

1969

Welded and rolled T-1 steel columns--a summary report, June 1969

C. K. Yu

L. Tall

Follow this and additional works at: <http://preserve.lehigh.edu/engr-civil-environmental-fritz-lab-reports>

Recommended Citation

Yu, C. K. and Tall, L., "Welded and rolled T-1 steel columns--a summary report, June 1969" (1969). *Fritz Laboratory Reports*. Paper 1836.

<http://preserve.lehigh.edu/engr-civil-environmental-fritz-lab-reports/1836>

This Technical Report is brought to you for free and open access by the Civil and Environmental Engineering at Lehigh Preserve. It has been accepted for inclusion in Fritz Laboratory Reports by an authorized administrator of Lehigh Preserve. For more information, please contact preserve@lehigh.edu.

Welded and Rolled "T-1" Steel Columns

WELDED AND ROLLED "T-1" STEEL COLUMNS -- A SUMMARY REPORT

by

C. K. Yu and L. Tall

This work has been carried out as part of an investigation sponsored by the United States Steel Corporation. Technical guidance was provided by the Task Group 1 of the Column Research Council.

Fritz Engineering Laboratory
Department of Civil Engineering
Lehigh University
Bethlehem, Pennsylvania

June 1970

Fritz Engineering Laboratory Report No. 290.16

TABLE OF CONTENTS

	<u>Page</u>
ABSTRACT	i
1. INTRODUCTION	1
2. MECHANICAL PROPERTIES AND RESIDUAL STRESS	7
2.1 Stress-Strain Relationship	7
2.2 Residual Stress	12
Residual Stress in T-1 Constructional Alloy Plates	15
Residual Stresses in Welded Built-Up T-1 Shapes	18
Residual Stresses In Rolled Heat-Treated T-1 Shapes	20
2.3 Summary	22
3. CENTRALLY LOADED COLUMNS	25
3.1 Introduction	25
3.2 Theoretical Analysis	26
3.3 Experimental Program and Test Results	32
3.4 Design Implications	35
4. LOCAL BUCKLING	38
4.1 Introduction	38
4.2 Theoretical Analysis	41
4.3 Test Program and Results	47
4.4 Summary	51
5. BEAM-COLUMNS	54
5.1 Introduction	54
5.2 Theoretical Analysis	57

5.3	Experimental Investigations	66
5.4	Comparison Between the Results of Theoretical Analysis and Tests	69
6.	SUMMARY AND CONCLUSIONS	72
7.	NOMENCLATURE	78
8.	ACKNOWLEDGEMENTS	81
9.	APPENDIX	82
10.	TABLES	85
11.	FIGURES	102
12.	REFERENCES	147

ABSTRACT

The requirements of economy and light weight in large size modern structures lead to the development and the use of weldable quenched and tempered constructional alloy steels. High strength steels with the yield strength in excess of 200 ksi have been developed. This paper summarizes the research conducted on welded and rolled "T-1" steel columns. "T-1" steel is a high strength constructional alloy steel with a minimum yield stress of 100 ksi and has the ASTM designation of A514 and A517.

Studies were concerned with the strength of T-1 steel columns of thin-walled members such as box- and H-sections. The investigation included studies of residual stresses and mechanical properties, local buckling, centrally loaded columns, and beam-columns. The study also included a pilot investigation into a higher strength steel, 5Ni-Cr-Mo-V steel.

The residual stresses present in rolled heat-treated shapes, in plates due to cutting and due to both edge and center welds, and in welded built-up shapes, all

of T-1 steel, were studied experimentally. It was found that the residual stresses in T-1 steel rolled shapes are in general much lower than the counterparts in mild steel because of the heat-treatment process, and in welded plates or shapes the magnitude of compressive residual stress is in a reverse proportion to the width-thickness ratio of the plate or component plate. Based on the results obtained, thermal residual stress distribution in T-1 steel shapes and plates can be predicted with reasonable accuracy.

The mechanical properties of the steel were determined experimentally through tension specimen tests and full-section stub column tests. The stress-strain relationship of T-1 steel could not be idealized as elastic-perfectly-plastic, and a representative stress-strain curve which consists of elastic range, nonlinear transition range and strain hardening range was prepared for theoretical computations involving T-1 steel.

The buckling strength of thin-walled centrally loaded columns made of T-1 steel was studied experimentally. A theoretical analysis was performed for pinned-end columns, based on the Shanley-Engesser tangent modulus theory and considering both the effects of residual stresses and non-linearity of the stress-strain curve. It was found that

both the residual stress distribution in the section and the shape of the stress strain curve have a pronounced influence on the reduction of column strength. The results obtained for T-1 steel columns were also compared with those results obtained on mild steel columns; T-1 steel columns in general exhibit a higher strength on a nondimensional basis.

The study of the local buckling phenomenon was carried out for both plates and shapes. Solutions were obtained on the basis of a finite difference approximation of the differential equation with variable coefficients. The numerical results were presented in the form of plate buckling curve of stress versus width-thickness ratio for plates with various boundary conditions, or for H- and box-sections, containing idealized distributions of residual stresses.

The ultimate strength and the local-deformation behavior, as well as the local buckling phenomenon of T-1 steel beam-columns, were investigated. Because of the nonlinearity of the stress-strain relationship of the steel and the particular pattern of residual stress, the moment-curvature-thrust of T-1 steel shapes are different from those of mild steel shapes. Interaction curves were

developed for T-1 steel beam-columns under equal end moment conditions.

The theoretical analyses were compared with their corresponding full scale experiments, it was shown good correlation exists between them. Suggestions are presented for the design of columns and beam-columns made of T-1 steel.

1. INTRODUCTION

The problem of stability in compression members in steel structures has received a great deal of attention from researchers in recent years. The influence on inelastic stability of residual stresses in steel shapes, and of the inelastic behavior of the stress-strain relationship, has been recognized.

"T-1" steel displays mechanical properties considerably different from those of the conventional low carbon steels. It has a nonlinear stress-strain relationship and a yield stress approximately three times higher than that of structural carbon steels. Additionally, previous research has shown that the magnitude of residual stresses essentially is independent of the yield stress if the steels are not heat-treated after rolling; heat-treatment can reduce the magnitude of the residual stresses in the structural shape. Consequently, the ratio of residual stress to yield stress for heat-treated T-1 steel shapes and plates is much less than that for structural carbon steels. The use of this high strength steel in structural members may effect a somewhat different behavior than that observed in the structural carbon steel

members toward which most previous investigations have been directed.

The objective of this study, in general, has been to present information for which design criteria could be prepared for T-1 steel columns. Specifically, the following details are included:

1. The determination of the residual stresses in, and the mechanical properties of, T-1 steel plates and shapes, both rolled and welded.
2. The investigation of the buckling strength of centrally loaded columns, especially those made of T-1 steel.
3. The investigation of the local buckling strength of columns including the solutions for the buckling of component plates and of plate assemblies.
4. The investigation of the ultimate strength and load-deformation characteristics of T-1 steel beam-columns.

According to the objectives, the study was divided into five phases; (1) mechanical properties and residual stresses, (2) centrally loaded columns, (3)

local buckling, (4) 5Ni-Cr-Mo-V steel columns, and (5) beam-columns. Phase (4) is concerned with 5Ni-Cr-Mo-V steel which is not T-1 steel but has certain similarities and is included in this study as a supplementary investigation.

Extensive studies have been made on topics related to elastic perfectly-plastic columns and to aluminum columns. In the first case, it is considered that the material has a stress-strain relationship that can be represented by two straight lines with slopes equal to the modulus of elasticity and zero, respectively; the residual stresses in the section are generally included. For the second case, even though the columns are loaded into the inelastic range, these shapes generally are considered as free of residual stresses since aluminum shapes are stretched after quenching to achieve straightness; the stretching removes most of the residual stresses. For T-1 constructional alloy steel columns, both the residual stresses in the section and the nonlinearity of the stress-strain relationship must be considered in the buckling strength analysis. Consequently, the results of previous investigations can not be applied directly to the present study. An independent analysis is required for predicting the strength of T-1 steel columns.

The buckling strength of a plate with residual stresses was evaluated by the energy method. The behavior of the plate was analyzed by the theory of elasticity and by the two theories of plasticity; one the total strain theory^{(1) (2) (3)} and the other the incremental theory.⁽⁴⁾ To simplify the numerical computation, the stress-strain relationship was assumed as elastic perfectly-plastic. The numerical analysis was carried out by using a finite difference approach and by means of a digital computer. Solutions were obtained for elastic, elastic-plastic, and plastic buckling of a plate with residual stresses, when the plate is simply supported at the loading edges and at the other edges is: (a) elastically restrained, (b) simply supported, and (c) fixed; solutions for plate assemblies which consist of cross sections of columns were also included.

The ultimate strength and load-deformation behavior of T-1 steel beam-columns were studied. The term beam-column denotes a member which is subject simultaneously to axial force and bending moment. The bending moment in the member may be caused by externally applied end moments, eccentricity of longitudinal forces, initial out-of-straightness of axially loaded

columns, or by transverse forces, in addition to axial force and end moments. In this study, only the types of beam-columns which are subject to constant axial force and varying end moments were investigated. Furthermore, the beam-columns studied were assumed to be laterally supported, that is, they were designed to fail in the bending plane without twisting, and were loaded at the ends with equal moments which cause a simple curvature bending only. The theoretical analysis was achieved by means of a numerical integration procedure. The nonlinear property of the stress-strain curve, various patterns of residual stress resulting from cooling after either rolling or welding, and the strain reversal effect, all were included in determining the moment-thrust-curvature relationship. The load-deformation relationship of the beam-columns was obtained by a direct stepwise integration procedure. The local buckling behavior of beam-columns was determined experimentally and was compared with theoretical solutions available.

This report presents a summary of an extensive analysis of the buckling strength of centrally loaded columns, the local buckling of plates and plate assemblies, and the ultimate strength of beam-columns made of T-1 steel.

Both residual stresses and the nonlinearity of the stress-strain relationship of material were found to have a pronounced influence on the strength of compression members.

2. MECHANICAL PROPERTIES AND RESIDUAL STRESS

2.1. Stress-Strain Relationship

Stress-strain curves and the related mechanical properties are the basic means of determining the quality and the usefulness of metals and of providing fundamental knowledge for their use in the design of metal structures and parts. The structural metals that are widely used at present may be divided into four categories: (1) structural carbon steels, (2) high strength low-alloy steels, (3) constructional alloy steels, and (4) aluminum alloys. These metals have two different types of stress-strain curves -- those exhibiting a yield point, and those not indicating this. For structural carbon and high strength low-alloy steels, the stress-strain curves are of the first type; that is, the stress is linearly proportional to strain up to the yield point and thereafter is constant or nearly constant over a large range of strain. Therefore, their mechanical properties can be characterized simply, by such terms as modulus of elasticity, upper yield point, static yield level, strain-hardening strains, and strain hardening modulus as shown in Fig. 1. For constructional alloy steels and aluminum alloys, the stress-strain curves are of the second type; that is, the stress deviates from a linear relationship with strain at stresses

below the yield strength and usually does not exhibit a region in which the stress remains constant over a large range of strains. There is no apparent yield point or yield stress level in this second type of stress-strain curve. Usually, a nominal yield point is determined by the 0.2% strain offset method.⁽⁵⁾ This stress-strain relationship with no apparent yield point will be described as a "nonlinear" relationship in this report.

To describe the nonlinear curves, Ramberg and Osgood have developed a set of curves in terms of three parameters: namely, the modulus of elasticity and two secant strengths.⁽⁵⁾ The comparison of these curves with those from tests of aluminum alloy, stainless steel and chromium nickel steel sheets, shows a satisfactory agreement.

Although the Ramberg-Osgood representation fits the stress-strain curves of most metals used in aircraft construction, it cannot be used to describe the stress-strain relationships of constructional alloy steels, such as T-1 steel, simply because the stress-strain curves of these steels usually approach a straight line with a very small slope after the "knee" portion of the curve. A new type of mathematical equation was developed to

represent the stress-strain relationship of T-1 steel.

A total of fifty-eight tension coupon tests and eight compression coupon tests were conducted on specimens taken from various rolled H-shapes and plates made of A514 steel. The tension specimen dimensions were determined according to the ASTM Standards for the tension test specimen.⁽⁶⁾ The speed of testing for the tension specimens was within the recommended ASTM limits, that is, the crosshead speed did not exceed 1/16 in. per minute per inch of gage length. The load-elongation curve was plotted by an automatic recording device. After exceeding the elastic limit, the testing machine was stopped at appropriate strain intervals to determine the stress-strain relationship at the zero strain rate.⁽⁷⁾ A typical stress-strain curve obtained from this type of test is shown on Fig. 2. Table 1 gives the results of all the tension coupon tests, and Fig. 3 shows the histogram plots for the mechanical properties of T-1 steel.

From the test curves, it can be observed that the proportional limit ranges from $0.65 \sigma_y$ to $1.0 \sigma_y$ with an average value of $0.82 \sigma_y$ and that the curve is a straight line after the yield stress, the yield stress being obtained by the 0.2% offset method.⁽⁶⁾ In order to determine

a representative stress-strain curve from all the test results, a method suggested by the Column Research Council⁽⁸⁾ was used. From the proportional limit to the yield stress, the strain departures from the modulus line (Fig. 2) for various fixed percentages of individual yield stress were recorded. For the case when not enough static points were taken in the transition part of the stress-strain curve, a method developed by Cozzone and Melcon⁽⁹⁾ was used to determine the transition portion of the static stress-strain curve; as shown in Fig. 4, a line OA' is drawn from the origin to the static yield point (determined by 0.2% offset) and extended to intersect the "dynamic" stress-strain curve at point A. To obtain the static stress-strain curve several lines were drawn as OB, OC, OD and the corresponding static points B', C', D' were determined. For example, the point B' was determined by means of the equation $OB' = OB \times OA' / OA$. The curve through B', C', and D' is the static stress-strain curve in the transition region. Dividing the measured strain by ϵ_y , where ϵ_y is equal to σ_y / E , and averaging all the offset values at the same stress level, a representative stress-strain curve in dimensionless form was obtained as shown in Fig. 5a.

The stress-strain curve for T-1 steel can be

therefore, described by the following three equations:

$$\frac{\sigma}{\sigma_y} = \frac{\epsilon}{\epsilon_y} \quad \text{when } 0 \leq \frac{\sigma}{\sigma_y} \leq 0.8$$

$$\begin{aligned} \frac{\sigma}{\sigma_y} = & 1.0 + 0.005 \left(\frac{\epsilon}{\epsilon_y} - 1.52 \right) \\ & + 0.3647 \left(\frac{\epsilon}{\epsilon_y} - 1.52 \right)^3 \\ & + 0.3276 \left(\frac{\epsilon}{\epsilon_y} - 1.52 \right)^5 \end{aligned} \quad (1)$$

$$\text{when } 0.8 \leq \frac{\sigma}{\sigma_y} \leq 1.0$$

and

$$\frac{\sigma}{\sigma_y} = 1.0 + 0.005 \left(\frac{\epsilon}{\epsilon_y} - 1.52 \right)$$

$$\text{when } 1.0 \leq \frac{\sigma}{\sigma_y}$$

A comparison of Eq. 1 with the experimentally obtained typical stress-strain curve and tangent modulus curve in the transition region is shown in Fig. 5b. The accuracy of Eq. 1 is adequate.

Several compression coupon tests were conducted and the results are shown on Table 2. The size of specimen used for compression tests is in accordance with the recommendation of the Column Research Council⁽⁸⁾ and no

lateral supports were used since the specimen itself was sufficiently stocky.

It was observed that both the modulus of elasticity and the yield stress determined by compression coupon tests are nearly the same as those obtained from the tension specimen tests. However, the compression tests indicate that the transition portion of the stress-strain curve has a sharper knee and a higher strain-hardening modulus than those of the tension tests. The difficulty of preparation of specimens and alignment make the compression coupon test less desirable. In this study, because of the limited number of compression specimen tests conducted, no statistical analysis could be performed and the results obtained from the tension specimen tests were taken as representative of the mechanical properties of T-1 steel for both tension and compression, even though actually they are slightly different from each other.

2.2 Residual Stress

Due to the importance of the effects of residual stress on the behavior of structural members, especially compressive members such as columns, much research has

been carried out in this field during the past decade. Residual stresses are a consequence of the plastic deformation of material; the sources of this plastic deformation can be many, such as thermal stresses due to uneven cooling of various parts of the structural shapes, cold bending or straightening of the member.

During the cooling process for a rolled section, there is usually more area of surface in contact with the cooling medium, either air or liquid, at the edges of the section than at its center. This causes a faster cooling rate at the edges and normally forms compressive residual stress there and tensile residual stress at the center and junctions. For a welded built-up section, welding causes temperatures to rise rapidly in the region near the deposited weld while most of the remaining portion of the section is unaffected. However, when the weld-affected zone starts to cool, the rest of the section gradually rises in temperature. The whole section on cooling to the ambient temperature experiences non-uniform thermal changes that cause nonhomogeneous plastification, and thus the formation of residual stress. Residual stresses due to welding or cooling from rolling are simply thermal stresses remaining when the material has cooled to ambient temperature. (10)

The theoretical analysis of thermal residual stress has been studied extensively, as for example, by Boulton and Lance Martin,⁽¹¹⁾ Gruning,⁽¹²⁾ Rodgers and Fetcher,⁽¹³⁾ Weiner,⁽¹⁴⁾ Tall,⁽¹⁵⁾ Estuar,⁽¹⁶⁾ and Alpsten.⁽¹⁷⁾ However, the difficulty of theoretically predicting thermal residual stress in plates or shapes is due to the uncertainty of many variables which affect the temperature distribution and thermal stresses. Therefore, to simplify the problem for theoretical analysis, quite a number of assumptions, sometimes far removed from reality, must be made.⁽¹⁵⁾ Consequently, theoretically obtained values of residual stress generally do not give satisfactory correlation with the actual measurements. Furthermore, other kinds of residual stresses such as those due to cold bending or rotary straightening may exist together with thermal residual stress, complicating the theoretical analysis even further. This has lead to reliance on actual residual stress measurements.

The program for the investigation of residual stresses in T-1 steel shapes and plates consisted of three parts, all experimental: (1) residual stresses in T-1 constructional alloy steel plates,⁽¹⁸⁾ (2) residual stresses in welded built-up T-1 shapes,⁽¹⁹⁾ and (3) residual

stresses in rolled heat-treated T-1 shapes.⁽²⁰⁾

All specimens for residual stress measurement were sufficiently long so that a uniform state of stress existed in the portion where the residual stresses were measured. The method of "sectioning"⁽⁷⁾ was used for the measurement of residual strains, because it is simple and gives the average strain within the gage length.

Residual Stresses in T-1 Constructional Alloy Steel

Plates

The plate sizes tested were selected so as to represent the component parts of commonly used built-up members. The plates chosen encompassed a range larger than any hitherto tested in any simple program. Table 3 summarizes the plate dimensions and the tests conducted.

The plates were cut to a specified size from wide plates by flame-cutting. The plates tested included unwelded plates, center-welded plates and plates welded along one or both edges, the latter two simulating the components of welded built-up H- and box-shapes. Manual shielded-metal-arc welding processes were employed. The electrodes used for most of the manual welds were E70 series, which are commonly used in industry and,

correspondingly, the wire and flux combination used was L70 and L840 for automatic submerged-arc welding.

For determination of possible differences in magnitude and distribution of residual stresses due to the use of different electrode types, a higher strength electrode also was used. Automatic welding, using L100 series with 709 flux, was performed on Plates T-5-5 and T-5-6.

The plates were welded by professional welders in the welding shop of a large industrial plant and the information related to welding was recorded, such as voltage, amperage, speed of electrode travel, type of electrode, and position of beads. Table 4 gives the detailed information.

The results⁽¹⁸⁾ of residual stress measurements indicate that for most of the plates the residual stresses at the top and bottom faces were different but that the difference was so small compared to the yield strength of the material that the average value could be used. The results obtained are presented in a tabular form in Tables 5, 6 and 7, where the values of residual stresses are the averages of both top and bottom faces of a plate.

For as-cut unwelded plates, the residual stresses result from flame-cutting and other fabrication processes. Residual stresses in 6" x 1/2" and 12" x 1" plates, with flame-cut unwelded plates included, are shown in Figs. 6 and 7 as an illustration. For plates of different size and welding method, the patterns of residual stress distribution are similar. Table 5 shows the residual stresses distribution in all the as-cut unwelded plates measured. The maximum compressive residual stress is in the range of 3 to 10 ksi, and the average is approximately 6 ksi. The average maximum compressive residual stress for plates wider than 12 in. is approximately 4 ksi; this average compressive stress extended across 60 to 95% of the plate width. The maximum tensile residual stress is at the edges and ranges from 26 ksi to 86 ksi.

In Figs. 6 and 7, the distribution of residual stress across the width of center-welded plates of sizes 6" x 1/2" and 12" x 1" are shown. The salient dimensions of the residual stress distribution and the average of top and bottom face measurements are given in Table 6. Tensile residual stress were observed at the flame-cut edges and at the weld in center-welded plates. The compressive residual stress have a maximum of about 24 ksi

in plates welded by automatic welding, and a lower value of 16 ksi for plates welded manually. The average compressive residual stress varies from 6 ksi to 18 ksi. The highest tensile residual stress was found to be about 84 ksi at the weld.

For edge-welded plates the results are shown in Table 7 and in Figs. 6 and 7 for two typical plates. The maximum compressive residual stress obtained is 20 ksi, with 10 ksi as the average. The tensile residual stresses at the welded edges are comparatively high, attaining the yield strength in the weld, approximately 80 ksi for most plates.

Comparing the results obtained, it was found for welded plates, that neither weld size, electrode strength, the condition of manual or automatic welding, nor number of weld passes, have a significant effect on the shape and magnitude of residual stress in plates. The distribution of the residual stress in T-1 plates may be represented very closely by straight lines as shown in Tables 5, 6, and 7.

Residual Stresses in Welded Built-up T-1 Shapes

Five shapes were included in the study.⁽¹⁹⁾ Two

of the shapes were welded H-shapes from flame-cut plates; one shape was welded from sheared plates; and two shapes were box shapes welded from flame-cut plates. Table 8 shows the shapes tested and their dimensions. The welding was carried out by the automatic submerged-arc-welding procedure utilizing Lincoln L70 wire and L840 flux.

The pattern of residual stress distribution obtained from measurements are presented in Figs. 8 and 9. The results for welded H-shapes are the readings of both top and bottom faces, whereas the readings shown for box shapes are the outside face reading only. Two sets of measurements taken from different sections are presented for each shape; these show that there is little variation in residual stress along the length of the shape. Table 9 gives a summary of results.

Figure 8 shows the residual stresses for the welded H-shapes. The pattern of residual stress distribution has tensile residual stresses at the junction of flange and web and at the flange tips, and compressive stresses over the rest of the shapes. Fig. 9 shows the residual stress distribution for welded box shapes; tensile residual stresses exist near the junctions and compressive residual stresses over the remaining area. The magnitude of

compressive residual stress appears to be inverse to the width-thickness ratio of the component plates, that is, the more stocky the plates, the higher the compressive residual stress.

Figures 10 and 11 show the residual stress distribution measured in the 6H27 welded shape and the 6 x 6 welded box shape, respectively, and they are compared with the residual stress distribution in plates subjected to similar welds at the center or edges. It is seen that both the magnitude and pattern of residual stress are similar; this indicates that residual stresses in component plates give a close representation of the residual stresses in the welded shapes themselves if the dimension of the plate elements are similar.⁽¹⁹⁾

Residual Stresses In Rolled Heat-Treated T-1 Shapes

Nine rolled and heat-treated T-1 steel shapes varying from light-weight shapes to medium-weight shapes were included in the study.⁽²⁰⁾ Representative shapes were chosen so that the results obtained would enable the prediction of the residual stresses in other wide-flange shapes in this medium-size range. Table 10 lists the shapes tested.

Some of the residual stress measurements are shown in Fig. 12. A typical residual stress distribution has compressive stress at the flange tips and tensile stress at the junctions of flanges and web. The maximum value of compressive residual stress is about 8 ksi for all shapes investigated. The average compressive residual stress at flange is about 3 ksi for shapes with flanges less than 1/2 in. in thickness and about 4 to 5 ksi for shapes with flange thickness more than 1/2 in. The maximum compressive residual stress in the web is small also, less than 5 ksi. The average for the light shapes is between 1 and 2 ksi and slightly higher for the heavier shapes, between 2 and 3 ksi. The tensile stresses in the flange center and web ends do not exceed 5 ksi; the average for all shapes is between 2 and 3 ksi. The average values of residual stresses in the shapes investigated are tabulated in Table 11.

Figure 13 shows the residual stresses in a 8WF31 shape for four different steels, including that for T-1 steel. The pattern of the residual stress distribution is similar, especially in the flange, which has the greatest effect on column strength. The difference in magnitude is most pronounced for the T-1 steel shape as compared to the other three shapes. The magnitude of residual

stress in T-1 steel shape is only one third to one-half that observed in the other steels. The heat-treatment after hot-rolling lowers the magnitude of residual stress and, thus, low residual stresses may be regarded as characteristic of rolled T-1 steel shapes.

2.3 Summary

The results of the experimental investigation on the residual stress distribution in T-1 steel plates and shapes, welded and rolled, can be summarized as follows. (18,19,20)

1. Residual stresses in the component plates give a close representation of the residual stresses in the welded shapes themselves, provided the relative sizes of plate elements are nearly the same.
2. Flame cutting and edge welding cause tensile residual stress at the flame-cut or welded edge.
3. Geometry is the major influence on the magnitude and distribution of residual stress. Weld size, electrode strength, the condition of manual or automatic welding, and the number of weld passes, have little

significant effect on the shape and magnitude of residual stress in plates or welded built-up sections.

4. Welded built-up shapes have residual stresses considerably higher than those in the rolled shapes.
5. For rolled steel shapes, the magnitude of residual stress is independent of the yield stress of the material; that is, regardless of which steel a shape is made, the magnitude of the compressive residual stress at the flange edges is approximately the same. Heat-treatment may lower the magnitude appreciably, as in T-1 steel rolled shapes which have a compressive residual stress at the flange edges of about 5 ksi.
6. Patterns of residual stress distribution in rolled heat-treated T-1 steel shapes may be represented by straight lines as shown in Fig. 14a.
7. Welding residual stresses in T-1 steel shapes may be approximated by several straight lines, with the tensile residual stress approaching the yield stress of the weld metal at the weld. For flame-cut plates, tensile residual stresses

often exist at the flange tips. The approximate patterns of residual stress distribution in welded built-up shapes are shown in Fig. 14b.

8. For plates or sections with a thickness less than one inch, residual stresses may be assumed to be the same across the thickness. For sections with a thickness greater than one inch, variation of residual stress through the thickness must be considered in the prediction of the column strength.
9. The variation of residual stress is small in any fiber along a member which has not been cold bent or otherwise mechanically straightened.

3. CENTRALLY LOADED COLUMNS

3.1 Introduction

Since the publication of Shanley's papers,^(21,22,23) the tangent modulus load has been recognized as the smallest value of the axial load at which bifurcation of equilibrium can occur. It was shown that, immediately after the tangent modulus load, the column can sustain increasing axial load with increasing deflection. Thus, the actual ultimate load of a perfectly straight column will be somewhat higher than the tangent modulus load. Because of the inevitable initial out-of-straightness of the columns, it has been found that if the initial out-of-straightness is small, the ultimate load usually is close to the tangent modulus load. For this reason, the tangent modulus load has been considered as the design criterion for a centrally loaded column.^(23,24)

Much research has been carried out on the column buckling strength analysis in the past decade. The most significant contribution of these previous investigations is the discovery and recognition of the importance of the influence of residual stresses on column strength. However, almost all of this research was restricted in application to materials having an elastic perfectly-plastic stress-strain relationship. For other materials

which exhibit a nonlinear type of stress-strain relationship, the residual stress effects either were neglected, or else accounted for by means of an empirical formula. Nevertheless, residual stresses do influence the buckling strength of columns made of materials with a nonlinear type stress-strain curve. The study reported here is devoted to an investigation of the strength of T-1 steel columns, considering the combined effects of residual stresses and the nonlinearity of the stress-strain curve. Theoretical column curves were developed based on the average residual stress distribution measured in the medium size shapes, and on mechanical properties obtained from tension specimens. The results of theoretical analysis were compared with full scale column tests, and design suggestions for T-1 steel columns were made.

3.2 Theoretical Analysis

Several customary assumptions are made in the theoretical analysis:

1. The column is initially perfectly straight.
2. Plane sections remain plane before and after bending.
3. The stress-strain relationship in any "fiber" of the column is the same as that observed in a tensile coupon.

4. The magnitude and pattern of distribution of residual stress are the same at any cross-section of the column.
5. The effect of shear deformation is neglected.
6. The external load is applied axially to the centroid of the cross section causing uniform strain over the cross section and through the whole length before bifurcation.
7. The cross section is constant along the length of the column.
8. The cross section is of such proportion that the possibility of torsional buckling can be precluded.

An initially straight axially loaded prismatic column will maintain its straight configuration up to a critical load at which it can be in equilibrium in either a straight or slightly bent position. Based on the Engesser-Shanley theory,⁽²²⁾ at the instant of bifurcation, the requirements of equilibrium of internal and external forces are (see Fig. 15)

$$\int_A \Delta \sigma \cdot dA = 0$$

and

$$\int_A \Delta \sigma \cdot y \cdot dA = P_v$$

(2)

where $\Delta\sigma$ is the increment of stress located a distance y from the neutral axis (or the axis of constant strain). P is the external axial force and v is the deflection in the direction of axis y . For an infinitesimal amount of bending the increment in stress predicted by small deflection theory is

$$\Delta\sigma = \phi \cdot E_t \cdot y = -\frac{d^2v}{dx^2} E_t \cdot y \quad (3)$$

Here E_t is the tangent modulus corresponding to the axial stress at the point. Substitution of Eq. 3.2 into 3.1 yields the expressions

$$\int_A E_t y dA = 0 \quad (4a)$$

and

$$\frac{d^2v}{dx^2} \int_A E_t y^2 dA + P v = 0 \quad (4b)$$

in which x is the coordinate along the length of the column.

From Eq. 4a the location of the neutral axis is determined. For a symmetrical section with a symmetrical residual stress distribution, this axis coincides with one of the principal axes of the section.

The critical load P_{cr} is obtained from Equation 4 as

$$P_{cr} = \pi^2 \frac{\int_A E_t y^2 dA}{L^2} \quad (5)$$

where L is the effective length of the column.

The buckling strength of a column depends on the tangent modulus of each elemental area and therefore is a function of residual stress distribution as well as mechanical properties.

If the column remains in the elastic range up to the critical load, then $E_t = E$ over the whole cross section and the critical load is the Euler load,

$$P_{cr} = \pi^2 \frac{EI}{L^2} \quad (6)$$

In the presence of residual stresses, the tangent modulus may vary from point to point on the section for a stress-strain relationship of either the elastic-perfectly-plastic or the non-linear type. The calculation of critical loads becomes much more complicated. If the notation I_m , effective moment of inertia, is introduced,

$$I_m = \int_A \frac{E_t}{E} y^2 dA \quad (7)$$

then,

$$P_{cr} = \frac{\pi^2 E I_m}{L^2} \quad (8)$$

The numerical method of computing I_m at a given P level was developed for columns of H- or box cross sections, containing either cooling or welding type residual stresses. The stress-strain curve of the material is assumed to be of either the non-linear type or the elastic-perfectly-plastic type. However, the method is, by its nature, applicable for columns with any kind of residual stress distribution and stress-strain curve, and it is suitable for computation by a digital computer.

As shown in the foregoing section, in order to evaluate the buckling load P_{cr} , the effective moment of inertia I_m must first be calculated. Here I_m depends on the residual stress distribution, the magnitude of applied force, and the stress-strain relationship of the material. Generally, it will not be practical to calculate P_{cr} directly; ⁽²⁵⁾ instead, the equivalent length L is determined. The numerical computation is accomplished as follows:

1. Divide the section into a sufficient number of finite area meshes as shown in Fig. 16.
2. Record the residual strain at the center of

each mesh (assuming the residual stresses distributed over each mesh are uniform and the same as that at the center point of the mesh).

3. Assume a uniform strain applied to the column. The total strain at a point is equal to the residual strain plus the applied uniform longitudinal strain.
4. From the tangent modulus strain equation and the stress-strain equation, determine the tangent modulus and the stress, respectively, corresponding to the total strain in each mesh determined in step 3.
5. Sum up the internal axial force on all the meshes $P = \int_A \Delta \sigma dA$ and compute the modified moment of inertia I_m from Eq. 7.
6. Compute the equivalent column length for the calculated P and I_m

$$L = \pi \sqrt{\frac{EI_m}{P}} \quad (9)$$

7. Increase the applied uniform longitudinal and repeat steps 1 through 6 until the entire column strength curve is obtained.

For dimensionless analysis, Eq. 9 can be rewritten in the form

$$\lambda = \frac{L}{\pi} \sqrt{\frac{\sigma_y}{E}} \cdot \frac{L}{r} = \sqrt{\frac{I_m/I}{P_{cr}/P_y}} \quad (10)$$

The function λ defined by Eq. 3.10 will hereafter be referred to as slenderness function. The dimensionless analysis in this fashion eliminates the mechanical properties, such as σ_y and E , in the computation. Only the shape of the stress-strain curve, and the pattern and the ratio of residual stress distribution remains as variables.

The numerical computation was carried out by means of a digital computer and all of the programs were written in Fortran IV language. Programs were prepared for rectangular, box- and H-columns. For symmetrical sections with symmetrical residual stresses, the cases considered here, only one-quarter of the section need be used in the computation for the buckling strength of columns.

3.3 Experimental Program and Test Results

Sixteen T-1 steel columns were tested under pinned-end conditions⁽²⁶⁾ and one 5Ni-Cr-Mo-V steel was

tested⁽²⁵⁾ under a flat-end condition.⁽²⁵⁾ The test program, as shown in Table 12, included rolled H-shapes and welded H- and box-shapes. The slenderness ratios of columns were selected in such a way that the columns would buckle in the inelastic range; that is, L/r varies from 30 to 60. Most columns were tested with restraint in the strong axis direction, and so were bent with respect to the weak axis.

The set-up of a typical column test is shown in Fig. 17. The strain readings at the ends and at sixth points along the column were recorded by SR-4 electrical strain gages. The deflection at mid-height was measured by a mechanical dial gage and the deflection at every sixth point was measured by a theodolite. End rotations were determined by two level bars mounted respectively on the top and bottom base plates.⁽²⁷⁾

Alignment was performed before the starting of testing. The alignment was based on the four corner strain gages at each end of the specimen and at mid-height. The alignment was considered satisfactory if the deviation of any of the four corner gage readings did not exceed 5 per cent of their average value at the maximum alignment load. This criterion was applied at each of

the three control sections. (27)

The test was started with an initial load about 1/15 to 1/10 of the calculated ultimate load capacity of the column. Besides recording the data, a point-by-point plot of the load-deflection curve and load-strain diagram were made as the testing proceeded. The load was applied in appropriate increments as determined by the load-deflections curve.

The test maximum loads were compared with the theoretical tangent modulus loads. The theoretical column curves determined were based on the residual stress distributions obtained from the average of all the actual residual stress measurements. The measurements of residual stresses were conducted on plates or shapes with thickness less than, or equal to, 1 inch. The theoretical column curves so obtained are limited in scope to "thin" welded H- or box- section of T-1 steel, either heat-treated rolled or welded built-up, with thickness less than 1 inch, and to "small size" shapes with flange width or web depth less than 10 inches. It is only in this range that sufficient data is available to ensure the idealization of residual stresses from which the theoretical tangent modulus strength was determined.

The patterns and magnitude of the idealized residual stress distribution for welded and rolled H-shapes and for welded box-shapes, all of T-1 steel, are shown in Fig. 18.

Figures 19 to 22 show the comparison between the results of theoretical analysis and the test points.^(25,26) For those columns bent about the weak axis, that is, the principal axis parallel to the web plate, and for square box columns, good correlation exists between the results of the theoretical analysis and tests. However, for the one welded H-shape column tested by bending with respect to the strong axis, a large discrepancy is observed. It was noticed during this test that twisting of the column preceded the unloading, and therefore, caused somewhat of a reduction of the column strength. However, since only one column was tested about the strong axis, the results are by no means conclusive.

3.4 Design Implications

Because all the experiments except one were carried out for either H-shaped columns bent about the weak axis or for square box-shape columns, the design

suggestions stated here are applicable only for weak axis bending of H-shapes or for square box-shapes.

The residual stresses in T-1 or 5Ni-Cr-Mo-V steel shapes, either welded or rolled, are smaller than those in the same shapes of mild steel, especially when compared on a nondimensional basis. This gives a smaller influence on the reduction of column strength due to residual stresses for T-1 steel shapes than for their counterparts of mild steel. This is true even though the nonlinearity property of the stress-strain relationship of T-1 steel causes somewhat of a reduction of column strength at certain ranges of slenderness ratio. The overall reduction is still less than that for mild steel columns. As shown in Figs. 23 and 24, the ultimate loads of T-1 steel columns are compared with those of A7 steel. T-1 steel columns are considerably stronger than A7 steel columns, especially for welded shapes.

The "CRC column strength curve", which also serves as a basis for the allowable column stress in the AISC Specifications, was originally derived based on a compressive residual stress arbitrarily assumed equal to $0.5 \sigma_y$ for A7 steel rolled wide flange shapes. It

exhibited good correlation with test results of hot-rolled WF shapes of mild steel. Nevertheless, the CRC column curve does not give a good prediction of column strength of welded shapes made of mild steels. The difference between them could be as much as 30% below the values predicted by the CRC column curve.

However, for welded shapes of T-1 steel, most of the test points are either close to or above the CRC column curve. This indicates that the CRC curve may be regarded as being applicable to welded T-1 H-shapes bent about the weak axis and to welded T-1 box-shapes.

For rolled shapes, T-1 steel H-columns bent about the weak axis are generally stronger than columns of mild steel, as shown in Fig. 24, and therefore their strengths are higher than those predicted by the CRC column curve. A curve which fits the test results is given by

$$P_{cr} = P_y - \frac{\sigma_y^2}{5\pi^2 E} \left(\frac{L}{r}\right)^2$$

or

$$\frac{P_{cr}}{P_y} = 1 - \frac{1}{5} \lambda^2$$

(11)

This equation may be considered as the column design basis for rolled T-1 steel shapes bent with respect to the weak axis.

4. LOCAL BUCKLING

4.1 Introduction

Local buckling may be defined as the bifurcation of equilibrium of adjacent theoretically flat plates into distorted shapes in their own planes. The efficient design of a column requires a cross section with comparatively thin plates, and thus, local buckling may increase in significance as steels of higher yield point are used. Hence, consideration must be given to the stability of plate elements so that the most economical cross section can be designed.

The buckling load of plates may be substantially different from the ultimate load which the plates can carry, as opposed to a column for which the buckling load has been found to be of a magnitude similar to the ultimate load, for practical conditions. Plates may be able to sustain loads in the buckled state, with ultimate loads considerably exceeding the buckling load. However, the difference between the buckling load and the ultimate load becomes significant only for relatively thin plates; the plate elements of structural steel columns are, on the contrary, relatively thick. Once buckling occurs in

plate elements of columns, the stiffness for axial compression of the plates is reduced, and this in turn reduces the bending rigidity of the column, possibly leading to overall failure of the column. Hence, the buckling load of plate elements or plate assemblies is more important as a guide for the design of column cross sections than in determining the ultimate load.

A column cross section consists of a number of plate elements. Since the plate elements are connected to each other, a complete analysis of local buckling must be made for the plate assembly as a unit. If an individual analysis is made for each plate element, the restrictions at the unloaded edges of each plate must be determined. However, if such individual analyses are made on plate elements for several combinations of particular edge conditions, such as free, simply supported, and fixed, the results may be useful in estimating the overall buckling strength of the cross section. Hence, the study of this investigation includes the analysis of plate elements and the analyses of plate assemblies.

The local failure of plate elements of a column is a particular case of plate instability in which the plates can be considered as simply supported at the two

opposite loading edges on which the distributed thrust is applied. The other two edges are free of loading and the supporting conditions would be, in general, either fixed for translation and elastically restrained for rotation, or else free. Since exact solutions can be made for most of the cross sections of structural columns, the following analysis considers only special boundary conditions at the unloaded edges to obtain buckling solutions for plate elements. These are the combinations of free, simply supported and fixed at the unloaded edges.

At the two opposite loading edges the boundary conditions for local buckling are simple supports. The boundaries at the other two edges of the plate elements are either free, when the edge does not meet with the other plate, or else elastically restrained for rotation when the edge intersects with the other plates. In this study, only rigid connections, such as joints in rolled shapes and welded intersections, are considered for the intersection. Particular attention is given to column cross sections of box-, and H-shapes.

When residual stresses exist, the stress in the plate cannot be considered as uniform. The plates may yield, partially, at a certain loading due to the existence

of compressive residual stress; thereafter, the plate is no longer homogeneous. The tangent modulus concept is introduced for the buckling in this state of stress, namely, that no strain reversal is assumed to occur at the instant of buckling.

The analytical solutions are not feasible to solution, in general, without a considerable amount of effort; consequently, approximate methods must be considered. The solutions were obtained by a finite difference approximation of the differential equations. A digital computer was used to obtain the numerical solutions.

4.2 Theoretical Analysis

The basic differential equation governing plate buckling, which is applicable both in the elastic and in the inelastic domain of the plate, is

$$E \left[\frac{\partial^2}{\partial z^2} \left(I k_1 \frac{\partial^2 w}{\partial z^2} + I k_2 \frac{\partial^2 w}{\partial y^2} \right) + 4 \frac{\partial^2}{\partial z \partial y} \left(I k_4 \frac{\partial^2 w}{\partial y^2} \right) + \frac{\partial^2}{\partial y^2} \left(I k_2 \frac{\partial^2 w}{\partial z^2} + I k_3 \frac{\partial^2 w}{\partial y^2} \right) \right] + t \sigma_z \frac{\partial^2 w}{\partial z^2} = 0 \quad (12)$$

where $k_1 = \frac{1 + 3 \left(\frac{E_t}{E_s} \right)}{(5 - 4\nu + 3e) - (1 - 2\nu)^2 \left(\frac{E_t}{E} \right)}$

$$k_2 = \frac{2 - 2(1 - \nu) \left(\frac{E_t}{E} \right)}{(5 - 4\nu + 3e) - (1 - 2\nu)^2 \left(\frac{E_t}{E} \right)}$$

$$k_3 = \frac{4}{(5-4\nu+3e) - (1-2\nu)^2 \left(\frac{E_t}{E}\right)}$$

$$k_4 = \frac{1}{2+2\nu+3e}$$

$$e = \frac{E}{E_s} - 1$$

E , E_t and E_s are the modulus of elasticity, tangent modulus and secant modulus, respectively, as shown in Fig. 25; ν is poisson's ratio. The coordinate systems for plate elements and for plate assemblies are shown in Fig. 26. The coordinate x is perpendicular to the middle plane of the plate, y is normal to the thrust and in the middle plane, and z is the coordinate parallel to the thrust and to the residual stress. When a plate assembly is considered, a coordinate system is set to each plate and they are distinguished by subscript numbers.

Equation 12 was derived by Bijlaard⁽²¹⁾⁽²²⁾⁽²³⁾ for a plate. When a plate assembly is considered, an equation can be set up for each plate element forming the same number of simultaneous equations as the number of plate elements.

The stress σ_z is a function of the residual strain distribution and the strain distribution due to the thrust. Both of these strain are assumed to be constant along the z -direction; however, the residual strain may

vary whereas strain due to thrust is constant, in the y direction. Since k_1 through k_4 are functions of strain intensities, they are also variables in the y-direction and thus, function of the coordinate y. Residual strain distribution in plates, rolled or welded, generally is complicated, and therefore an analytical solution for Eq. 12 is quite a difficult task, if not an impossible one.

In this study, the governing equation, Eq. 12, was solved by the finite difference method.⁽³¹⁾⁽³²⁾ The deflected shape of the plate was expressed as a product function of which one term is a simple known function; Eq. 12 was thus reduced to an ordinary differential equation. The deflected shape of the plate was assumed to be defined by the following product function which satisfies the boundary conditions at the loading edges

$$w = Y \sin \frac{p\pi}{L} z \quad (13)$$

Where Y is a function of the coordinate y along and p is the number of half waves in the z-direction. It is known that the lowest buckling stress can be obtained by considering a plate buckling into a half wave in the z direction; thus, it is necessary to consider only p equal to 1. Substituting Eq. 13 into Eq. 12, the basic differential

equation can be shown to lead to the following form, where the equation is divided by a constant I_0 .

$$\begin{aligned} & \frac{d^2}{dy^2} \left(\frac{I}{I_0} k_3 \frac{d^2 Y}{dy^2} - \frac{\pi^2}{L^2} \frac{I}{I_0} k_2 Y \right) \\ & - 4 \frac{\pi^2}{L^2} \frac{d}{dy} \left(\frac{I}{I_0} k_4 \frac{dY}{dy} \right) - \frac{\pi^2}{L^2} \frac{I}{I_0} k_2 \frac{d^2 Y}{dy^2} \\ & + \frac{\pi^2}{L^2} \left(\frac{\pi^2}{L^2} \frac{I}{I_0} k_1 - \frac{t \sigma_r}{EI_0} \right) Y = 0 \end{aligned} \quad (14)$$

This differential equation, Eq. 14 must be satisfied at each mesh part in the y direction. This formulates a number of simultaneous equations equal to the number of mesh points. The determinant of the simultaneous equations is set equal to zero to determine the eigenvalues. For the buckling analysis of a partially yielded plate, the distribution of stress and stiffness of the material are a function of the loading and of the residual stress distribution so that it is easier to solve for a critical width ratio under a known loading rather than for a critical load on a plate with known geometry. The detail of the procedure of numerical computation is described in Ref. 33.

The buckling curves for plates with different residual stress patterns and boundary conditions which resemble those of component plates of column cross sections are shown in Figs. 27 through 30. The figures are plotted with the ratio of average critical stress to the static

yield stress as ordinate and with the non-dimensionalized width-thickness ratio as abscissa.

The assumed residual stress patterns reduce the buckling strength in all cases considered. The reduction in the elastic buckling strength is rather constant for a residual stress pattern regardless of the width-thickness ratio. The sudden jump of the plate buckling curve for plates with welding type residual stress is due to the penetration of yielding over a large portion of the area at the same instant.

These figures show also that it is possible for a plate to buckle with no external load. This phenomenon was explained for the first time in this study;⁽³⁴⁾ it is necessary only for a particular magnitude and distribution of residual stress to exist, for a particular b/t ratio.

A critical value of width-thickness ratio exists in all cases considered; plates with width-thickness ratio less than this critical value sustain the full yielding load. The critical value depends on the magnitude of residual stress for the assumed residual stress distribution of the cooling type, whereas it is constant for practical

purposes for the assumed residual stress patterns of the welding type.

Numerical results of the local buckling analysis on cross sections can be obtained in a form similar to the plate buckling curve. However, the fact that there are so many factors, such as geometric shape, residual stress distribution and the stress at which the section buckles, on which the critical width-thickness ratio depends, makes it quite difficult to prepare curves which cover a wide variety of column cross sections with various patterns of residual stress distributions. Instead, numerical results were obtained for a few cases to illustrate the effect of residual stresses. Box- and H- sections were selected with idealized residual stress patterns of the welding type as shown in Figs. 31, and 32. The assumed patterns are more severe for local buckling strength than the residual stress distribution found in medium size welded built-up shapes of T-1 steel and are somewhat conservative when compared to those found in similar shapes of structural carbon steel. Thus, the patterns are not intended to predict the strength of any real column, but are only for comparison purposes.

The analysis is made such that the minimum critical width-thickness ration of the flange plate is

obtained as a solution in non-dimensionalized form, with the given ratio between the widths of the web and the flange, b_w/b_f and with the given ratio between the thicknesses, t_w/t_f , where the subscripts w and f denote the values for web and flange plates, respectively.

The results are obtained in the same form as the plate buckling curve demonstrated in Fig. 31 for a box-section. The reduction of buckling strength due to the presence of residual stress is similar to that found for the buckling of plates with residual stress. Figure 32 shows the reduction factors for some box- and H- sections.

Since the critical width-thickness ratio can be obtained without much difficulty for column cross sections free of residual stress, or found from the literature⁽³⁵⁾⁽³⁶⁾ tabulated for most of the practical column cross sections, the reduction factor makes it possible with a simple multiplication to determine the critical width-thickness ratio of column cross sections containing residual stress.

4.3 Test Program and Results

A series of two welded square box-columns of T-1 steel were tested.⁽³⁷⁾ The section was selected to simulate

the plates simply supported at the unloaded edges. The lengths of the test columns were chosen such that column buckling could not occur (upper limits), and at the same time, such that the end disturbances would not affect the plate buckling behavior of the test section as well as the distribution of residual stresses (lower limit). The width-thickness ratios of the specimens were selected such that the critical loads were reached in both the elastic range and in the elastic-plastic range. Two identical specimens were cut from a long fabricated piece for both shapes, thus a total number of four specimens were tested. Table 13 shows the detail of the specimens.

Prior to the buckling tests, tensile coupon tests and residual stress measurements were carried out. The static yield stress had average values of

116 ksi for specimens T-1A and T-1B and

104 ksi for specimens T-2A and T-2B.

Figure 33 shows the distribution of residual stresses in the specimens, from which the following average values of non-dimensionalized compressive residual stresses were obtained.

$$\frac{\sigma_{rc}}{\sigma_y} = 0.12 \text{ in specimens T-1A and T-1B and}$$

$$\frac{\sigma_{rc}}{\sigma_y} = 0.16 \text{ in specimens T-2A and T-2B.}$$

Local buckling tests were made under the "as-placed" condition in an 800 kip screw-type universal testing machine. The ends of each specimen were milled to aid in the alignment of the column. The end fixtures consisted of a flat plate at the base and a plate with a set of wedge disks at the top. The set of disks was used for alignment so that all four component plates were loaded uniformly. Thus, each component plate satisfied conditions of simple supports at the unloaded edges. The deflection was measured at the center of the width of each side plate and at quarter points of the width for two plates on the opposite sides. The test set-up is shown in Fig. 34.

The critical stresses were determined by the so called "top of the knee method"⁽³⁸⁾ from the load-deflection relationship of the test specimens. Test results are summarized in Table 14 and compared with theoretical predictions in Fig. 35.

The specimens T-1A and T-1B, which buckled in

the elastic region, showed good agreement with the prediction, (with a slightly lower stress). Two theoretical predictions were made for specimens T-2A and T-2B, which buckled in the elastic-plastic range; one based on the total strain theory of plasticity and the other based on the incremental theory. The incremental theory predicted no buckling until the specimen reached the yield load, whereas the total strain theory predicted 92% of the yield load. Although both predictions were for loads higher than the test results, the difference is very small for the prediction of the total strain theory. It can be concluded, therefore, that the experiments correlated with the theoretical prediction of elastic and elastic-plastic buckling of steel plates with residual stresses, except for the prediction based on the incremental theory. The lack of correlation of the incremental theory was expected from the results of experimental studies on aluminum-alloy plates. (30)(36)

The test results of both critical stress and ultimate strength are also plotted on the plate buckling curve in Fig. 36, together with the results of similar tests on A7 square tubes given in Ref. 34. The non-dimensionalized comparison of test results in Fig. 36 shows that the welded T-1 plates are stronger than similar

plates of A7 steel. This is to be expected from the study on residual stresses, and a similar conclusion was obtained for the comparison of T-1 and A7 welded columns.

The specimens T-1A and T-1B buckled in the elastic range and showed significant post-buckling strength as seen in Fig. 36. On the other hand, specimens T-2A and T-2B buckled in the elastic-plastic range and had a relatively small reserve of post-buckling strength.

4.4 Summary

This chapter has considered the plate buckling strength and the local buckling strength of column sections, both containing residual stresses and loaded into the inelastic range of the material.⁽³⁹⁾ Since the coefficients of the basic differential equation governing plate buckling are variables, it is quite difficult to obtain rigorous solutions. Instead, solutions are obtained on the basis of a finite difference approximation to the differential equation.

Numerical results for plates with various edge conditions are presented in plate buckling curves of non-dimensionalized stress against non-dimensionalized width-thickness ratio. Numerical results of local buckling strength were obtained for a few cases.

A series of four welded built-up rectangular tubes of "T-1" constructional alloy steel were tested to substantiate the theoretical results.

The following conclusions may be drawn from this study for both plate buckling and the local buckling of columns: (39)

(1) The finite difference approximation of the differential equation was found to be powerful in obtaining the eigenvalue of the basic differential equation governing plate buckling.

(2) The elastic buckling strength depends largely on the magnitude and distribution of residual stresses.

(3) The effect of residual stresses on the elastic-plastic buckling depends greatly on the width-thickness ratio of the plates.

(4) A critical value of width-thickness ratio exists; plates with width-thickness ratio less than this critical value sustain the full yielding load. Based on the results of numerical analysis, it is found that the AISC specifications for critical width-thickness ratios can be extended directly to T-1 steel shapes, rolled or welded.

(5) The incremental theory of plasticity predicts

a much higher critical width-thickness ratio (and consequently a much higher critical stress) than the total strain theory.

(6) The comparison with the tests shows correlation between the theoretical results and the test results; for elastic-plastic buckling, the theoretical results based on the total-strain theory give good correlation with the experimental results, but the results based on the incremental theory predict a much higher critical stress.

(7) Comparison of experiments on welded square tubes shows that the tubes of T-1 steel are stronger for local buckling than those of A7 steel when compared on a non-dimensionalized basis.

(8) The square tubes buckling in the elastic range showed a significant post-buckling strength, while the tubes buckling in the elastic-plastic range had a relatively small reserve of post buckling strength.

5. BEAM-COLUMNS

5.1 Introduction

A beam-column may be defined as a member which is subject to forces producing significant amounts of both bending and compression. The bending moment in the member may be caused by externally applied end moments, eccentricity of longitudinal forces, initial out-of-straightness of axially loaded columns, or transverse forces in addition to axial forces and end moments. Several typical beam-columns are shown in Fig. 37. In this study, only the types of beam-columns which are subject to constant concentric axial forces and end moments are discussed.

The ultimate strength analysis of beam-columns was first treated as a stability problem by Von Karman.⁽⁴⁰⁾ He suggested a double integration procedure which was based on the equilibrium and the compatibility conditions of all the sections along the member, and this established the theoretical background for all the subsequent analyses of beam-columns. However, Von Karman's exact concept was difficult to apply to practical problems without the facilities of fast calculating-devices. Consequently, approximate solutions, either by assuming a certain function

for the shape of a deflected member or by simplifying the mechanical properties of the real material, were presented by Westergaard and Osgood⁽⁴¹⁾ and by Jezek.⁽⁴²⁾ Von Karman's work was extended by Chwalla who, in a series of papers published between 1928 and 1937,⁽⁴³⁾ presented the results of analyses of beam-columns of several different cross-sectional shapes subjected to eccentric loads. Chwalla's most significant contributions were the establishment of the foundation for the concept of column deflection curves.⁽⁴⁴⁾ Twenty years passed without significant progress beyond Chwalla's work. In the past decade, by means of electronic computers, investigations of the behavior of beam-columns have been extended to provide more extensive analyses which include the effect of residual stresses. The analysis of beam-columns has been accomplished essentially in two ways. One is to consider straight members subject to longitudinal loads with a constant eccentricity, or else to consider initially crooked members subject to axial forces at the ends. Recent developments in this type of approach include the contributions of Batterman and Johnston,⁽⁴⁵⁾ Malvick and Lee,⁽⁴⁶⁾ and Birnstiel and Michalos.⁽⁴⁷⁾ The other approach to beam-column problems is that in which the axial force is assumed to be held constant and the end

moments or transverse loads are varied. Dealing with beam-column problems in this sense permits the use of the concept of column deflection curves for the determination of the load-deformation and other needed relationships in the design of beam-columns in multi-story frames.⁽⁴⁴⁾ Extensive research on this subject has been carried out at Lehigh University, the main investigators being Ojalvo,⁽⁴⁸⁾ Levi,⁽⁴⁹⁾ Galambos,⁽⁵⁰⁾ Lay,⁽⁵¹⁾⁽⁵²⁾ and Lu.⁽⁵³⁾ Charts and tables are available and can be used directly in the design of beam-columns, with or without sway, in multi-story frames.⁽⁵⁴⁾⁽⁵⁵⁾⁽⁵⁶⁾

The previous investigations have been limited to materials with an elastic perfectly-plastic stress-strain relationship and restricted to sections with residual stresses of the cooling-after-rolling type. Also, it was assumed that during the entire loading history, no reversal of the strain of the plastified sections is permitted, and the reversal of curvatures after ultimate loads, that is, the unloading effect, is neglected. The present investigation studied the behavior of rolled and welded beam-columns made of T-1 steel. Because of the non-linearity of the stress-strain curve and the different residual stress distributions, the behavior of T-1 steel beam-columns could differ significantly from those that have previously been investigated.

A computer program was prepared to include not only the true mechanical properties and residual stresses in the section, but to include also the effects of strain reversal and unloading of moments. At present, the program covers only equal end moment cases. However, if desired, it can be modified for the cases of unequal end moments. Numerical solutions thus obtained are compared with the full scale experiments and also with the analytical solutions obtained by extrapolation procedures. (44)

5.2 Theoretical Analysis

A prerequisite for performing ultimate strength analyses of beam-columns is a knowledge of the relationship existing between the bending moment and the axial force acting on a cross section, and the resulting curvature.

The basic equations are

$$\int_A \sigma \, dA = P$$

and

$$\int_A \sigma \cdot y \cdot dA = M_i \quad (15)$$

Here, y is the distance of a finite element area dA from the bending axis and σ is the stress in this element (See Fig. 16). The stress at each element is a function of strain, and therefore the stress-strain relationship must be defined first. Generally, the monotonic stress-strain relationship can be

described well by the data obtained from a tension specimen test, and recorded or represented by a mathematical equation,

$$\sigma = f(\epsilon) \quad (16)$$

However, if the stress-strain relationships are history-dependent, Eq. 16 is invalid if the strain reverses. In this study, the incremental stress-strain relationship is given by (as shown in Fig. 38)

$$\begin{aligned} \sigma &= f(\epsilon) && \text{for } \epsilon = \epsilon^* \\ \sigma &= \sigma^* - 2f\left(\frac{\epsilon^* - \epsilon}{2}\right) && \text{for } -\epsilon^* \leq \epsilon \leq \epsilon^* \\ \sigma &= -f(\epsilon) && \text{for } \epsilon < -\epsilon^* \end{aligned} \quad (17)$$

in which σ^* and ϵ^* are the largest compressive stress and strain to which the material of any element has been subjected. The sign convention used here is plus for compression, and minus for tension.

The total strain at any point in a loaded beam-column is composed of a residual strain (ϵ_r), a constant strain over the entire cross section due to the presence of axial load (ϵ_c) and the strain due to curvature (ϵ_ϕ), that is

$$\epsilon = \epsilon_r + \epsilon_c + \epsilon_\phi \quad (18)$$

Here, $\epsilon_\phi = y \cdot \phi$ (19)

where ϕ is the curvature at the section under consideration. When the stress-strain relationship is known, it is obvious that if P is specified, and by assuming a value for the curvature ϕ , the corresponding M_i can be determined by satisfying both Equations 15. If the axial force is applied first on the member and held constant through the whole loading process, a moment-curvature relationship can be established.

The numerical procedure for the determination of the M - P - ϕ^* curve is a trial- and -error process. For a given residual stress distribution, ϵ_r is known; and for the given curvature ϕ , ϵ_ϕ is known. By assuming an ϵ_c value for the whole cross section, the total strain, and therefore the stress, at each element area is determined. The summation of total internal forces must be equal to the given P , otherwise ϵ_c must be revised until Eq. 15a is satisfied. Then, the corresponding M_i can be evaluated by means of Eq. 15b. By increasing the value of ϕ and repeating the calculation, a complete moment-curvature relationship can be determined for a specified axial force, P .

In this study, the stress-strain relationship

* M - P - ϕ denotes moment-thrust-curvature.

of the material and residual stress distribution is programmed in subroutine subprogram forms. Both the material properties and the strain reversal effect are included. A set of M-P- \emptyset curves is presented in Fig. 39. The section is a welded T-1 steel H-shape built up from flame-cut plates. The M-P- \emptyset curves are plotted for P/P_y varying from 0.5 to 0.9. It is clear that for P/P_y less than 0.7 (the proportional limit σ_p/σ_y is 0.8, and the maximum compressive residual stress σ_{rc}/σ_y is equal to 0.1), the case in which strain reversal is considered gives results which are identical to the corresponding one in which the stress-strain relationship is assumed to follow the monotonic stress-strain curve only. However, for P/P_y larger than 0.7, significant differences are shown for the two cases. Therefore, the influence of strain reversal is pronounced if the section exhibits a combination of compressive residual stresses and thrust which cause yielding immediately after thrust is applied.

In addition to the effect of strain reversal, the pattern of distribution and magnitude of residual stress also change the shape of the M-P- \emptyset curve. Figure 40 presents three types of residual stress distributions which represent the idealized residual stresses in (A) a rolled low carbon steel section, (B) a rolled heat-treated

T-1 steel section and (C) a welded built-up T-1 steel shape with flame-cut plates. If the mechanical properties are assumed to be elastic-perfectly plastic, the M-P- ϕ curves for the three types of residual stress distribution are curves (1), (2), and (4) in Fig. 40. It is noticed that there are significant differences among them in the elastic-plastic range. Generally speaking, the M-P- ϕ curve for the rolled structural carbon-steel section, which has the largest compressive residual stress ratio (σ_{rc}/σ_y) among the three, exhibits a smoother knee whereas the rolled heat-treated T-1 steel shapes, for which the compressive residual stress ratio is the smallest and thus residual stress effect the least, show a sharper knee.

Furthermore, aside from the effect of residual stresses, the mechanical properties also play an important role with the M-P- ϕ curve. Again in Fig. 40, curves (2) and (3) are the M-P- ϕ curves for sections with identical residual stress distribution but different mechanical properties; one is of the elastic perfectly-plastic type and the other is representative of T-1 steel. For material with a non-linear type of stress-strain curve, such as that of T-1 steel, the M-P- ϕ curve is lower in the knee portion than that for which an elastic perfectly-plastic stress-strain curve is assumed. However, for curvature greater than that at the end of the

Knee, curve (3) is above curve (2), due to the strain hardening property of the T-1 steel. Curves (4) and (5) are also presented in Fig. 40 for welding type residual stresses and a similar behavior is observed.

It should be noticed here that all the values shown in Fig. 40 are in non-dimensional form. For elastic perfectly-plastic materials, a yield stress and yield strain indeed exists. However, for T-1 steel, all the values are based on a nominal yield stress determined by a 0.2% offset and a yield strain that is equal to σ_y/E . Naturally, the yield strain so defined is not the strain corresponding to the yield stress.

For most practically used beam-columns, the internal moments for a large portion of the member are within the knee range of the M-P- θ curve during the loading process. Therefore, the shape of the knee has a pronounced influence on the load-deformation relationship and the ultimate strength of the beam columns. This leads to the emphasis on the basic assumptions of the residual stress distribution as well as of the shape of the stress-strain curve and of the strain reversal phenomenon in the case when thrust is applied first and yielding occurs before the application of moment. The assumption that thrust is applied before the moment corresponds approximately to the actual behavior of

multi-story frames in which most of the axial forces in the columns are due to the dead load, and moments are due to the live load.

In the general design practice for planar structures it is often sufficient to know the ultimate strength of beam-columns. However, in plastic design, especially for multi-story buildings, it is necessary to determine the maximum moment of a joint of a subassemblage.⁽⁴⁴⁾ Therefore, not only the ultimate moment capacity but also the complete load-deformation curve of each individual beam-column must be known. The most practical and useful way of presenting the load-deflection relationship of a beam-column is the end moment vs. end rotation curve. A numerical method was used to determine the end moment vs. end rotation relationship of a beam-column. The procedure for numerical computation is outlined as follows:⁽⁵⁷⁾

1. Subdivide the length of the member which is under a constant thrust into n integration stations as shown in Fig. 41a. The distance between any two adjacent stations on the deflected member is λ ($=L/(n-1)$) (approximately equal to the arc length within the segment).
2. Assume that the segment in each sublength is a circular arc.

3. Assume an end rotation and an end moment at station 1.

4. Determine the curvature ϕ_1 at station 1 from the M-P- ϕ curve. (If present M_1 is less than the previous maximum M_1 , the unloading M-P- ϕ curve is to apply).

5. Deflection at station 2,

$$v_2 = v \sin (\theta_1 - \frac{1}{2} \phi_1 \cdot \lambda)$$

the slope at station 2, $\theta_2 = \theta_1 - \phi_1 \cdot \lambda$

6. The moment at station 2 is $M_2 = M_1 + Pv_2 -$

$$\frac{M_1 - M_n}{L} \cdot \cos (\theta_1 - \frac{1}{2} \phi_1 \cdot \lambda)$$

7. Determine ϕ_2 from the M-P- ϕ curve, and carry on the integration in the same manner as from steps (4) to (6). That is,

$$v_i = \lambda \cdot \sin (\theta_{i-1} - \frac{1}{2} \phi_{i-1} \cdot \lambda) + v_{i-1}$$

$$\theta_i = \theta_{i-1} - \phi_{i-1} \cdot \lambda$$

$$M_i = M_1 + Pv_i - \frac{M_1 - M_n}{L} \cdot \lambda \cdot \sum_2^{i-1} \cos (\theta_{i-1} - \frac{1}{2} \phi_{i-1} \cdot \lambda)$$

8. If the assumed M_1 and θ_1 is correct, then at the nth station, v_n should be zero, or a given value, if sidesway is permitted. Otherwise, decrease M_1 if v_n is negative, increase M_1 if v_n is positive, and repeat step (3) to (7) until v_n is within a certain allowable error.

9. Increase θ_1 and increase or decrease M_1 a certain amount and repeat the whole process as from step (1) to step (8) until the complete M- θ curve is obtained.

The numerical integration procedure suggested above is essentially the same as that used in the development of CDC*'s. The point of difference is the fact that the integration is carried out on the deflected shape of the member for fixed stations. Thus the history of every station can be recorded, and the unloading effect can be taken into account.

The interaction curves between P/P_y and M/M_p for equal end moment conditions (symmetrical bending) are shown in Fig. 42 for slenderness ratios equal to 20, 40, and 60. Beam-columns of rolled heat-treated shapes show higher ultimate strength than those of welded built-up shapes. This can be understood as the consequence of the smaller effect of residual stresses on the M-P- θ curves for rolled shapes than on those for welded shapes.

An approximate solution for the case L/r equal to 20, which is obtained by extrapolating from the results

*CDC column deflection curve

obtained from A36 steel beam-columns, is also presented in Fig. 42. For beam-columns made of steel other than A36, the slenderness ratio must be adjusted according to the following formula. (44)

$$\left(\frac{L}{r_x}\right)_{\text{equivalent}} = \left(\frac{L}{r_x}\right) \sigma_y \sqrt{\frac{\sigma_y}{36}}$$

The interaction curve determined from this extrapolation procedure is also presented in Fig. 42, for the case $L/r = 20$. It is shown that the approximate solution is slightly lower than the corresponding "exact solution".

5.3 Experimental Investigations

An experimental investigation of the behavior of beam-columns made of T-1 steel was carried out. (57) The program consisted of tests of two full scale beam-columns, one a rolled 8WF40 shape and the other an 11H71 shape. The members were tested in an "as-delivered" condition; no attempt was made to eliminate rolling or welding residual stresses by annealing. The magnitude and distribution of the residual stresses were determined by actual measurements, (58) and was found to be close to the idealized residual stress distribution for H-shapes, as shown in Fig. 40. Therefore, this idealized residual stress distribution was used for the determination of beam-column strength. The beam-columns

were tested under equal end moment (single curvature) conditions.

The procedure for testing beam-columns has been described in detail elsewhere,⁽⁵⁹⁾⁽⁶⁰⁾ and only a brief outline is given here for review and completeness.

The general set-up of the beam-column specimen is shown in Fig. 43a. The horizontal moment arms are rigidly welded to the end of the column. The sizes of the beams are comparatively larger than that of the column so that the beam sections remain in the elastic range during the whole loading process. Pinned-end fixtures were utilized to ensure that there are no end moments other than those imposed by the moment arms, applied at the column ends. In Fig. 43a, it can be seen that the axial force in the column is made up of the direct force applied by the testing machine, P and the jack force, F . To simulate the situation existing in the lower stories of a multi-story frame and to be in accord with the assumptions for the theoretical analysis, the tests were performed with the axial load held constant. Thus at each increment of load or deformation, the direct force, P , was adjusted so that the total force in the column remained at $0.55 P_y$, where P_y is the yield load of the column.

The direct axial force, P , was first applied on the column; the beam-to-column joints were rotated by applying the jack force to the ends of the moment arms. The column was therefore forced into a symmetrical curvature mode of deformation. In order to preclude any deformation out of the plane perpendicular to the strong axis, the column was braced at the third points by two sets of lateral braces. The lateral braces used were designed for the laboratory testing of large structures permitted to sway.⁽⁶¹⁾ In the early stages of loading, that is, in the elastic range, approximately equal increments of moment were applied to the column. In the inelastic range, comparatively larger deformations occur for the same moment of moment increment, therefore, end rotations instead of moment are used as a basis for loading in order to obtain a complete load-deformation curve with approximately evenly distributed test points.

At each increment of load or end rotation, the end rotations were measured by level bars (see Fig. 43b). The mid-height deflection, in the bending plane as well as out-of-plane, of the column was also measured by mechanical dial gages. SR-4 gages were mounted at the beam and column junctions as well as at several other locations along the column, as shown in Fig. 43b, to determine strain distribution

in the column or to serve as a means for checking moments. Figure 44 shows the photographs taken at the beginning and end of the test. The occurrence of local buckling of the compressed flange was determined by measuring the out-of-plane deformations of the flanges at five locations in the vicinity of mid-height of the beam-column with an inside micrometer.

5.4 Comparison Between the Results of Theoretical Analysis and Tests

The results of the tests can be presented in the form of end moment vs. end-rotation curves as shown in Figs. 45 and 46. In Fig. 45 the M- θ curve for the 8WF40 T-1 steel beam-column is shown. Figure 46 contains the M- θ curve for the 11H71 welded T-1 steel beam-column. The moments indicated by open points represent the total applied moment determined from the hydraulic jack load. The length of the moment arm is the distance from the centerline of the column to the center of the rod to which the hydraulic jack is connected. The end moments were also checked by the reading of the dynamometer which is inserted in series with the jack and by four sets of SR-4 strain gages which were affixed to the loading beam, near its junction with the column. The difference between the moment readings by these three means are shown in Fig. 47. It is apparent that they are rather consistent.

The length used to compute slenderness ratios of the columns were the distances between the points of intersection of the centerlines of the column and loading beams. For both beam-columns, the slenderness ratio, L/r , is 40. Because of the stiffness of the joint, the rigidity of the beam-column near the ends is greater than that of the remainder of the column. Therefore, the actual effective L/r is slightly less than that measured. Comparison of the experimental results with the theoretical reveals that the testing points are above the theoretically obtained $M-\theta$ curve (Figs. 45 and 46). This discrepancy is due in part to the fact that the actual slenderness ratio has been reduced somewhat by the installation of joint stiffeners and to the fact that the actual stress-strain relationship determined from tension specimen tests shows a slightly higher proportional limit than that of the average typical stress-strain curve on which the theoretical analysis was based. The tests are compared also to the theory in a plot of M_u/M_{pc} vs. L/r_x as shown in Fig. 48. The difference between theory and test is approximately 5% for both rolled and welded built-up shapes. From Fig. 48 it can also be observed that the difference of ultimate strength for rolled welded shapes vanishes for low slenderness ratios. This is apparently because of the fact that the internal moments in the greater portion of the member are

within the strain hardening region at ultimate load, and hence the residual stress effect is insignificant. In Figs. 45 and 46, the local buckling points are shown as cross marks. It is observed that there is good correlation between the local buckling points determined theoretically and experimentally. Also, it is interesting to note that for welded built-up shapes the occurrence of local buckling is at a comparatively larger end rotation than that for rolled heat-treated shapes. Apparently, this is because of the higher tensile residual stresses in the welded shape which increase the value of the critical strain necessary to cause total yielding of the flange. This indicates that welding residual stresses can actually increase the rotation capacity of the beam-column, if the termination of rotation capacity is taken as the local buckling point.

Furthermore, the initiation of local buckling does not seem to reduce to strength of beam-columns dramatically. The $M-\theta$ curves still follow their original path for some distance until pronounced out-of-plane deflections of the flanges are observed. If further study on the post local buckling behavior confirms this in the future, the use of beam-columns may be extended beyond the local buckling point.

6. SUMMARY AND CONCLUSIONS

This is a summary report on a study of the structural capabilities of T-1 steel. The mechanical properties of T-1 steel, and the magnitude and distribution of residual stresses in rolled heat-treated and welded plates and shapes were investigated, and applied to theoretical and experimental studies of local buckling, and of the buckling of columns and beam-columns.

Even though emphasis has been given to members of T-1 steel, the analytical methods developed in this study can be applied to columns or beam-columns of other material as well, as long as the stress-strain relationship of the material and the residual stresses in the section are defined.

The reports prepared in the course of this study are listed in the Appendix.

The following statements summarize the results obtained from the investigation:

1. The stress-strain relationship of T-1 steel can be closely simulated by three equations; a fifth order polynomial equation for the transition range and two linear equations for

the elastic and strain hardening range, respectively. The particular characteristic of this stress-strain relationship is that no obvious yield plateau is observed. Instead, strain hardening occurs immediately after the ending of the transition range, continues until the tensile strength is reached, and then starts to unload.*

2. The typical pattern and magnitude of residual stresses in rolled T-1 shapes can be represented by a triangular distribution with maximum compressive and tensile residual stress approximately equal to 5% of the yield stress. For welded shapes, the tensile residual stress at the weld is approximately equal to the yield stress, and the compressive residual stresses are about 10% of the yield stress; for flame-cut plates, tensile residual stresses of about 30% of the yield stress exist at the flange tips. The patterns of residual stress distribution are of a trapezoidal shape.
3. Geometry has the most pronounced effect on the magnitude and distribution of residual stress, as compared to such factors as weld size,

*Recent study conducted by the U.S. Steel Corporation indicates that two values of strain hardening modulus exist in the stress-strain curve—one, as shown in this report, immediately after yielding and another larger one between $\frac{\epsilon}{\epsilon_y}$ equal to 5 and 8.

- number of passes, electrode and welding method.
4. The shape of the stress-strain curve has a dominant influence on the final column strength curve. To assume the stress-strain relationship of T-1 steel to be elastic perfectly-plastic will overestimate column strength in the medium slenderness region or underestimate the strength of short columns.
 5. The reduction in buckling strength due to the existence of residual stress is less pronounced in columns of T-1 steel as compared with columns of structural carbon and low alloy high-strength steels.
 6. The comparison with test results and theoretical results shows that the column strengths of constructional alloy steel members can be predicted by the tangent modulus loads.
 7. It is shown experimentally that welded H- or box- columns and rolled wide flange columns are stronger than their counterparts of lower yield strength steels, when compared on a non-dimensional basis.
 8. The results of both experiments and theoretical analysis for the column strength of T-1 steel

shapes show that the CRC basic column strength curve is a good approximation for strength.

9. In the investigation of local buckling of plates, the comparison between the theoretical results and the test results; for elastic-plastic buckling, the theoretical results based on the total strain theory gives good correlation with the experimental results, but the results based on the incremental theory predicts a much higher critical stress.
10. Comparison of experiments on welded square tubes shows that the tubes of T-1 steel are stronger for local buckling than those of A7 steel when compared on a non-dimensional basis.
11. The square tubes buckled in the elastic range, showed significant post buckling strength, while the tubes buckled in the elastic-plastic range, had a relatively small reserve of post-buckling strength.
12. The effect of residual stresses on the elastic-plastic buckling depends greatly on the width-thickness ratio of the plates. Theoretical and experimental results indicate that the (1963) AISC Specification for critical width-thickness ratio may be extended to T-1 steel

shapes, welded or rolled.

13. The mechanical properties of the material, pattern and magnitude of residual stresses and the strain reversal effect, all are important in the final shape of M-P- θ curves which in turn is the sole basis for the determination of the load-deformation characteristics of beam-columns.
14. For beam-columns, the strain reversal effect is more pronounced for non-linear materials than for linear materials if other conditions, that is, residual stresses and thrust, are identical.
15. Two full scale beam-column tests, one rolled 8WF40 shape and the other an 11H71 welded shape were conducted. A comparison between the theoretical curves and the corresponding experimental M- θ curves has shown that the theory can predict not only the ultimate strength but also the complete history of a beam-column.
16. Comparing the direct integration solutions to the extrapolation solutions obtained from previous investigations in A36 steel shapes,

it is shown that for T-1 steel shapes, both rolled and welded built-up shapes, the direct integration solutions provide a higher ultimate strength. Hence, the extrapolation procedure may provide an approximate but conservative estimate of the strength of T-1 steel shapes.

7. NOMENCLATURE

A	Area of cross section
b	Width of plate element - subscripts t and w refer to flange and web, respectively
d	Depth of section
E	Modulus of elasticity
E_{st}	Strain-hardening modulus
E_t	Tangent modulus
f	a function
I	Moment of inertia - subscripts x and y refer to the x and y axes (strong and weak axes), respectively
I_m	Effective moment of inertia ($= \frac{E_t}{E} y^2 dA$) subscripts x and y refer to the x and y axes, respectively
L	Column effective length, length of a beam-column
M	Bending moment - subscripts R and L refer to moments at the right and left ends, respectively, of a beam-column, i refers to internal moment
M_p	Plastic moment
M_{pc}	Reduced plastic moment
M_u	Ultimate moment
P	Axial load
P_{cr}	Buckling (critical) load
P_y	Axial yield load in a column

r	Radius of gyration - subscripts x and y refer to strong and weak axes radii
t	Thickness of plate element - subscripts t and w refer to flange and web, respectively
u, v, w	Displacement in the x , y , and z directions, respectively
x, y, z	Coordinate axes, coordinates of the point with respect to x , y , and z axes
ϵ	Strain
ϵ_c	Strain due to axial load
ϵ_{cr}	Critical strain
ϵ_p	Strain at proportional limit
ϵ_r	Residual Strain
ϵ_{rc}	Maximum compressive residual strain
ϵ_{rt}	Maximum tensile residual strain
ϵ_{st}	Strain at start of strain hardening
ϵ_t	Total strain
ϵ_y	Yield strain ($= \sigma_y/E$)
ϵ_θ	Strain due to curvature
ϵ^*	Largest strain any element area experienced
θ	End rotation of a member
λ	Slenderness function, distance between two adjacent integration stations
Σ	Summation
θ	Curvature
θ_p	Curvature at M_p

ϕ_{pc}	Curvature at M_{pc}
σ	Stress
σ_{cr}	Critical stress
σ_p	Stress at proportional limit
σ_r	Residual stress
σ_{rc}	Maximum compressive residual stress
σ_{rt}	Maximum tensile residual stress
σ_y	Yield stress (determined by 0.2% offset method for non-linear stress-strain relationship)
σ^*	Largest stress any element area experienced
σ_1	Secant yield stress
ν	poisson's ratio

8. ACKNOWLEDGEMENTS

The investigation was conducted at Fritz Engineering Laboratory, Department of Civil Engineering, Lehigh University, Bethlehem, Pennsylvania. The U.S. Steel Corporation sponsored the study, and appreciation is due to Charles G. Schilling of that company who provided much information and gave many valuable comments.

Column Research Council Task Group 1, under the chairmanship of John A. Gilligan, provided valuable guidance. Appreciation is due to the author's colleagues, especially to Y. Ueda, F. Nishino, E. Odar and K. Okuto, who assisted in various parts of the study. Lynn S. Beedle, Director of Fritz Laboratory, provided encouragement and advice throughout the study.

9. APPENDIX: REPORTS RESULTING FROM THIS STUDY

1. Ueda, Y.
ELASTIC, ELASTIC-PLASTIC AND PLASTIC BUCKLING OF PLATES WITH RESIDUAL STRESSES, Ph.D. Dissertation, Lehigh University, September, 1962. (F.L. Report No. 290.1)
2. Nishino, F.
BUCKLING STRENGTH OF COLUMNS AND THEIR COMPONENT PLATES, Ph.D. Dissertation, Lehigh University, September, 1964. (F.L. Report No. 290.10)
3. Nishino, F. and Tall, L.
NUMERICAL METHOD FOR COMPUTING COLUMN CURVES, Fritz Laboratory Report No. 290.6, December, 1966.
4. Nishino, F. and Tall, L.
RESIDUAL STRESS AND LOCAL BUCKLING STRENGTH OF STEEL COLUMNS, Fritz Laboratory Report No. 290.11, January, 1967.
5. Odar, E., Nishino, F., and Tall, L.
RESIDUAL STRESSES IN "T-1" CONSTRUCTIONAL ALLOY STEEL PLATES, Welding Research Council Bulletin No. 121, April, 1967. (F.L. Report No. 290.4)
6. Odar, E., Nishino, F., and Tall, L.
RESIDUAL STRESSES IN WELDED BUILT-UP "T-1" SHAPES, Welding Research Council Bulletin No. 121, April 1967. (F.L. Report No. 290.5)
7. Odar, E., Nishino, F., and Tall, L.
RESIDUAL STRESSES IN ROLLED HEAT-TREATED "T-1" SHAPES, Welding Research Council Bulletin No. 121, April, 1967. (F.L. Report No. 290.5)
8. Okuto, K.
A PILOT EXPERIMENTAL INVESTIGATION OF A514 STEEL BEAM-COLUMNS, M.S. Thesis, July, 1967 (F.L. Report No. 290.13)

9. Nishino, F., Ueda, Y. and Tall, L.
EXPERIMENTAL INVESTIGATION OF THE BUCKLING
OF PLATES WITH RESIDUAL STRESSES, ASTM Special
Technical Publication No. 419, August 1967
(F.L. Report No. 290.3)
10. Ueda, Y. and Tall, L.
BUCKLING OF PLATES WITH RESIDUAL STRESSES,
Vol. 27, IABSE Publications, December, 1967,
Zurich. (F.L. Report No. 290.2)
11. Yu, C. K., and Tall, L.
A PILOT STUDY ON THE STRENGTH OF 5Ni-Cr-Mo-V
STEEL COLUMNS, Experimental Mechanics, Vol. 8
No. 1, January, 1968. (F.L. Report No. 290.12)
12. Yu, C. K.
INELASTIC COLUMNS WITH RESIDUAL STRESSES,
Ph.D. Dissertation, Lehigh University, March,
1968, (F.L. Report No. 290.14)
13. Yu, C. K., and Tall, L.
A514 STEEL BEAM COLUMNS, Fritz Laboratory Report
No. 290.15, October, 1968. To be published.
14. Yu, C. K. and Tall, L.
WELDED AND ROLLED HEAT-TREATED "T-1" STEEL
COLUMNS - A SUMMARY, Fritz Laboratory Report
No. 290.16, June 1969. To be published.
15. Nishino, F. and Tall, L.
RESIDUAL STRESSES AND STRENGTH OF THIN-WALLED
COLUMNS, Fritz Laboratory Report No. 290.7,
in preparation.
16. Nishino, F. and Tall, L.
EXPERIMENTAL INVESTIGATION OF THE STRENGTH OF
"T-1" STEEL COLUMNS, Fritz Laboratory Report
No. 290.9, June 1969.
17. Tall, L.
THE STRENGTH OF WELDED A514 STEEL STRUCTURAL
COMPONENTS, Fritz Laboratory Report No. 290.17,
December, 1968. Published in the International
Institute of Welding, Annual Meeting, July 1969.
18. Nishino, F., Tall, L., and Okumura, T.
RESIDUAL STRESS AND TORSIONAL BUCKLING STRENGTH
OF H AND CRUCIFORM COLUMNS, Transactions, Japan
Soc. Civil Engrs., No. 160, December 1968.

19. Yu, C. K., and Tall, L.
SIGNIFICANCE AND APPLICATION OF STUB COLUMN
TEST RESULTS, Fritz Laboratory Report No.
290.18, June 1969

10. TABLES

TABLE 1 TENSION SPECIMEN TEST RESULTS
(A514 STEEL PLATES OR SHAPES)

Shape	Tension Specimen No.	Proportional Limit (σ_p/σ_y)	Static Yield Stress, σ_y (ksi) (0.2% offset)	Modulus of Elasticity E (ksi)	Strain Hardening Modulus E_{st} (ksi)	Ultimate Stress σ_u	Reduction of Area (%)	Elongation in Gage Length*** (%)
8WF40	AW	0.84	107	28,500	172	119	46	11.6
	AF-1	0.88	109	29,000	197	123	55	14.6
	AF-2	0.78	113	27,700	122	126	58	13.8
	AF-3	0.86	111	29,000	193	125	58	15.0
	AF-4	0.85	111	30,000	108	---	56	14.6
	EW	0.86	125	29,500	172	136	55	10.7
	EF-1	0.76	129	27,000	110	139	57	11.5
	EF-2	0.79	127	29,100	150	137	57	12.1
	EF-3	0.75	130	28,100	120	140	53	11.1
	EF-4	0.90	131	28,900	155	---	---	---
11H71	JF-32	0.81	113	30,200	197	124	46	10.0
	JF-31	0.85	113	28,400	177	125	40	9.2
	JW-20	0.78	104	29,400	169	117	52	12.8
	JF-11	0.90	115	29,200	106	128	42	9.5
	JF-12	0.86	115	27,900	116	125	46	11.0
8WF17	AF-1	0.78	113	27,000	154	125	40	9.0
	AF-2	0.83	111	27,200	134	122	54	9.0
	AW-3	0.70	109	28,500	140	119	48	8.3
8WF31	BW-2	0.84	111	29,600	75	121	--	---
	BF-3	0.67	114	31,200	70	123	--	---
	BF-4	0.65	113	30,200	81	122	--	---
	BW-5	0.87	110	28,400	95	120	--	---
	BF-6	0.83	112	28,900	125	123	--	---
	12WF36	DF-11	0.93	106	27,400	72	119	--
DF-12		0.88	113	30,200	60	125	--	---
DW-13		0.77	111	28,300	55	123	--	---
12WF45	EF-11	0.88	115	28,000	87	125	--	---
	EF-12	0.77	116	29,800	70	128	--	11.1
12WF120	FF-1	0.84	105	29,600	258	116	--	---
	FF-2	0.76	88	29,300	260	105	--	---
1/2" Plates	T-7-1	0.91	115	29,400	102	125	43	10.0
	T-7-2	0.87	113	28,100	86	123	41	10.5
	T-7-3	0.87	115	27,300	128	126	39	10.0
	T-7-4	0.71	114	28,800	126	125	--	10.5
	T-11-1	0.84	112	28,100	131	123	40	11.0
	T-11-5	1.00	113	27,300	106	125	39	10.0
	T-5-1	1.00	113	28,500	70	124	50	9.7
	T-5-2	0.76	112	29,700	114	123	52	10.0
	T-5-4	0.80	112	29,800	89	122	--	---
	T-5-7	0.90	113	29,300	83	124	44	---
	T-5-10	0.68	112	30,100	127	123	--	---
	T-2-8	0.87	111	27,400	---	126	--	---
	T-2-8A	0.96	111	30,600	108	122	--	---
	T-2-6A	0.90	111	26,900	101	120	--	---
	T-2-6B	0.92	110	27,500	129	120	--	---
	T-2-6C	0.96	110	27,300	127	120	--	---
1" Plates	T-4-1A	0.64	105	31,000	---	113	--	---
	T-4-1B	0.75	113	30,400	200	119	--	---
	T-4-1C	0.74	102	30,500	---	110	--	---
	T-4-6A	---	112	31,800	198	122	--	---
	T-4-6C	0.78	111	31,900	198	121	--	---
	T-4-3A	0.99	111	32,000	150	121	--	---
	T-4-5A	0.84	111	26,000	200	120	--	---
	T-4-8A	0.76	110	29,200	---	121	--	---
	T-4-8B	0.86	110	31,200	241	121	--	---
T-4-8C	0.80	110	30,400	197	121	--	---	
1/2" Plates	T-10-1	1.00	118	28,200	111	129	42	-9.0
	T-10-3	1.00	117	28,000	100	129	35	8.7
Average		0.82	112	28,900	144	123	48	10.8

* Second letter, "W" or "F", denotes specimen from web or flange coupon, respectively.

** The values of E should be regarded as indicative only since they were measured directly from the autographically recorded curve.

*** Gage length was 8 inches.

TABLE 2 SUMMARY OF COMPRESSION SPECIMEN TEST RESULTS

Specimen No.	Source	Area (in ²)	Static Yield Stress (ksi)	Modulus of Elasticity (ksi)	Strain Hardening Modulus (ksi)
C-1		0.3725	108	30,800	300
C-2	1/2" plates	0.3725	110	29,700	280
C-3	(as-delivered)	0.3724	110	31,200	310
C-4		0.3725	110	29,700	300
C-5		0.5991	110	29,700	320
C-6		0.5990	122	30,000	350
C-7	3/4" plates	0.5991	121	31,100	360
C-8	(as-delivered)	0.5990	122	31,600	350

TABLE 3 PROGRAM OF RESIDUAL STRESS MEASUREMENTS ON PLATES*

Center Welded Plates					WELDED PLATES**					UNWELDED PLATES	
Plate No.	Geometry (in.)	Type of Weld		Weld Size (in.)	Plate No.	Geometry (in.)	Type of Weld		Weld Size (in.)	Plate No.	Geometry
		Aut.	Man.				Aut.	Man.			
T-1-2	4 x 1/4	-	X	1/8	T-1-4	4 x 1/4	-	X	1/8	T-1	4 x 1/4
-6	4 x 1/4	-	X	1/8	-7	4 x 1/4	-	X	1/8	T-2	6 x 1/2
T-2-2	6 x 1/4	-	X	1/4	T-1-6	6 x 1/4	-	X	1/4	-	-
-4	6 x 1/4	X	-	1/4	-8	6 x 1/4	X	-	1/4	T-4	8 x 11
T-3	8 x 1	-	X	1/4	-	-	-	-	-	T-5	12 x 1/2
T-4-2	8 x 1	-	X	1/4	T-4-6	8 x 1	-	X	1/4	-	-
-4	8 x 1	X	-	1/4	-8	8 x 1	X	-	1/4	-	-
T-5-2	12 x 1/2	X	-	1/4	T-5-6	12 x 1/2	X	-	1/2	-	-
-4	12 x 1/2	X	-	1/2	-8	12 x 1/2	X	-	2 x 1/4	-	-
-5	12 x 1/2	X	-	1/2	-10	12 x 1/2	X	-	2 x 1/2	-	-
				(L100)							
T-6-2	12 x 1	-	X	1/2	T-6-14	12 x 1	-	X	1/2	T-6	12 x 1
-4	12 x 1	X	-	1/2	-16	12 x 1	X	-	1/2	-	-
-6	12 x 1	-	X	1	-18	12 x 1	-	X	1	-	-
-8	12 x 1	X	-	1	-20	12 x 1	X	-	1	-	-
-10	12 x 1	-	2VX	2V-1	-	-	-	-	-	-	-
-12	12 x 1	2VX	-	2V-1	-	-	-	-	-	-	-
T-7-2	16 x 1/2	X	-	1/2	T-7-4	16 x 1/2	X	-	1/2	T-7	16 x 1/2
-	-	-	-	-	-6	16 x 1/2	X	-	2 x 1/2	-	-
-	-	-	-	-	T-8-2	20 x 3/8	X	-	3/8	T-8	20 x 3/8
-	-	-	-	-	-4	20 x 3/8	X	-	2 x 3/8	-	-
T-9-2	24 x 1	X	-	1/2	T-9-4	24 x 1	X	-	1/2	T-9	24 x 1
-	-	-	-	-	-6	24 x 1	X	1	2 x 1/2	-	-

*All plates were cut from wide rolled plates by flame-cutting.

**All center welded plates are welded with single Vee groove, unless otherwise specified

2V - Double Vee Groove

X means tests being made.

TABLE 3 PROGRAM OF RESIDUAL STRESS MEASUREMENTS ON PLATES*

Plate No.	Pass	Volts	Amps	Electrode Travel (in/min)	Electrode Melt-Off (in/min)	Electrode Type	Type of Weld	Place of Weld	Flux	Beads
T-1-2	1	18	170	5.8	10.5	E7018(1/8"D)	M	C	-	
T-1-4	1	18	125	24.0	9.55	"	M	E	-	1/8"
T-1-6	1	18	170	7.0	10.4	"	M	C	-	As T-1-2
T-1-7	1	18	125	24.0	9.55	"	M	E	-	As T-1-4
T-2-2	1	20-22	130	8.0	9.9	"	M	C	-	
	2	20-22	210	8.8	8.5	E7018(3/16"D)	M	C	-	1/4"
T-2-4	1	32	350	12.0	120.0	L70(W)5/64"	A	C	L840	
T-2-6	1	22	160	9.2	10.4	E7018(5/32")	M	E	-	1/8"
	2	22	160	9.3	10.6	"	M	E	-	
T-2-8	1	28	300	30.0	111.1	L70(W)5/64"	A	E	L840	1/8"
	2	28	300	30.0	111.1	"	A	E	"	
T-3	1	20-22	130	6.6	10.2	E7018(1/8"D)	M	C	-	
	2	20-22	210	8.8	8.6	E7018(3/15"D)	M	C	-	1/4"
T-4-2	1	20-22	130	6.8	9.8	E7018(1/8"D)	M	C	-	
	2	20-22	210	9.2	8.6	E7018(E/16"D)	M	C	-	1/4"
T-4-4	1	32	350	15.0	120.0	L70(W)5/64"	A	C	L840	
T-4-6	1	22	160	9.0	10.4	E7018(1/8"D)	M	E	-	3/16"
	2	22	160	8.0	9.8	E7018(1/8"D)	M	E	-	
T-4-8	1	28	300	30.0	111.1	L70(W)5/64"	A	E	L840	1/8"
	2	28	300	30.0	111.1	"	"	"	"	
T-5-2	1	32	350	12.0	120.0	L70(W)5/64"	A	C	L840	
T-5-4	Tack Welds	20-22	130	4.9	9.8	E11018(1/8"D)	M	C	-	
	1	32	350	12.0	120.0	L70(W)5/64"	A	C	L840	3/8"
	2	32	350	12.0	120.0	"	A	C	L840	
T-5-5	Tack Welds	20-22	130	5.8	8.7	E11018(1/8"D)	M	C	-	
	1	32	400	18.0	120.0	L100(W)1/8"D	A	C	709-5	3/8"
	2	32	500	18.0	120.0	"	A	C	709-5	
T-5-6	1,2	30	350	24.0	44.4	L100(W)1/8"	A	E	709	1/4"
	3,4	30	350	24.0	44.4	L100(W)1/8"	A	E	709	1/4"
T-5-8	1,2	28	300	30.0	111.1	L70(W)5/64"	A	E	L840	1/8"
	3,4	28	300	30.0	111.1	L70(W)5/64"	A	E	L840	1/8"
T-5-10	1,2	28	300	21.0	111.1	L70(W)5/64"	A	E	L840	1/4"
	3,4	28	300	21.0	111.1	L70(W)5/64"	A	E	L840	1/4"
T-6-2	1	18	140	6.0	11.0	E7018(1/8"D)	M	C	-	
	2	18	170	6.0	10.3	"	M	C	-	
	3	20	210	4.6	9.4	"	M	C	-	
	4	20	210	5.6	9.7	"	M	C	-	
	5	20	210	7.5	10.5	"	M	C	-	
	6	20	210	7.0	10.1	E7018(1/8"D)	M	C	-	1/2"

Table 4—Records of Welding (Continued)

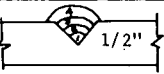
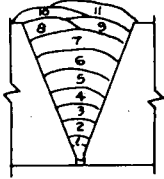
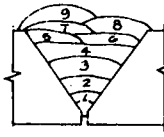
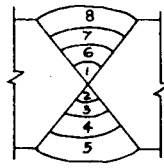
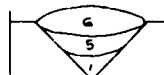




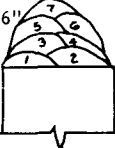

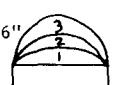





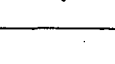


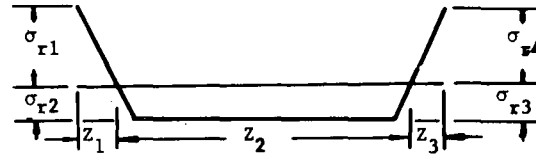
Plate No.	Pass	Volts	Amps	Electrode Travel (in/min)	Electrode Melt-Off (in/min)	Electrode Type	Type of Weld	Place of Weld	Flux	Beads
T-6-4	1,2	32	375	15.0	150.9	L70(W)5/64"	A	C	L840	
	3,4	32	375	15.0	150.9	L70(W)5/64"	A	C	L840	
T-6-6	Tack Welds	22	140	-	-	E7018(1/8")	M	C		
	1	22	140	5.3	9.7	E7018(1/8")	M	C		
	2	20	170	4.9	10.7	E7018(5/32")	M	C		
	3	20	210	4.6	9.7	E7018(3/16")	M	C		
	4	20	210	7.0	9.3	"	M	C		
	5	20	210	7.3	9.1	"	M	C		
	6	20	210	6.7	9.3	"	M	C		
	7	20	210	7.3	9.8	"	M	C		
	8	20	210	6.1	9.6	"	M	C		
	9	20	210	8.0	9.5	"	M	C		
	10	20	210	6.8	9.9	"	M	C		
T-6-8	1,2,3	32	400	16.0	179.8	L70(W)5/64"	A	C	L840	
	4,5,6	31	375	12.0	152.6	L70(W)5/64"	A	C	L840	
	7,8,9	31	375	12.0	152.6	L70(W)5/64"	A	C	L840	
T-6-10	Tack Welds	22	140	-	-	E7018(1/8")	M	C	-	
	Tack Welds	20	140	-	-	E7018(1/8")	M	2V-C		
	1	20	140	6.4	10.3	E7018(1/8")	M	2V-C		
	2	20	140	6.2	10.7	E7018(1/8")	M	2V-C		
	3	20	170	6.4	10.7	E7018(5/32")	M	2V-C		
	4	18	210	5.9	10.4	E7018(3/16")	M	2V-C		
	5	18	210	5.9	10.3	E7018(3/15")	M	2V-C	-	
	6	18	170	5.7	10.6	E7018(5/32")	M	2V-C	-	
	7	18	210	6.1	9.8	E7018(3/16")	M	2V-C	-	
T-6-12	Tack Welds	18	140	-	-	E7018(1/8")	M	-	-	
	1	32	325	18.0	130.6	L70(W)5/64"	A	2V-C	L840	
	2,3,4	32	400	16.0	179.8	L70(W)5/64"	A	2V-C	L840	
	5,6	32	400	16.0	179.8	L70(W)5/64"	A	2V-C	L840	

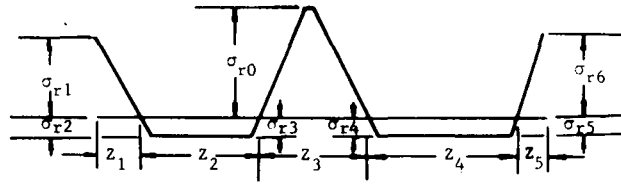
Table 4—Records of Welding (Continued)

Plate No.	Pass	Volts	Amps	Electrode Travel (in/min)	Electrode Melt-Off (in/min)	Electrode Type	Type of Weld	Place of Weld	Flux	Beads
T-6-14	1	22	160	3.1	9.6	E7018(5/32")	M	E	-	1/4" 
	2	22	160	8.1	10.3	E7018(5/32")	M	E	-	
T-6-16	1,2,3	30	300	20.0	105.8	L70(W)5/64"	A	E	L840	3/16" 
T-6-18	1	22	160	5.0	10.3	E7018(5/32")	M	E	-	7/16" 
	2	22	160	4.8	10.0	E7018(5/32")	M	E	-	
	3	22	160	5.8	10.3	"	M	E	-	
	4	22	160	5.8	10.3	"	M	E	-	
	5	22	160	6.2	10.8	"	M	E	-	
	6	22	160	6.2	10.8	"	M	E	-	
	7	22	160	4.6	10.4	E7018(5/32")	M	E	-	
T-6-20	1 to 11	30	300	20.0	105.8	L70(W)5/64"	A	E	L840	
T-7-2	1	32	375	18.0	152.6	L70(W)5/64"	A	C	L840	
	2,3,4	32	375	15.0	152.6	L70(W)5/64"	A	C	L840	
	Tack Welds	22	140	-	-	E7018(1/8")	M	C	-	
T-7-4	1,2,3	32	300	26.0	106.0	L70 5/64"	A	E	L840	3/16" 
T-7-6	1,2,3	32	300	26.0	106.0	L70 5/64"	A	E	L840	7/32" 
	4,5,6	32	300	26.0	106.0	L70 5/64"	A	E	L840	1/4" 
T-8-2	1,2	30	300	36.0	94.7	L70 5/64"	A	E	L840	1/8" 
T-8-4	1,2	30	300	36.0	94.7	L70(W)5/64"	A	E	L840	5/32" 
	3,4	30	300	36.0	94.7	L70(W)4/64"	A	E	L840	1/8" 
T-9-2	1,2	32	375	15.0	150.9	L70(W)5/64"	A	E	L840	
	3,4,5	32	375	15.0	150.9	L70(W)5/64"	A	E	L840	
T-9-4	1	30	300	32.0	94.7	L70(W)5/64"	A	E	L840	7/32" 
	2	30	300	28.0	94.7	L70(W)5/64"	A	E	L840	
	3	30	300	26.0	94.7	L70(W)5/64"	A	E	L840	
T-9-6	1,2,3	30	300	26.0	94.7	L70(W)5/64"	A	E	L840	
	4,5,6	30	300	26.0	94.7	L70(W)5/64"	A	E	L840	



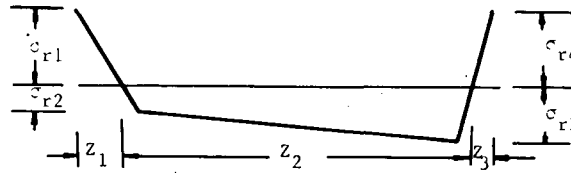
Test No.	Plate No.	Plate Size (in.)	Residual Stress in ksi				Distances in in.		
			σ_{r1}	σ_{r2}	σ_{r3}	σ_{r4}	z_1	z_2	z_3
T-1	-	-	-	-	-	-	-	-	-
T-2	1	6 x 1/2	76.0	8.03	5.28	72.6	0.85	4.3	0.85
	3		81.4	6.05	6.05	86.9	0.90	4.2	0.90
	5		85.8	6.05	6.05	79.2	0.90	4.2	0.90
	7		89.1	6.05	6.05	83.6	0.90	4.2	0.90
T-3	-	-	-	-	-	-	-	-	-
T-4	1	8 x 1	25.3	4.99	4.99	29.7	0.90	6.3	0.80
	3		31.9	7.70	7.70	49.5	1.00	6.0	1.00
	5		34.1	4.40	3.96	37.4	0.90	6.2	0.90
	7		28.6	4.40	3.96	30.8	0.85	6.2	0.95
T-5	1	12 x 1/2	41.8	6.60	3.63	36.3	0.90	10.2	0.90
	3		37.4	2.64	4.73	46.2	0.90	10.2	0.90
	7		40.7	3.96	3.19	40.7	0.90	10.2	0.90
	9		42.9	5.39	3.41	36.3	0.90	10.2	0.90
T-6	1	12 x 1	30.8	4.51	4.51	30.8	0.80	10.5	0.70
	3		42.9	3.96	3.96	40.7	0.70	10.6	0.70
	5		37.4	3.96	3.96	40.7	0.70	10.6	0.70
	7		42.9	2.97	2.97	51.7	0.80	10.6	0.60
	9		38.5	3.52	3.52	34.1	0.70	10.6	0.70
	11		45.1	3.52	3.52	44.1	0.70	10.6	0.70
	13		36.3	3.52	3.52	36.3	0.70	10.6	0.70
	15	12 x 1	36.3	2.97	2.97	42.9	0.70	10.6	0.70
	17		31.9	2.97	2.97	36.3	0.70	10.6	0.70
	19		50.6	3.96	3.96	36.3	0.70	10.6	0.70
T-7	1	16 x 1/2	48.4	1.98	2.97	48.4	0.70	14.60	0.70
	3		57.2	4.51	1.98	47.3	0.70	14.6	0.70
T-8	1	20 x 3/8	61.6	3.96	3.96	59.5	0.70	18.6	0.70
	3		67.1	3.74	3.63	58.3	0.80	18.5	0.70
T-9	1	24 x 1	46.2	3.96	1.98	30.8	0.70	22.60	0.70
	3		31.9	5.94	5.06	31.9	0.60	22.9	0.50
	5		27.5	5.94	11.0	38.5	0.60	22.8	0.60

Table 6- Residual Stress Distribution in Center-Welded Plates



Test No.	Plate No.	Size (in x in)	Residual Stresses (ksi)							Distances (in)				
			σ_{r0}	σ_{r1}	σ_{r2}	σ_{r3}	σ_{r4}	σ_{r5}	σ_{r6}	z_1	z_2	z_3	z_4	z_5
T-1	-	-	-	-	-	-	-	-	-	-	-	-	-	-
T-2	2	6 x 1/2	39.9	62.0	16.0	14.0	13.0	12.0	55.9	0.70	1.65	1.40	1.65	0.60
	4	6 x 1/2	78.0	44.9	24.0	22.0	18.0	13.9	39.1	0.40	1.80	1.65	2.00	0.15
T-3	A	8 x 1/2	65.7	26.4	14.5	9.02	9.02	12.7	23.5	0.20	2.50	2.30	2.80	0.20
	B	8 x 1/2	69.7	28.3	12.4	9.60	9.60	10.8	27.8	0.18	2.62	2.60	2.42	0.18
	C	8 x 1/2	70.2	31.2	8.03	7.81	7.04	7.70	29.2	0.20	2.60	2.50	2.55	0.15
	D	8 x 1/2	66.1	31.0	12.0	12.0	12.0	12.0	31.7	0.15	2.65	2.40	2.60	0.20
T-4	2	8 x 1	19.1	22.6	7.04	7.26	7.81	7.04	25.0	0.80	2.50	1.40	2.40	0.90
	4	8 x 1	30.3	27.1	7.81	9.02	11.0	10.5	31.2	0.80	2.40	1.60	2.40	0.80
T-5	2	12 x 1/2	87.8	31.5	16.1	16.1	15.0	14.1	19.6	0.80	4.20	2.20	4.10	0.70
	4	12 x 1/2	76.8	36.5	14.9	16.0	16.5	16.5	49.2	0.80	4.20	2.30	3.80	0.80
	5	12 x 1/2	79.5	53.5	14.9	11.9	11.9	14.9	40.8	0.80	4.30	1.90	4.20	0.80
T-6	2-A	12 x 1	31.1	27.1	9.82	6.1	10.0	8.03	24.1	0.60	4.40	1.60	4.70	0.70
	2-B	12 x 1	49.3	24.3	8.10	7.04	9.35	7.04	13.75	0.60	4.50	1.60	4.70	0.60
	4-A	12 x 1	26.95	35.1	10.0	10.0	11.9	10.0	27.9	0.70	4.40	1.80	4.40	0.70
	4-B	12 x 1	65.01	34.3	34.3	10.0	10.0	9.02	9.02	32.0	0.60	1.80	4.40	0.70
	6-A	12 x 1	51.6	25.6	11.9	13.9	10.0	11.9	7.15	0.60	4.40	2.00	4.40	0.60
	6-B	12 x 1	49.2	22.2	14.41	11.9	10.0	10.0	14.3	0.60	4.50	1.80	4.50	0.60
	8-A	12 x 1	49.7	20.6	14.0	14.0	14.0	17.1	14.1	0.60	5.40	1.00	4.50	0.50
	8-B	12 x 1	61.2	24.9	14.1	14.1	11.9	11.9	35.0	0.60	5.00	1.40	4.40	0.60
	10-A	12 x 1	46.2	20.5	15.8	6.05	8.03	11.9	15.1	0.50	4.60	1.80	4.70	0.40
	10-B	12 x 1	34.5	24.8	9.8	8.03	8.03	10.6	20.0	0.60	5.00	1.20	4.60	0.60
	12-A	12 x 1	47.4	23.0	20.0	10.6	10.0	24.6	5.06	0.60	4.50	1.80	4.60	0.50
	12-B	12 x 1	42.9	25.1	10.0	10.0	10.0	16.0	35.3	0.60	4.50	1.80	4.50	0.60
T-7	2	16 x 1/2	69.5	38.0	10.0	10.0	10.0	10.0	40.3	0.60	6.40	1.90	6.50	0.60
T-8	-	-	-	-	-	-	-	-	-	-	-	-	-	-
T-9	2-A	24 x 1	60.1	44.0	7.04	6.05	4.95	8.60	18.5	0.70	10.4	1.80	10.5	0.60
	2-B	24 x 1	71.5	37.8	6.05	4.95	4.95	6.05	22.4	0.60	10.5	1.80	10.4	0.70

Table 7—Residual Stress Distribution in Edge-Welded Plates



Test No.	Plate No.	Size (in x in)	Residual Stress in ksi				Distances (in)			Weld
			σ_{r1}	σ_{r2}	σ_{r3}	σ_{r4}	z_1	z_2	z_3	
T-1	-	-	-	-	-	-	-	-	-	-
T-2	6	6 x 1/2	78.1	15.1	2.97	86.0	0.8	4.20	1.0	S
	8		92.0*	2.97	16.0	85.0	0.8	4.20	1.0	S
T-4	6	8 x 1	99.0*	8.5	8.0	44.0	1.2	5.1	1.70	S
	8		78.0*	7.26	11.55	33.0	0.80	6.4	0.80	S
T-5	6-A	12 x 1/2	74.8	8.03	6.05	88.2**	1.00	10.1	0.90	D
	6-B		72.8	10.5	1.0	100.0**	0.90	10.1	1.00	S
	8-A		100.0*	6.05	6.05	98.6*	1.0	10.0	1.00	D
	8-B		93.5*	6.26	1.10	99.0*	0.90	10.2	0.90	S
	10-A		87.4*	8.80	10.0	73.6*	0.90	10.2	0.90	D
	10-B		75.9*	9.75	1.0	101.0*	0.90	9.1	1.00	S
T-6	14	12 x 1	-	-	-	-	-	-	-	-
	16-A		90.0*	6.05	4.06	42.8	0.60	11.2	0.20	S
	16-B		125.0**	7.02	2.96	42.8	0.70	11.0	0.30	S
	18		-	-	-	-	-	-	-	-
	20-A		95.0*	13.6	1.0	48.4	0.70	10.5	0.80	S
	20-B		98.0*	14.3	1.0	48.0	0.70	11.0	0.30	S
T-7	4	16 x 1/2	82.5*	10.6	1.0	50.5	0.70	14.6	0.70	S
	6		84.0*	6.71	6.27	83.6*	0.90	14.2	0.90	D
T-8	2	20 x 3/8	82.5*	6.05	4.40	60.5	0.70	18.3	1.00	S
	4		81.3*	5.61	5.50	81.4*	1.00	18.2	0.8	D
T-9	4-A	24 x 1	35.0	5.08	6.60	81.5*	0.7	22.6	0.7	S
	4-B		39.0	12.3	5.72	115.95*	0.60	22.7	0.70	S
	6-A		111.0*	5.50	5.50	124.0*	0.70	22.6	0.70	D
	6-B		109.0*	3.96	6.05	121.0*	0.80	22.6	0.60	D

S - Welded on one edge only

D - Welded on both edges

* - Residual stress at the welded edge

** - Residual stress at the edge welded with L100 electrode

TABLE 8 SHAPES TESTED

SHAPE	EDGE PREPARATION	PLATE SIZE(INCHES)
6H27	Sheared	6 x 1/2 flange 6 x 3/8 web
6H27	Flame-Cut	6 x 1/2 flange 6 x 3/8 web
10H61	Flame-Cut	9 x 3/4 flange 9 x 1/2 web
6 x 6-Box	Flame-Cut	6 x 1/4 5 1/2 x 1/4
10 x 10-Box	Flame-Cut	10 x 1/2 9 x 1/2

TABLE 9 RESIDUAL STRESSES IN WELDED BUILT-UP SHAPES

SHAPE	WELDED BUILT-UP SHAPES								WELDED BOX SHAPES COMPONENT PLATES			
	Residual Stresses in Flange (ksi)				Residual Stresses in Web (ksi)				Max(+)	Av.(+)	Max(-)	Av.(-)
	Max(+)	Av.(+)	Max(-)	Av.(-)	Max(+)	Av.(+)	Max(-)	Av.(-)				
6H27 (sheared)	+40	18-20	40	20-22	80	70-75	20	18-20	-	-	-	-
	Junct.											
6H27	+45	20-24	20	18-20	80	70-75	20	18-20	-	-	-	-
	Junct.											
10H61	+20	14-16	12	8-10	44	36-40	12	6-10	-	-	-	-
	Tips											
6"x6" Box	-	-	-	-	-	-	-	-	80	60-65	40	22-24
10"x10" Box	-	-	-	-	-	-	-	-	95	70-80	20	10-15

Readings are average of top and bottom faces for H shapes.

TABLE 9 RESIDUAL STRESSES IN WELDED BUILT-UP SHAPES

TABLE 10 SHAPES INCLUDED IN THE INVESTIGATION

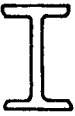
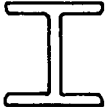
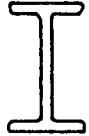
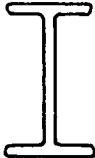
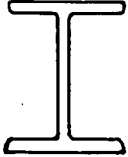
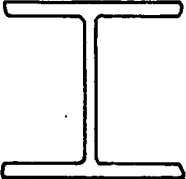
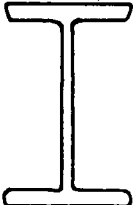
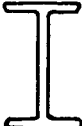
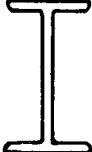
TEST NO.	SHAPE		DELIVERED LENGTHS
T-R-A	8WF17		2 x 10'
T-R-B	8WF31		1 x 40'
T-R-C	10WF25		1 x 10'
T-R-D	12WF36		2 x 13'
T-R-E	12WF45		2 x 15'
T-R-F	12WF120		3 x 36'
T-R-H	16WF64		2 x 15'
T-R-J	CB-102-33		2 x 11'
T-R-K	CBL-16-26		2 x 10'

TABLE 11 RESIDUAL STRESSES MEASURED IN ROLLED SHAPES

Test No.	Residual Stresses in ksi							
	Shape	Flange Edge*			Web Center			
		Top Face	Bottom Face	Average	Flange Center	Top Face	Bottom Face	Aver.
T-R-1-A	8WF17	-1.0	-4.5	-2.75	+1.5	-2.5	-1.5	-2.0
T-R-1-B	"	-1.0	-4.0	-2.5	+2.5	-1.5	-2.0	-1.75
T-R-2-A	8WF31	-3.0	-1.50	-2.25	+2.0	-2.5	-3.0	-2.75
T-R-2-B	"	-3.0	-3.5	-3.25	+2.0	-1.5	-2.0	-1.75
T-R-3-A	10WF25	-3.5	-3.0	-3.25	+2.25	0	+1.5	+0.75
T-R-3-B	"	-3.0	-2.5	-2.75	-0.5	+1.0	+1.5	+1.25
T-R-4-A	12WF36	-4.0	-3.4	-3.70	+2.0	-3.0	-3.0	-3.0
T-R-4-B	"	-4.0	-4.0	-4.0	+2.5	-3.5	-3.5	-3.5
T-R-5-A	12WF45	-4.75	-4.5	-4.65	+2.0	-3.0	-2.5	-2.75
T-R-5-B	"	-5.25	-6.5	-5.80	+3.0	-4.5	-4.5	-4.5
T-R-6-A	12WF120	-5.70	-5.0	-5.35	+3.20	-3.0	-1.5	-2.25
T-R-6-B	"	-8.1	-4.5	-6.3	+2.6	-3.5	-2.5	-3.0
T-R-7-A	16WF64	-4.27	-3.11	-3.75	+2.3	-1.0	+1	-0
T-R-7-B	"	-4.50	-2.10	-3.30	+2.0	-1.0	-0.5	-0.75
T-R-8	CB-102-33	-1.72	-2.21	-2.0	+1.0	+0.2	+0.5	+0.35
T-R-9	CBL-16-26	-2.50	-1.72	-2.11	+2.0	-3.0	+1.0	-1.0

*Average of four flange tips
 +Tensile residual stress
 -Compressive residual stress

Table 12 SUMMARY OF COLUMN TESTS

Steel	Making	Shape	Bending Axis	Slenderness Ratio (L/r)	Test
T-1	Rolled	8WF31	Weak	40	0.92
		12WF120	Weak	60	0.77
			Weak	30	0.89
			Weak	50	0.82
	Welded	6H27	Weak	45	0.82
			Weak	60	0.66
			Strong	30	0.83
		10H61	Weak	45	0.80
			Weak	60	0.69
			Strong	30	0.84
			Weak	35	0.90
			Weak	55	0.79
			6x6 Box	40	0.91
				60	0.69
10x10 Box	30	0.94			
	50	0.87			
-Ni-Cr- Mo-V	Rolled	10WF112	Weak	50	0.75

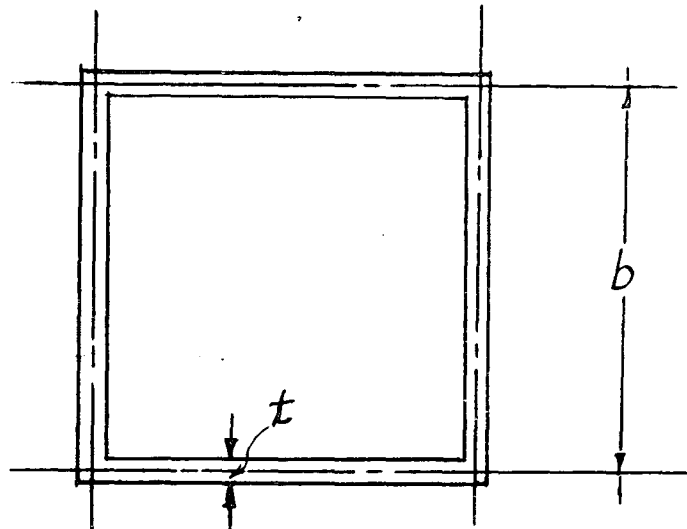
290.16

Table 13 DETAIL OF SPECIMENS FOR PLATE BUCKLING TESTS

Piece No.	Length (in.)	Description	Basic Tests	Specimen No.	Length (in.)	L/b	b/t*
1	200	11½"x11½"x¼" Box	Coupons Residual Stress	T-1A	60	5.31	44.0
				T-1B	60	5.34	44.0
2	140	7"x7"x¼" Box	Coupons Residual Stress	T-2A	35	5.18	26.2
				T-2B	35	5.18	26.2

290.16

*Average of four plates.



-100

Table 14 SUMMARY OF PLATE BUCKLING TESTS

Specimen	$\frac{b}{t} \sqrt{\frac{\sigma_y}{E}}$	σ_{rc}/σ_y	P_{max} (kips)	P_{cr} (kips)	P_{max}/P_y Test	P_{cr}/P_y Test	P_{cr}/P_y Predicted
T-1A	2.61	0.12	700	520	0.53	0.39	0.43
T-1B	2.61	0.12	694	510	0.52	0.38	0.43
T-2A	1.64	0.16	651	630	0.90	0.87	0.91
T-2B	1.64	0.16	657	645	0.91	0.89	0.91

11. FIGURES

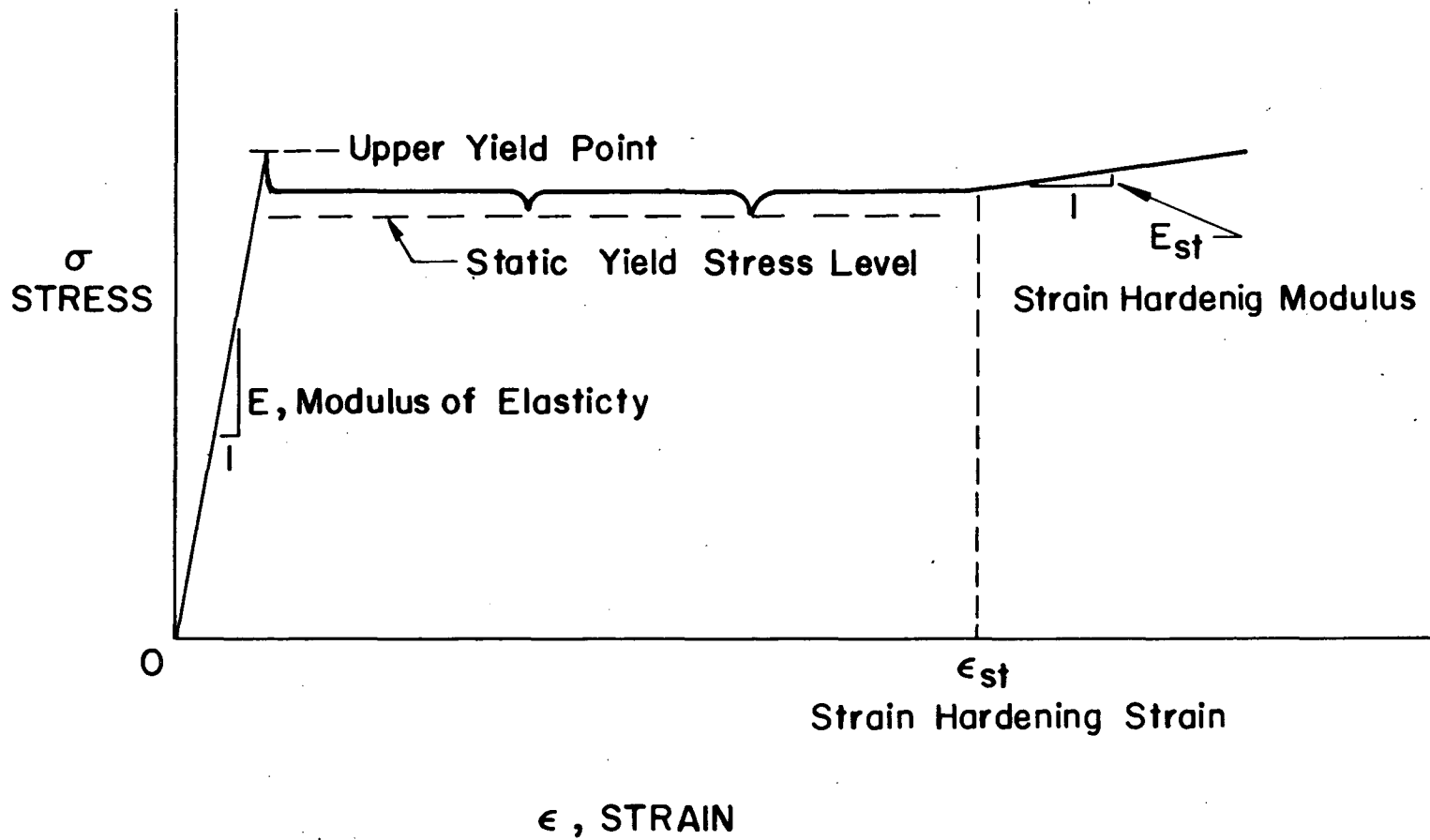


Fig. 1 Diagrammatic Stress-Strain Curve for Structural Carbon Steel

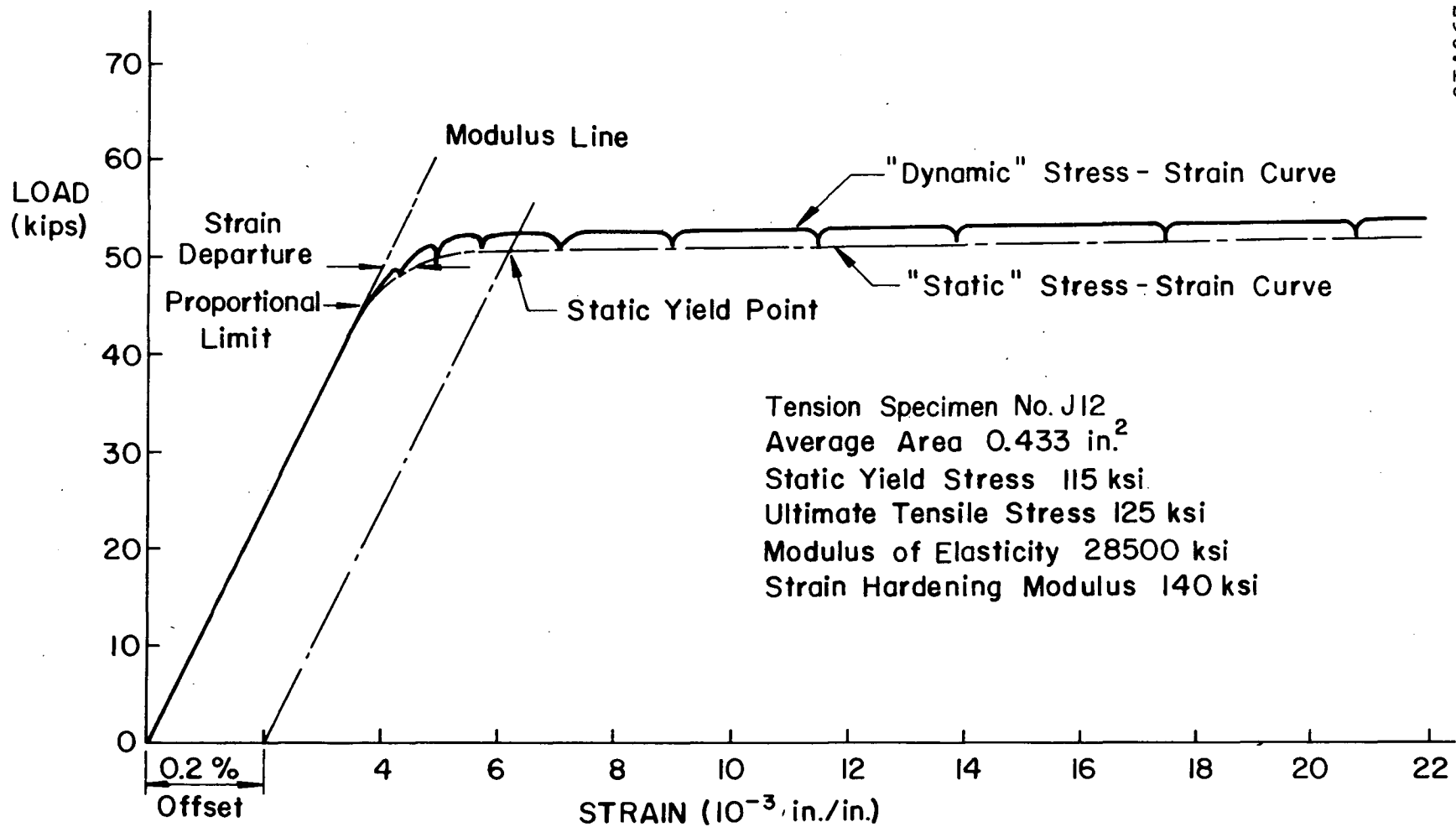


Fig. 2 Typical Stress-Strain Curve for a Typical T-1 Steel Tension Specimen Test

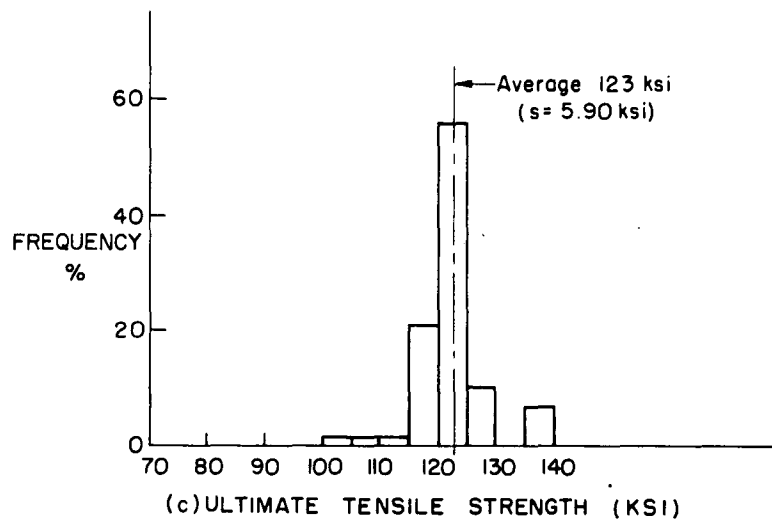
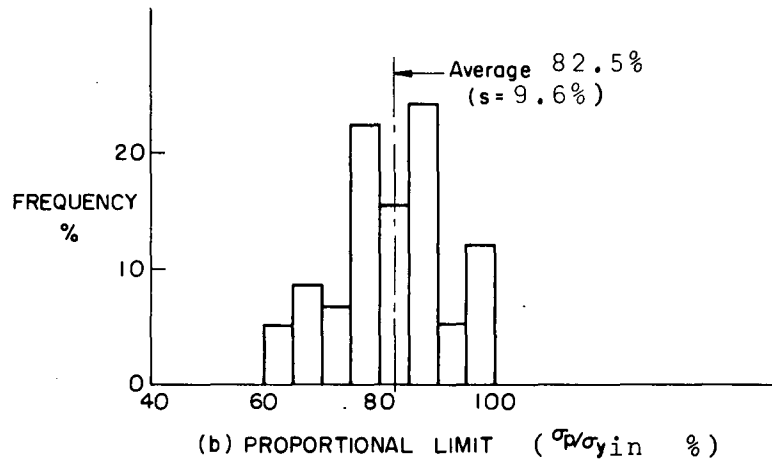
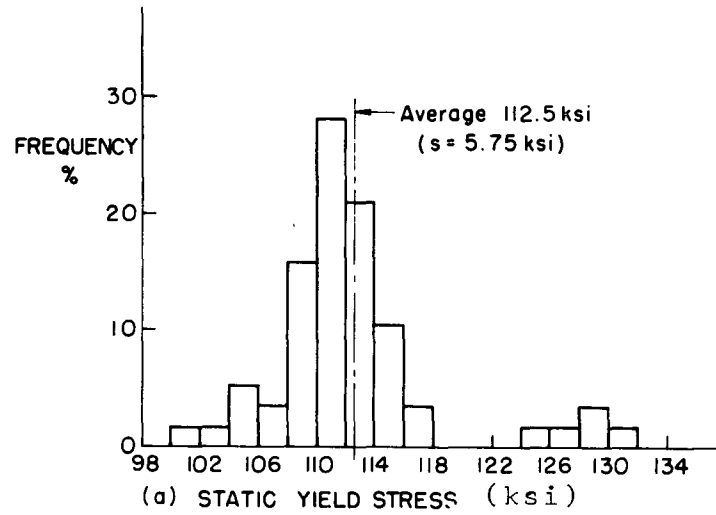
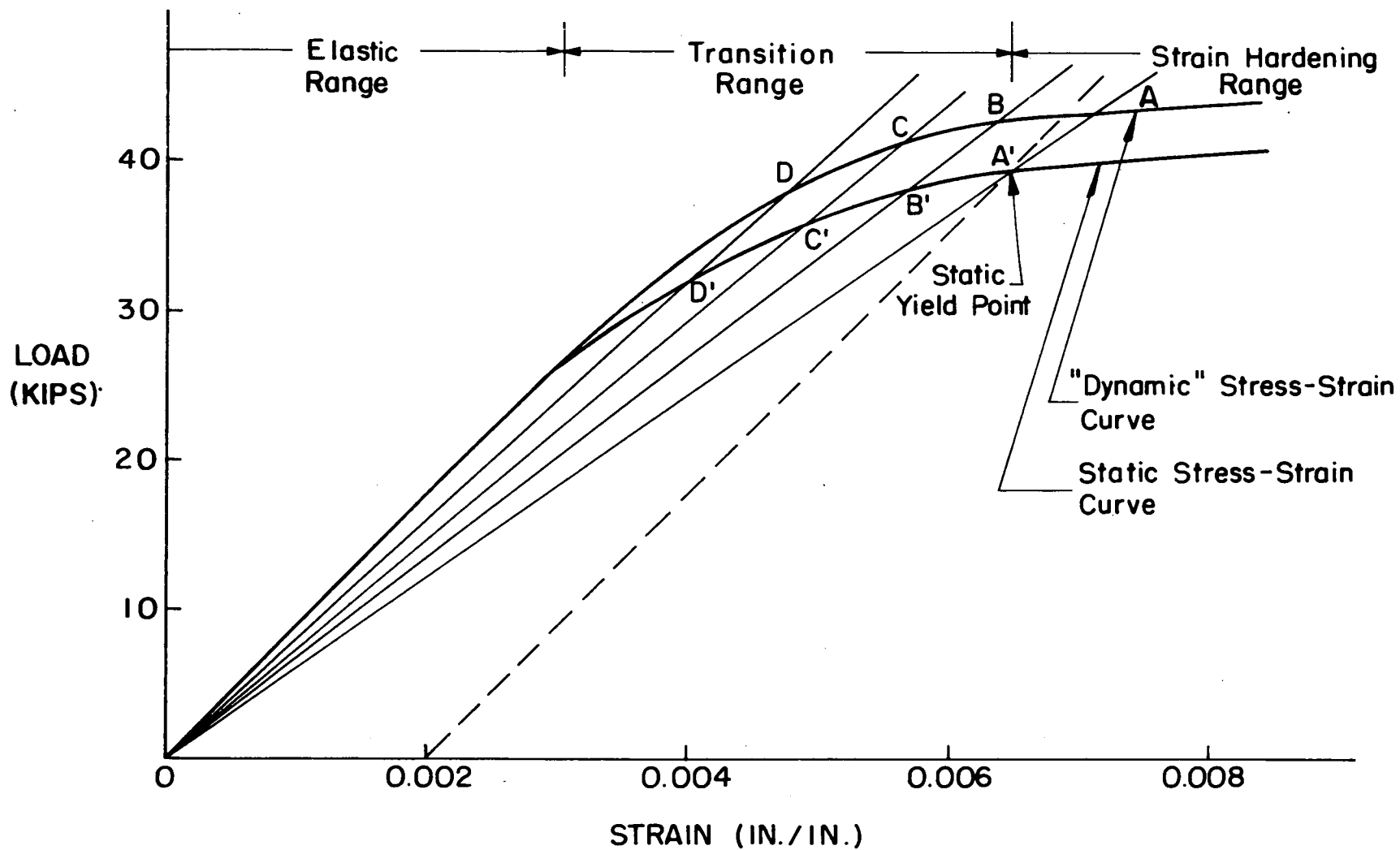
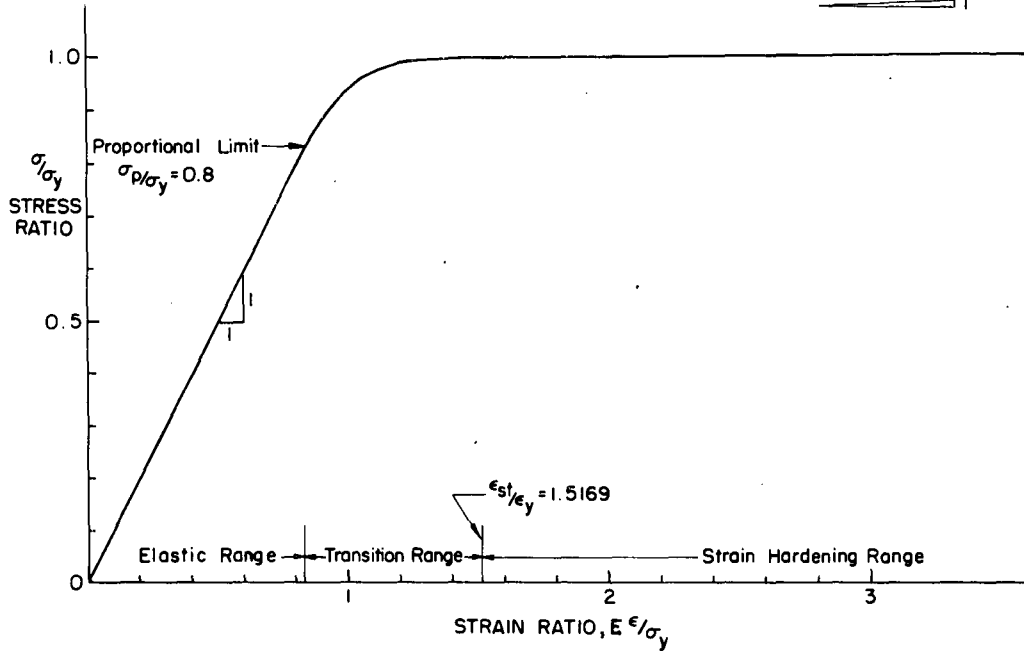


Fig. 3 Histograms for Mechanical Properties of T-1 Steel

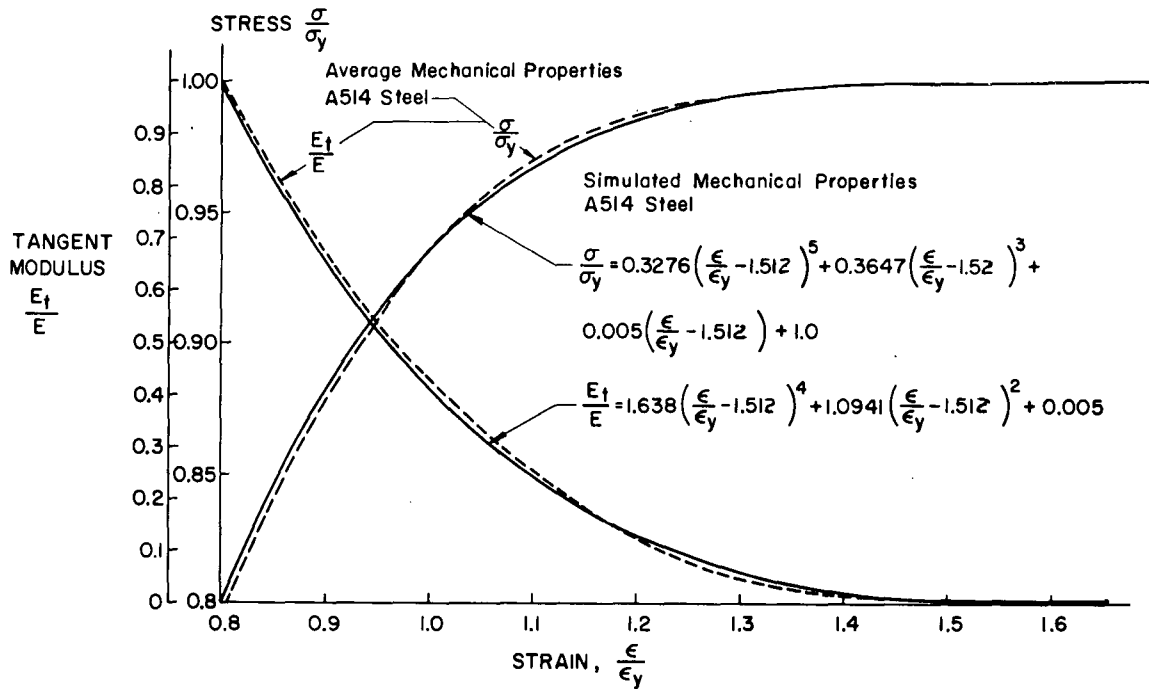


290.16

Fig. 4 Determination of the Static Stress-Strain Curve for Nonlinear Materials



(a) AVERAGE TYPICAL STRESS-STRAIN CURVE



(b) STRESS-STRAIN AND TANGENT MODULUS-STRAIN RELATIONSHIPS IN THE TRANSITION RANGE

Fig. 5 Stress-Strain Relationship for T-1 Steel

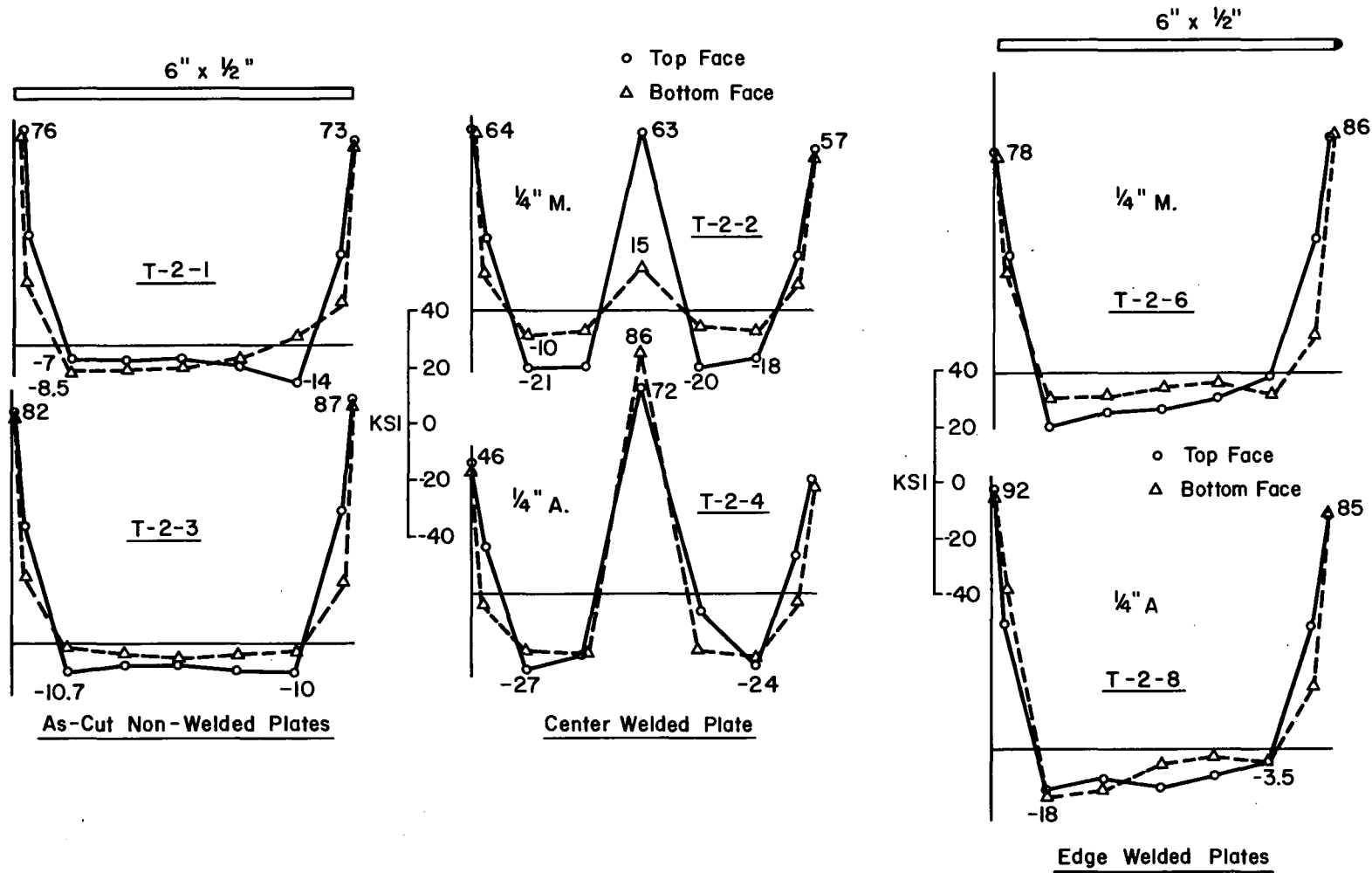


Fig. 6 RESIDUAL STRESSES IN 6" x 1/2" FLAME CUT PLATES

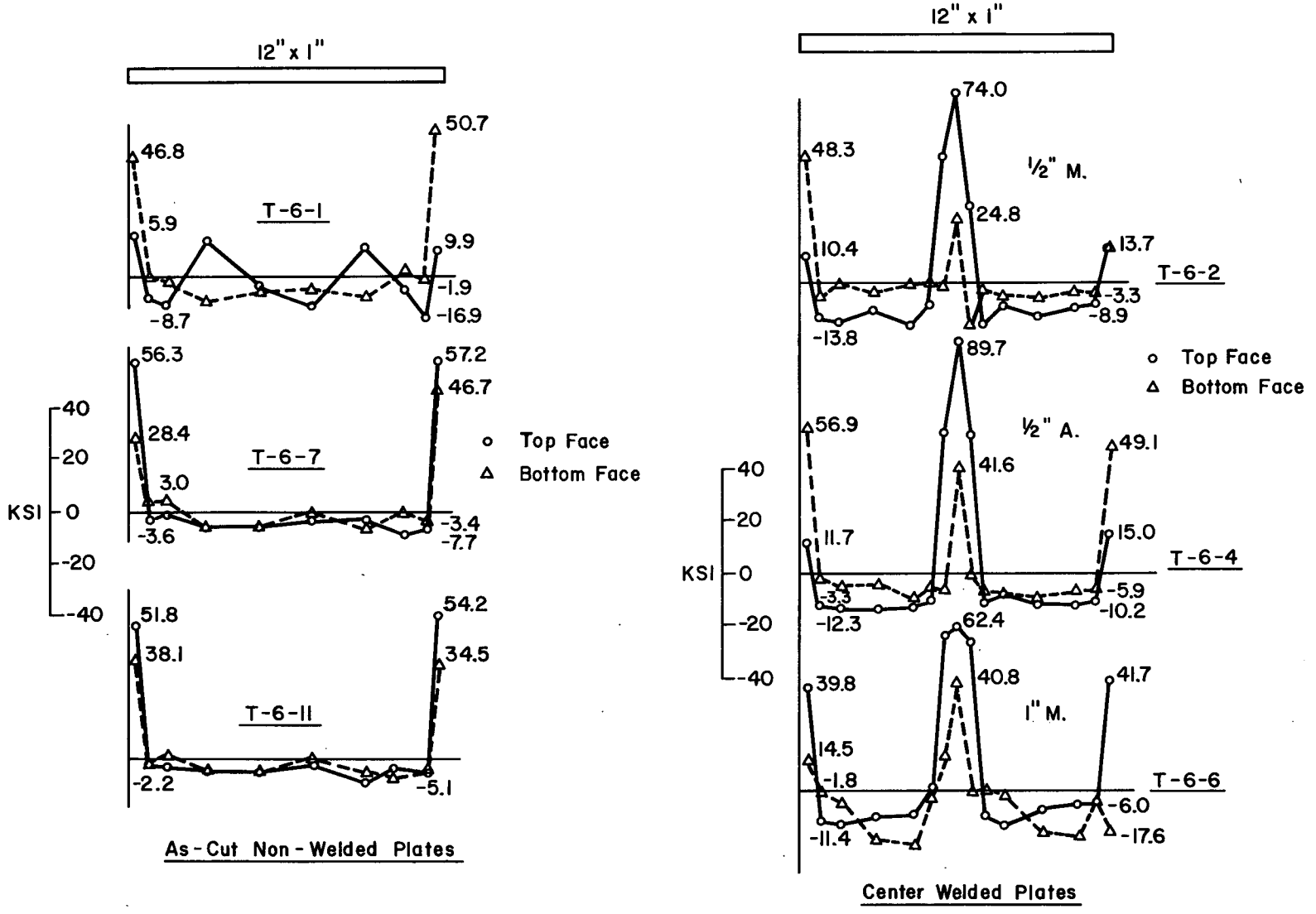


Fig. 7 RESIDUAL STRESSES IN 12" x 1" PLATES

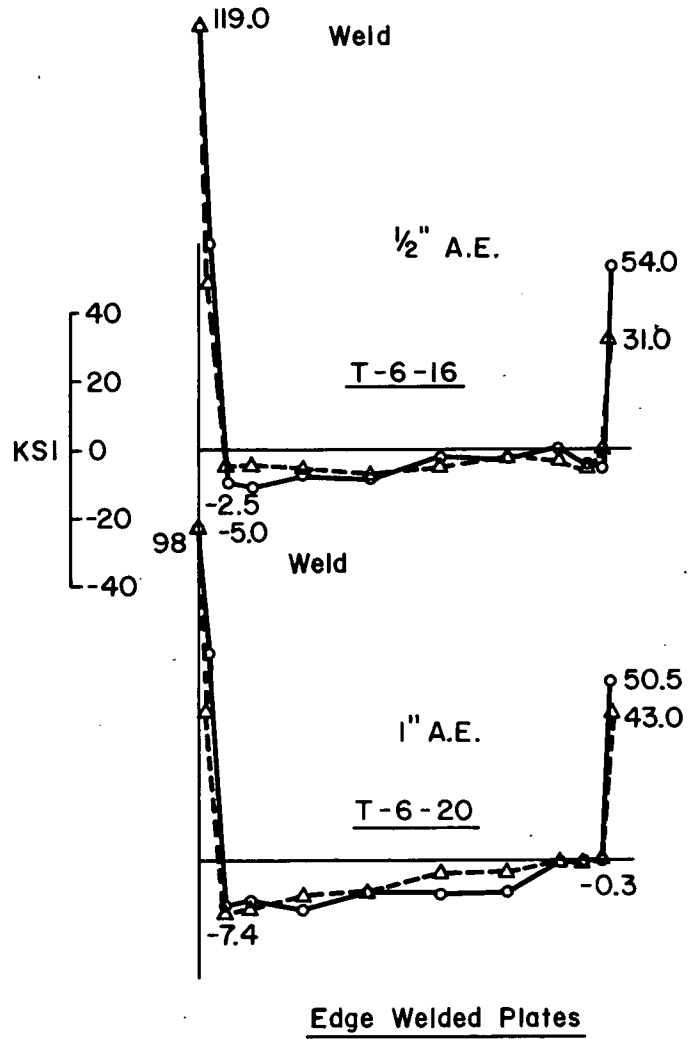
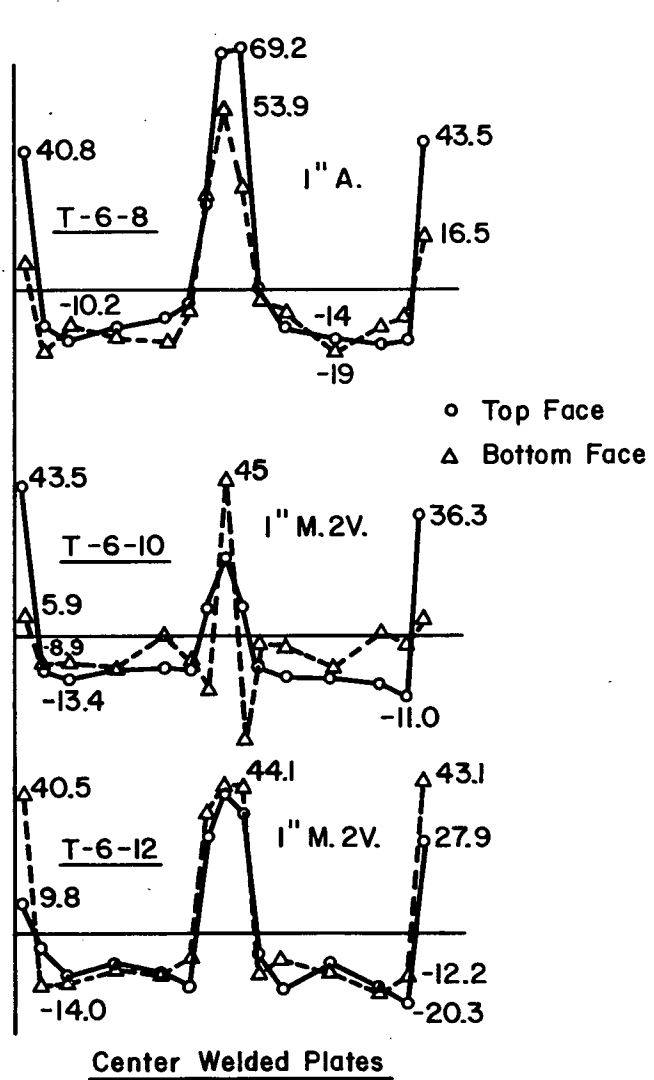
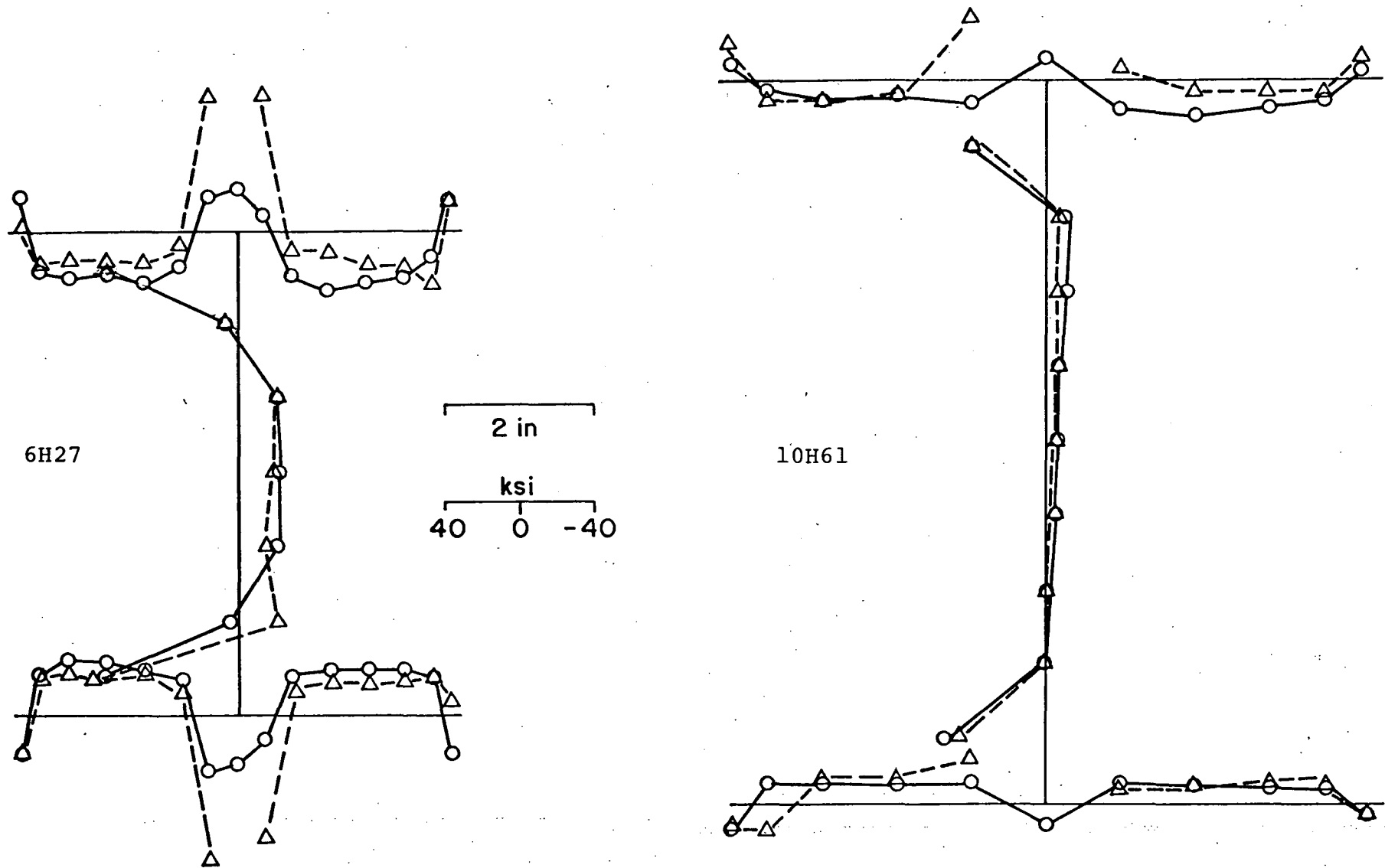


Fig. 7 RESIDUAL STRESSES IN 12" x 1" PLATES (Cont'd)



290.16

-111

Fig. 8 Residual Stresses in Welded H-Shapes

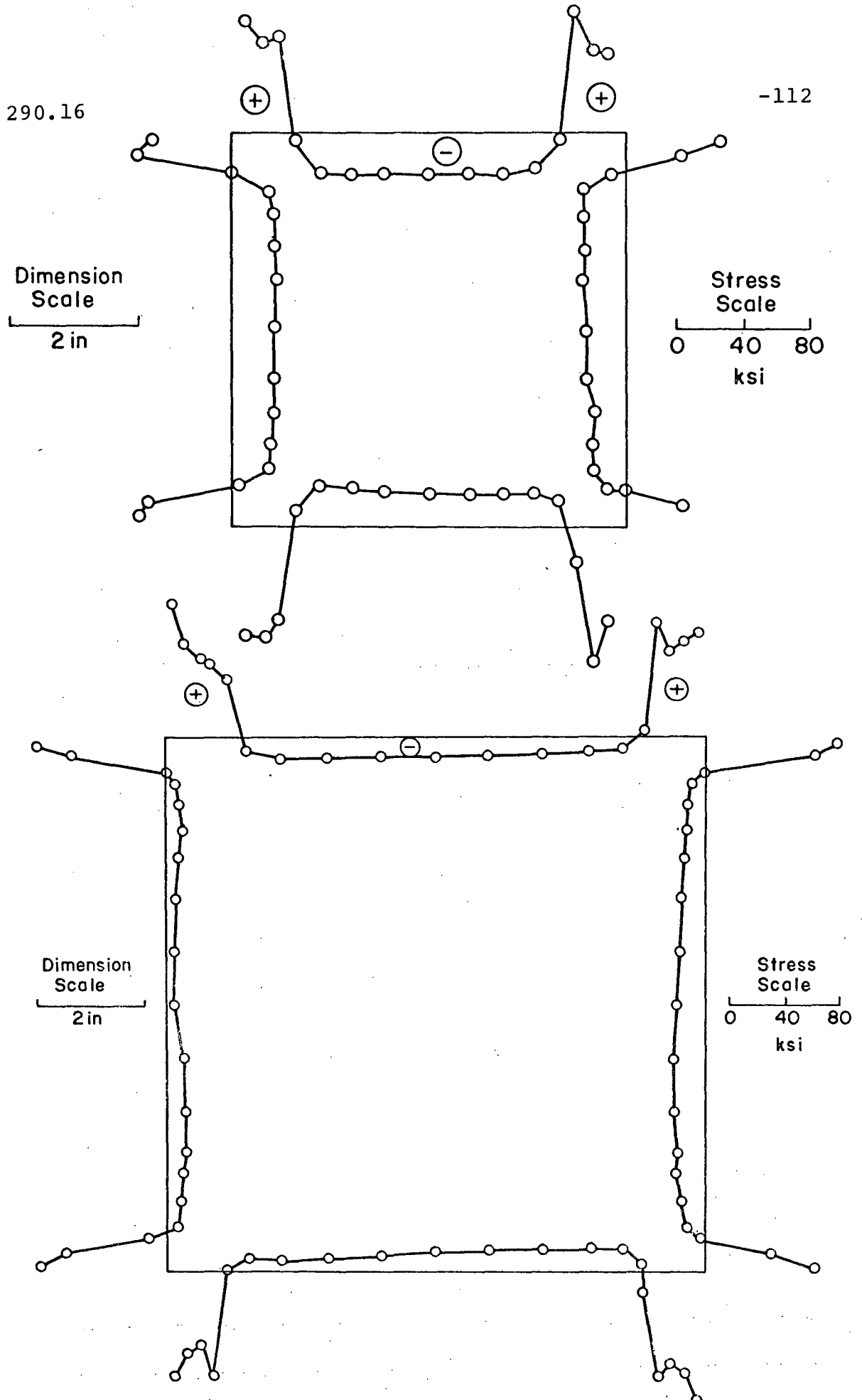


Fig 9 Residual Stresses in Welded Box Shapes

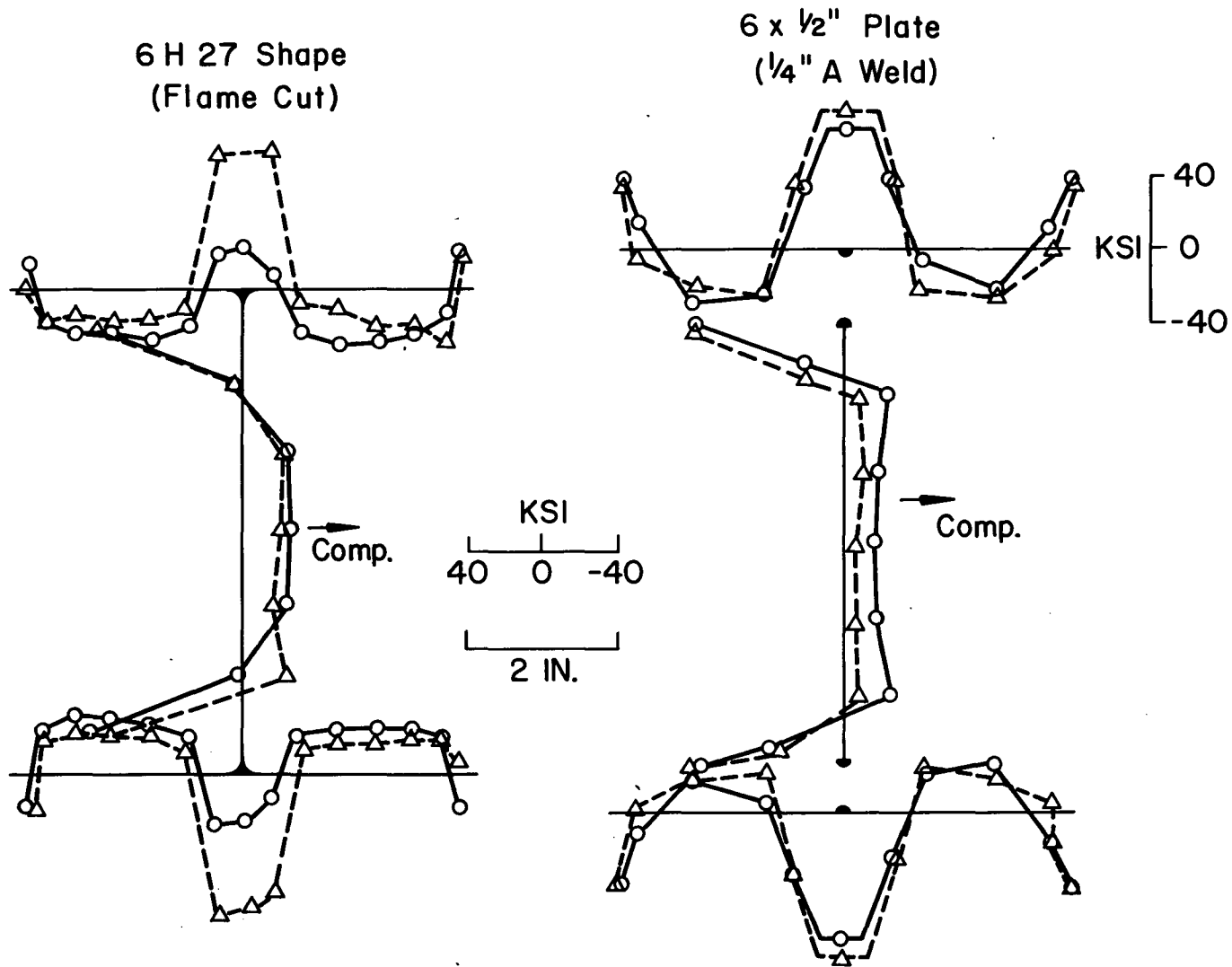


Fig. 10 COMPARISON OF WELDED H-SHAPE WITH ITS COMPONENT PLATES

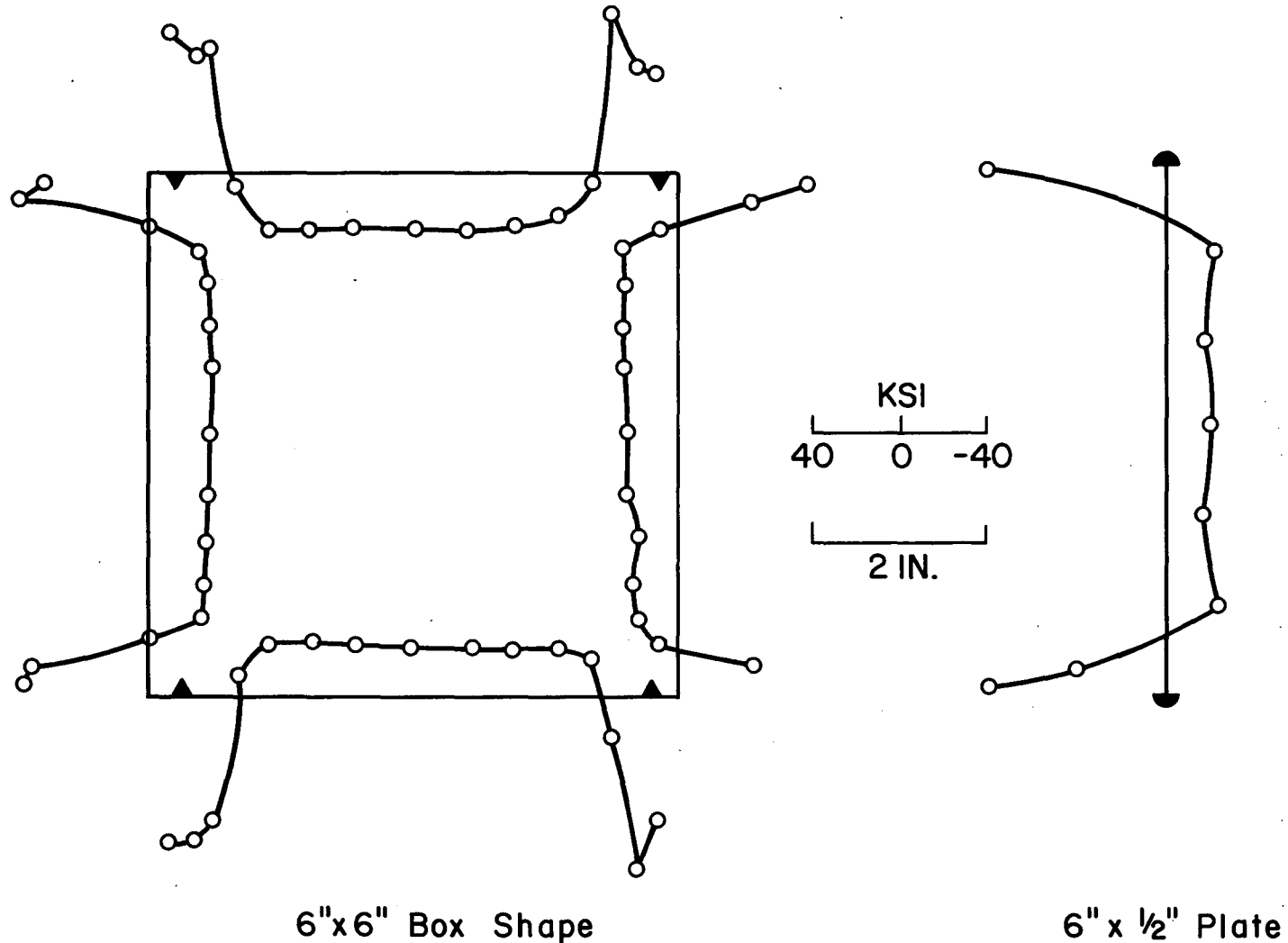


Fig. 11 COMPARISON OF WELDED BOX SHAPE WITH ITS COMPONENT PLATES

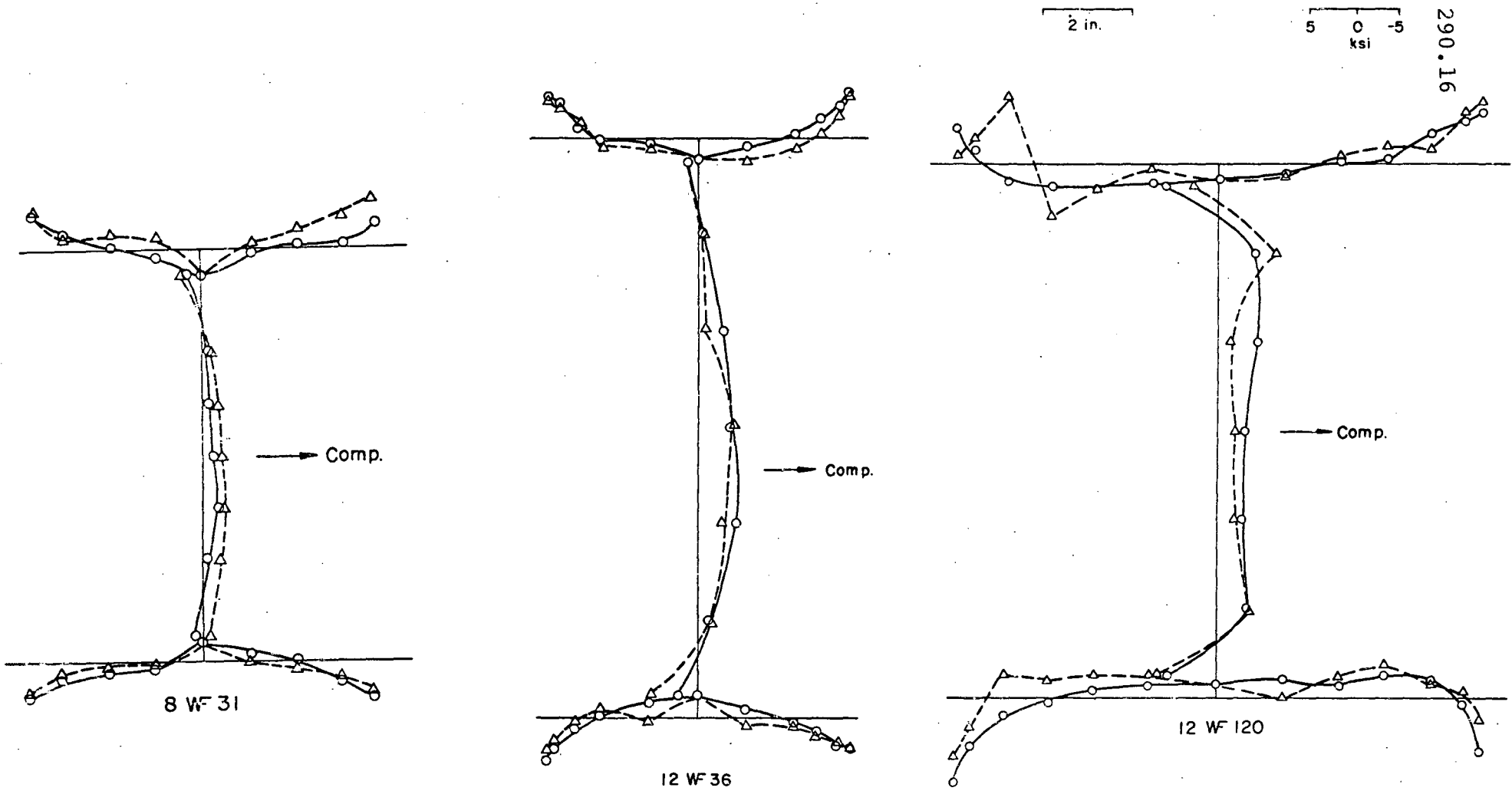


Fig. 12 Typical Residual Stress Distribution in Rolled Heat-Treated T-1 Shapes

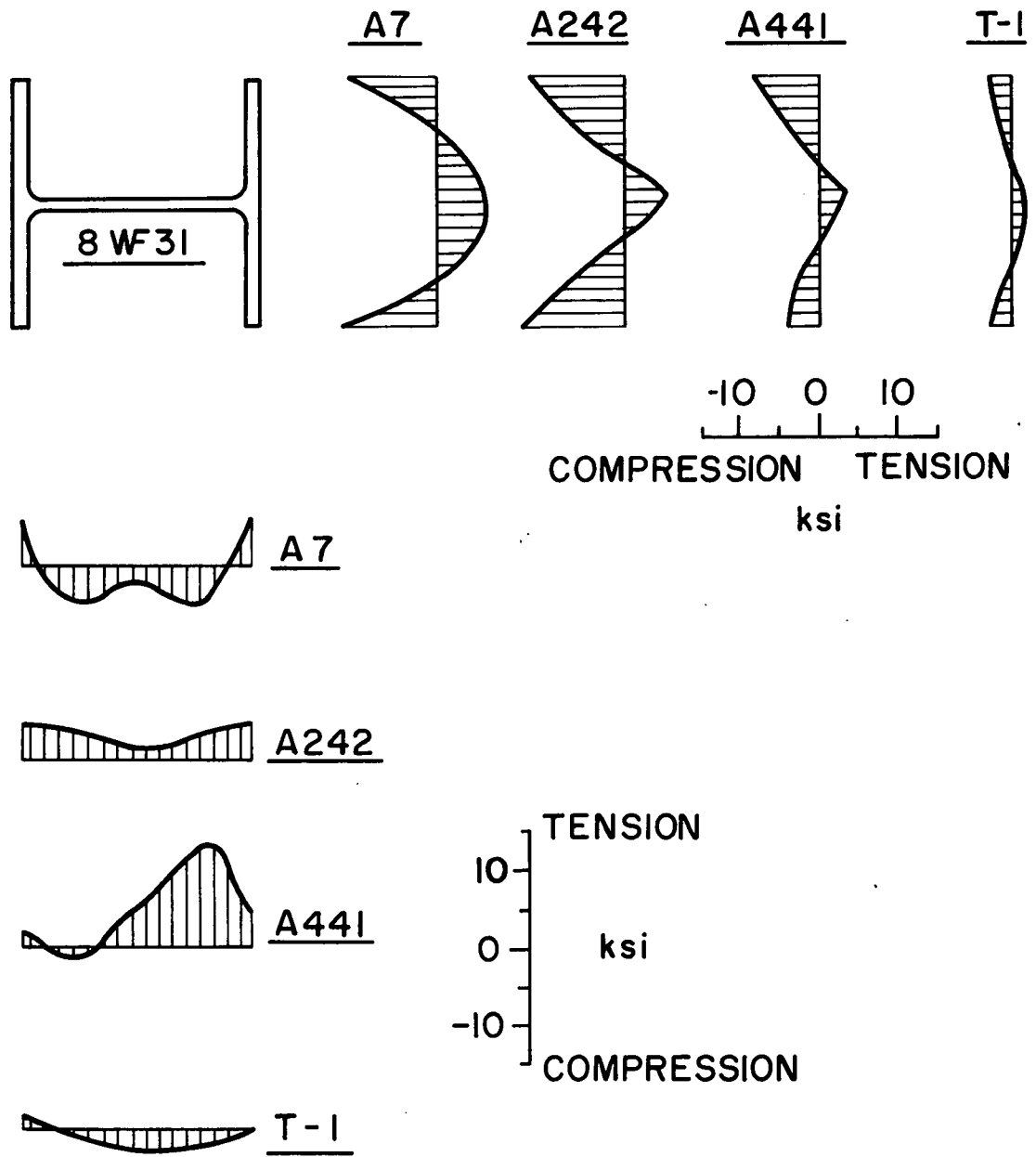
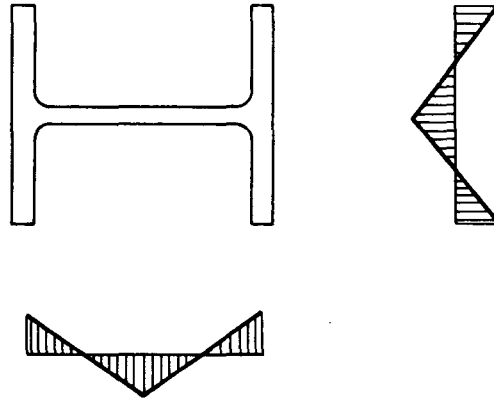
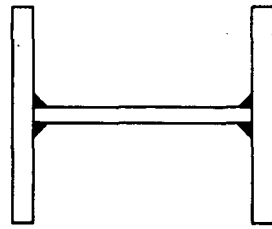


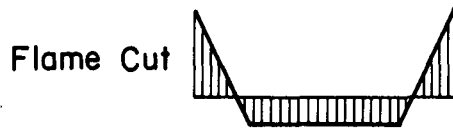
Fig. 13 COMPARISON WITH RESULTS OBTAINED FROM OTHER TESTS



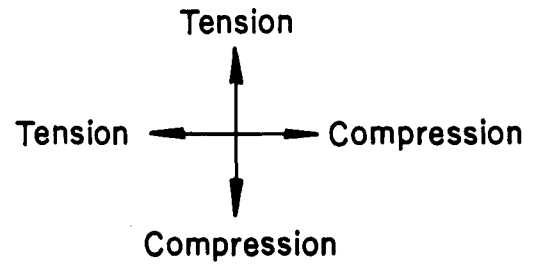
(a) Rolled Steel Shapes



Flame Cut



Flame Cut



(b) Welded

Steel Shapes

Fig. 14 Idealized Residual Stress Distribution in T-1 Shapes

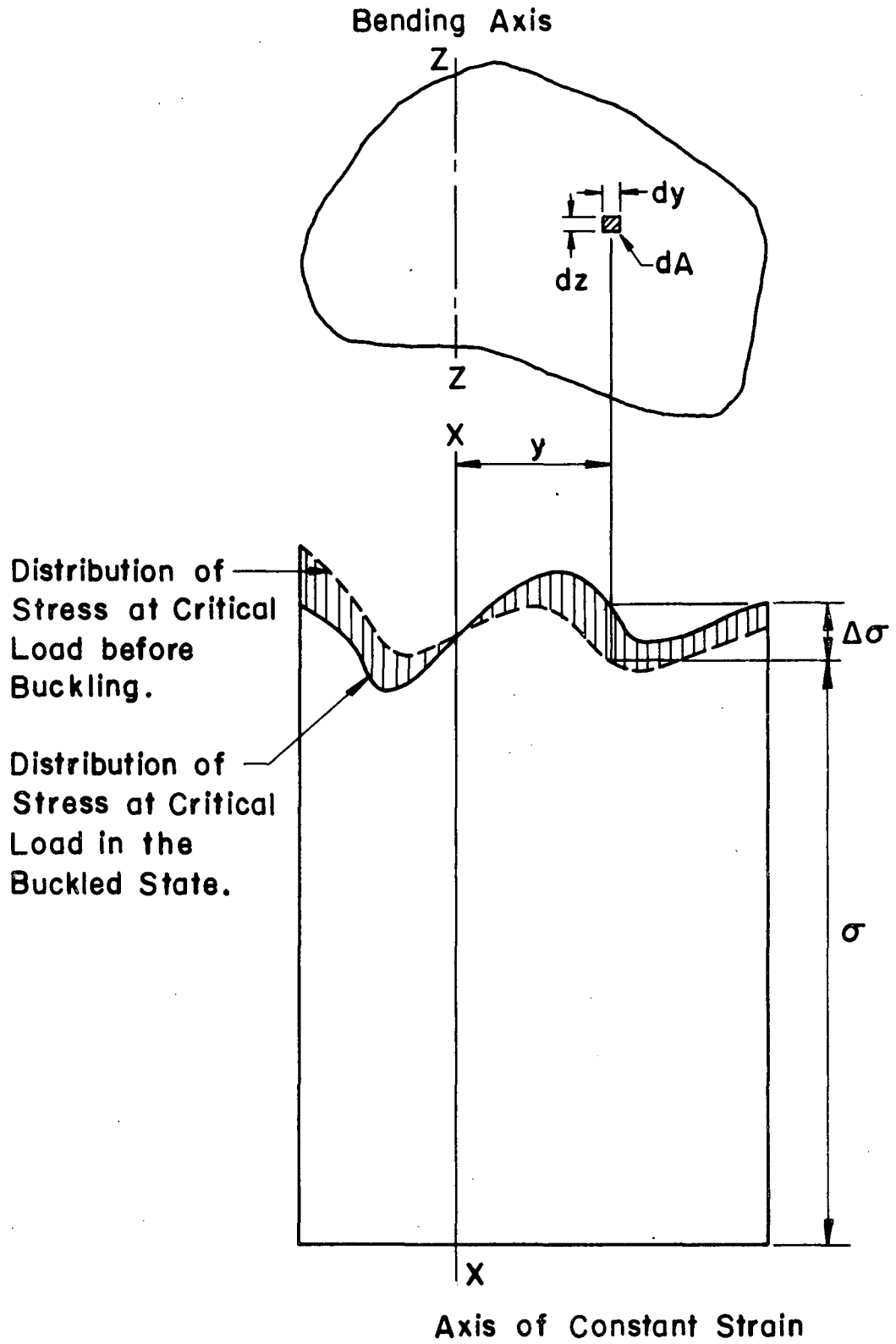


Fig. 15 Stress Diagram During Buckling

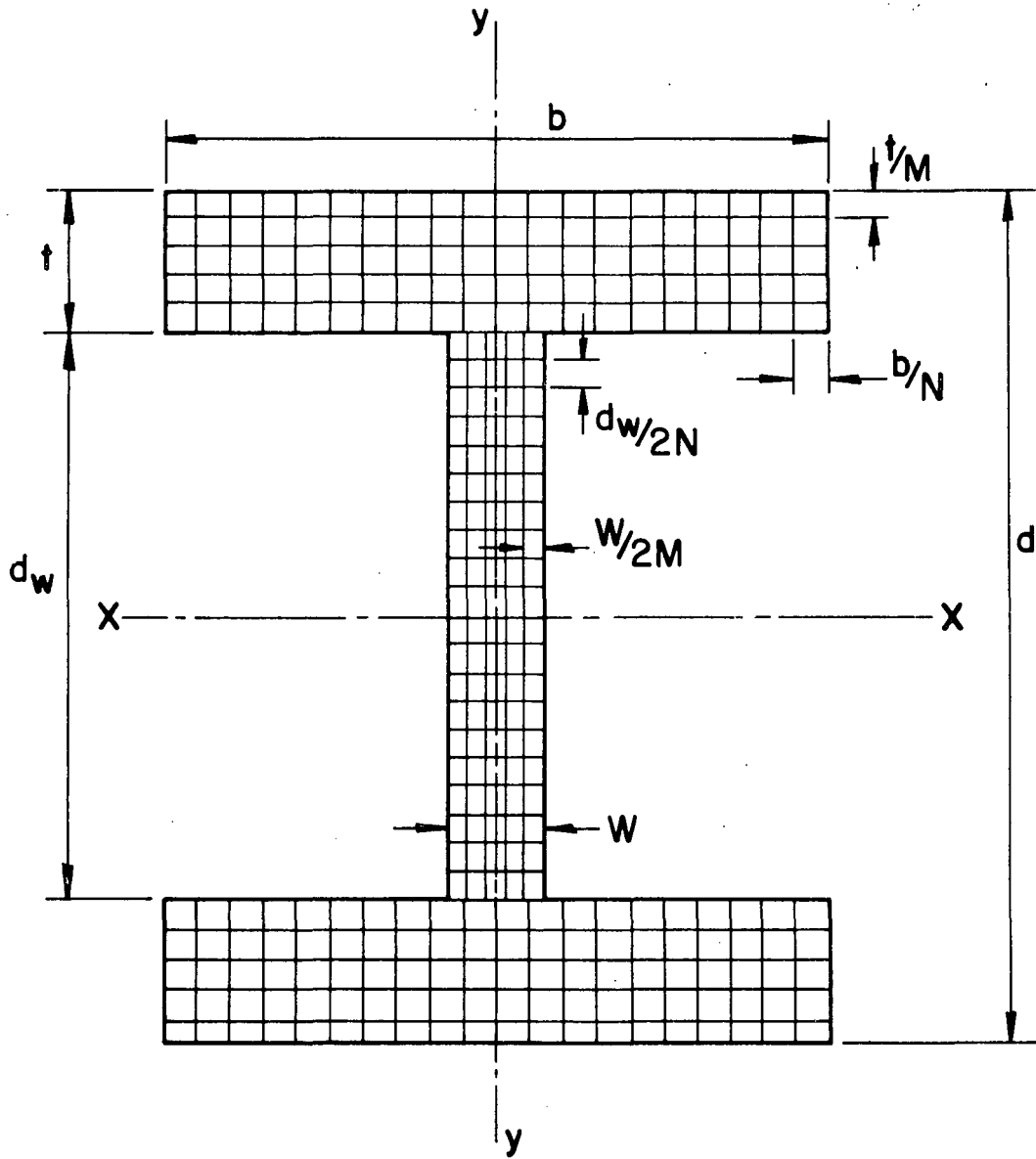
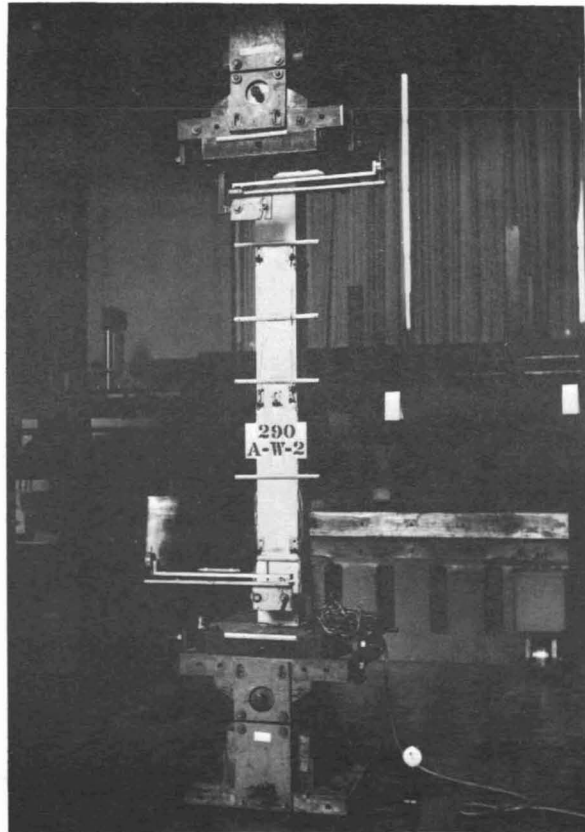
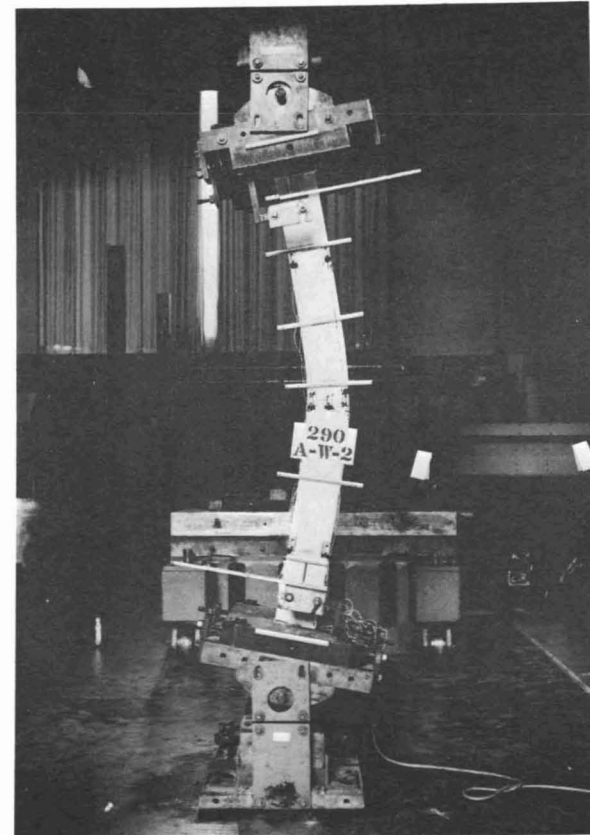


Fig. 16 Arrangement of Finite Area Elements



(a) Beginning of Test



(b) End of Test

Fig. 17 Set-Up of Pinned-End Column Test

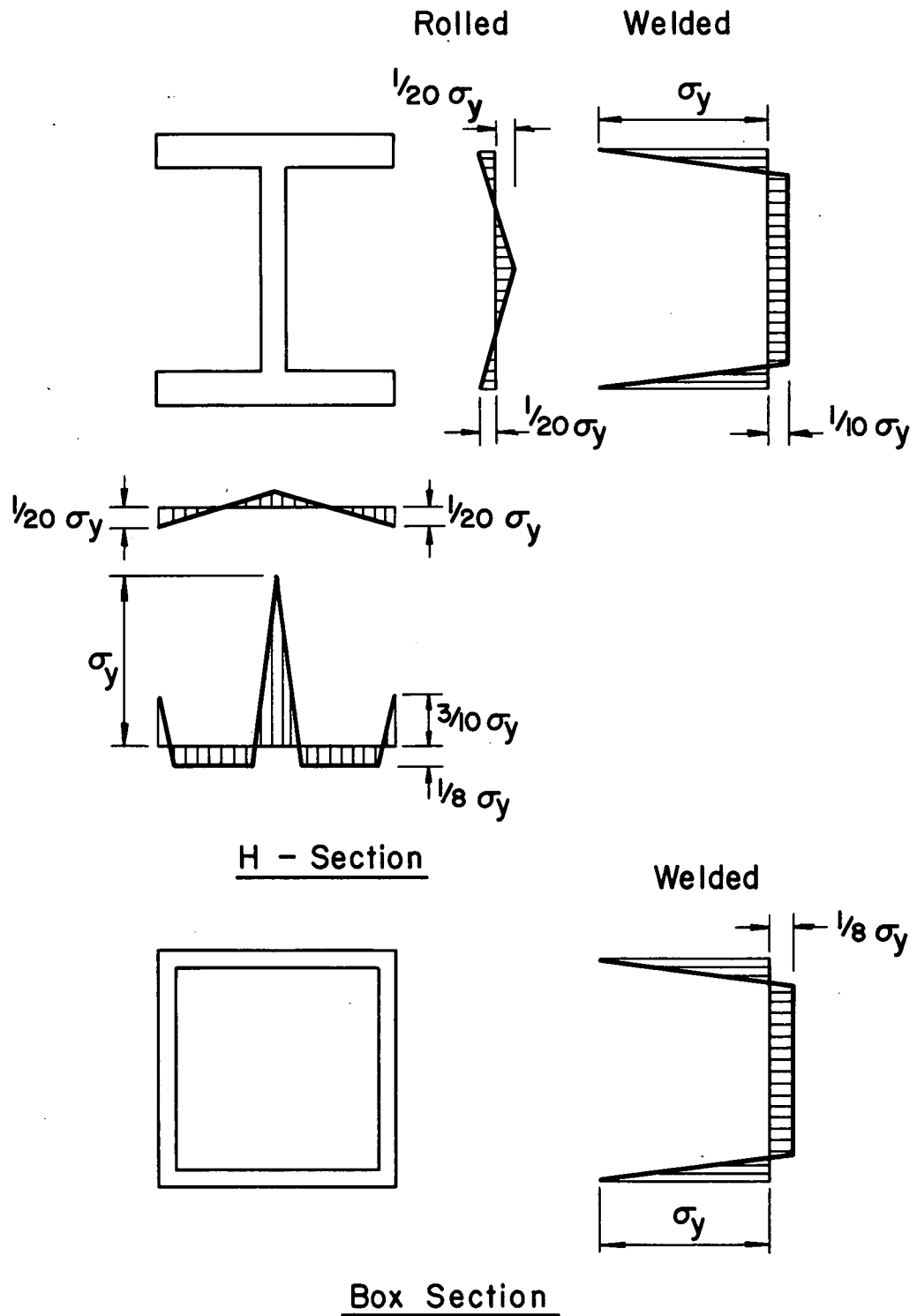


Fig. 18 IDEALIZED AVERAGE RESIDUAL STRESS DISTRIBUTION IN T-1 STEEL SHAPES

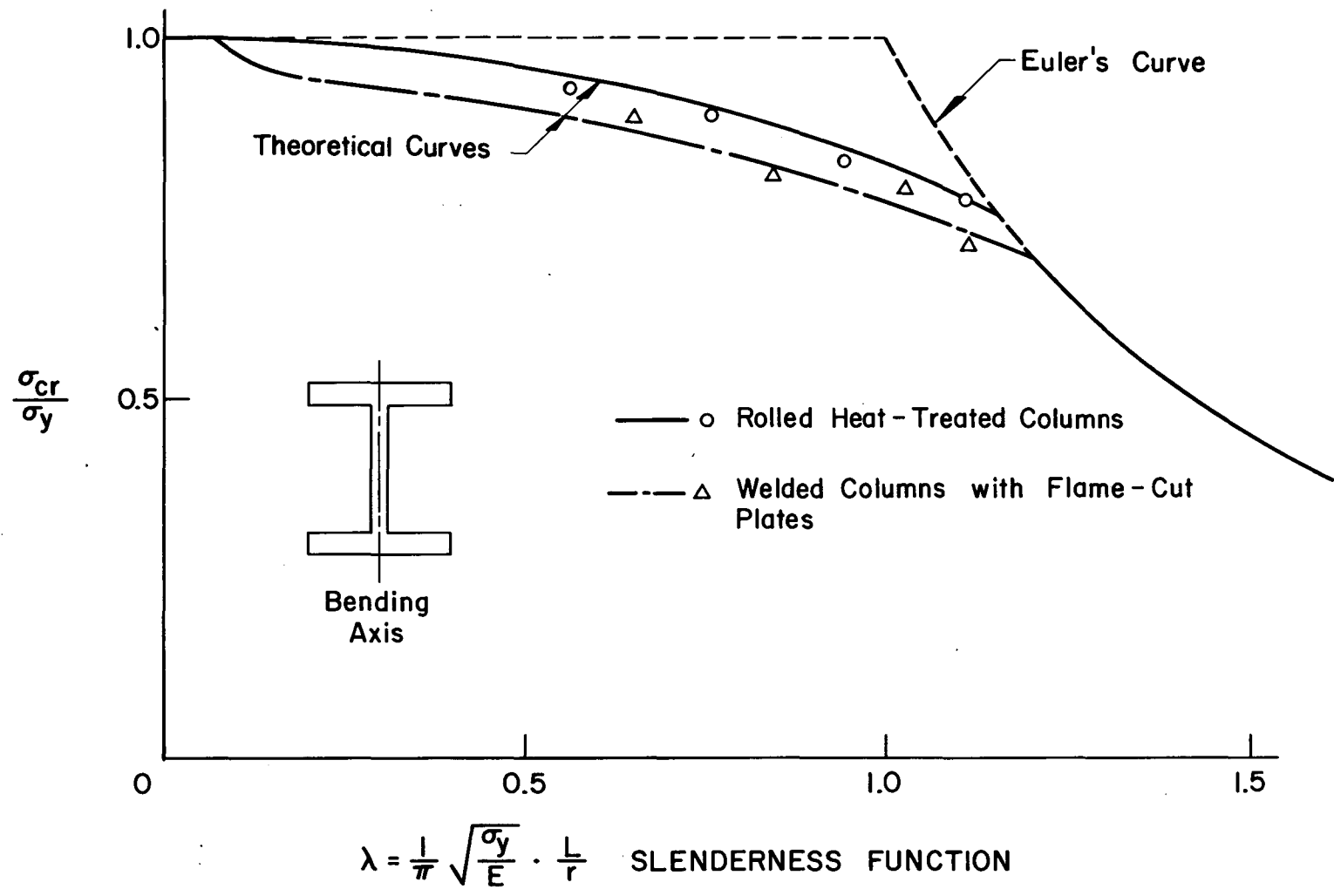


Fig. 19 COLUMN CURVES FOR H-SHAPES OF T-1 STEEL

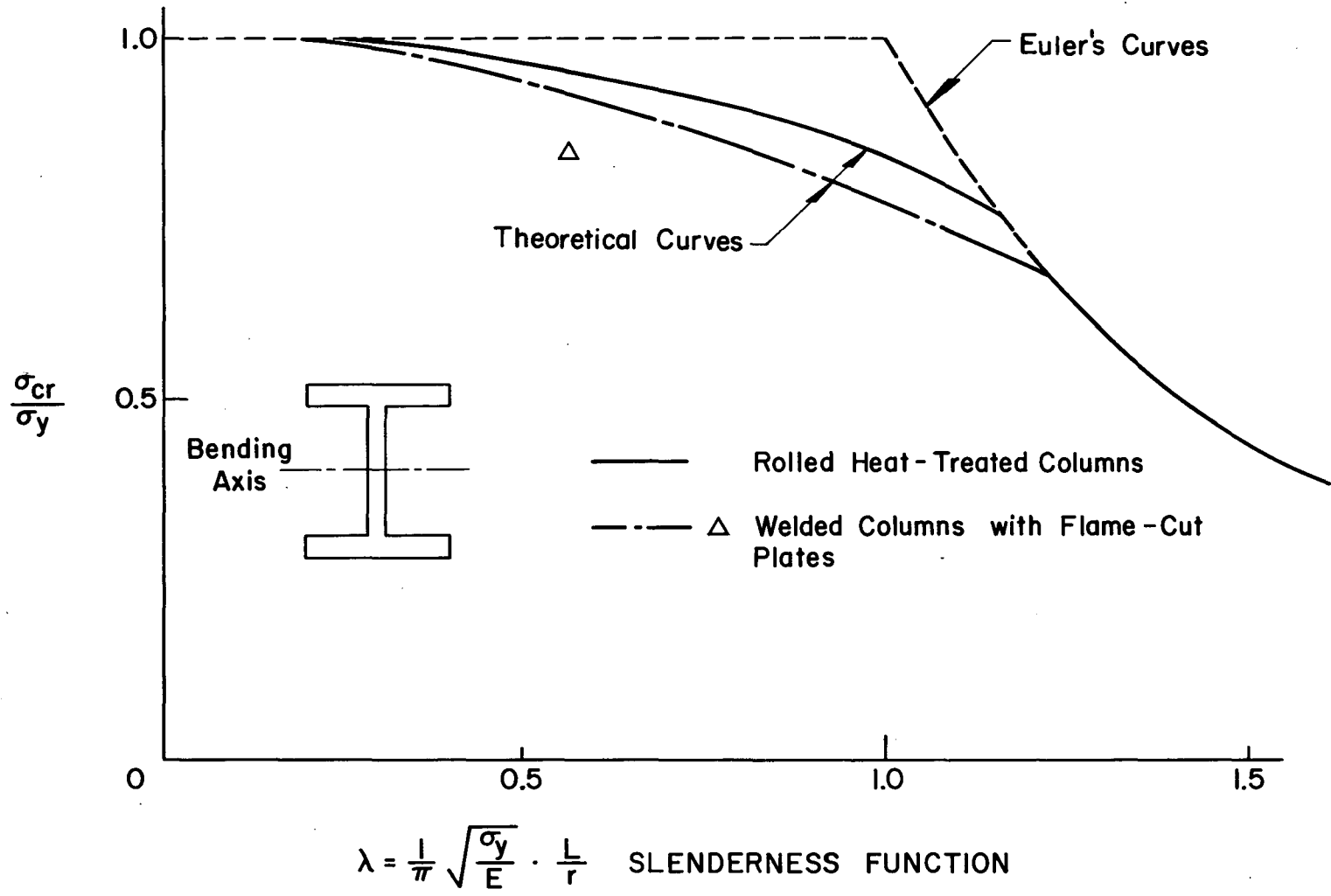


Fig. 20 COLUMN CURVES FOR H-SHAPES OF T-1 STEEL

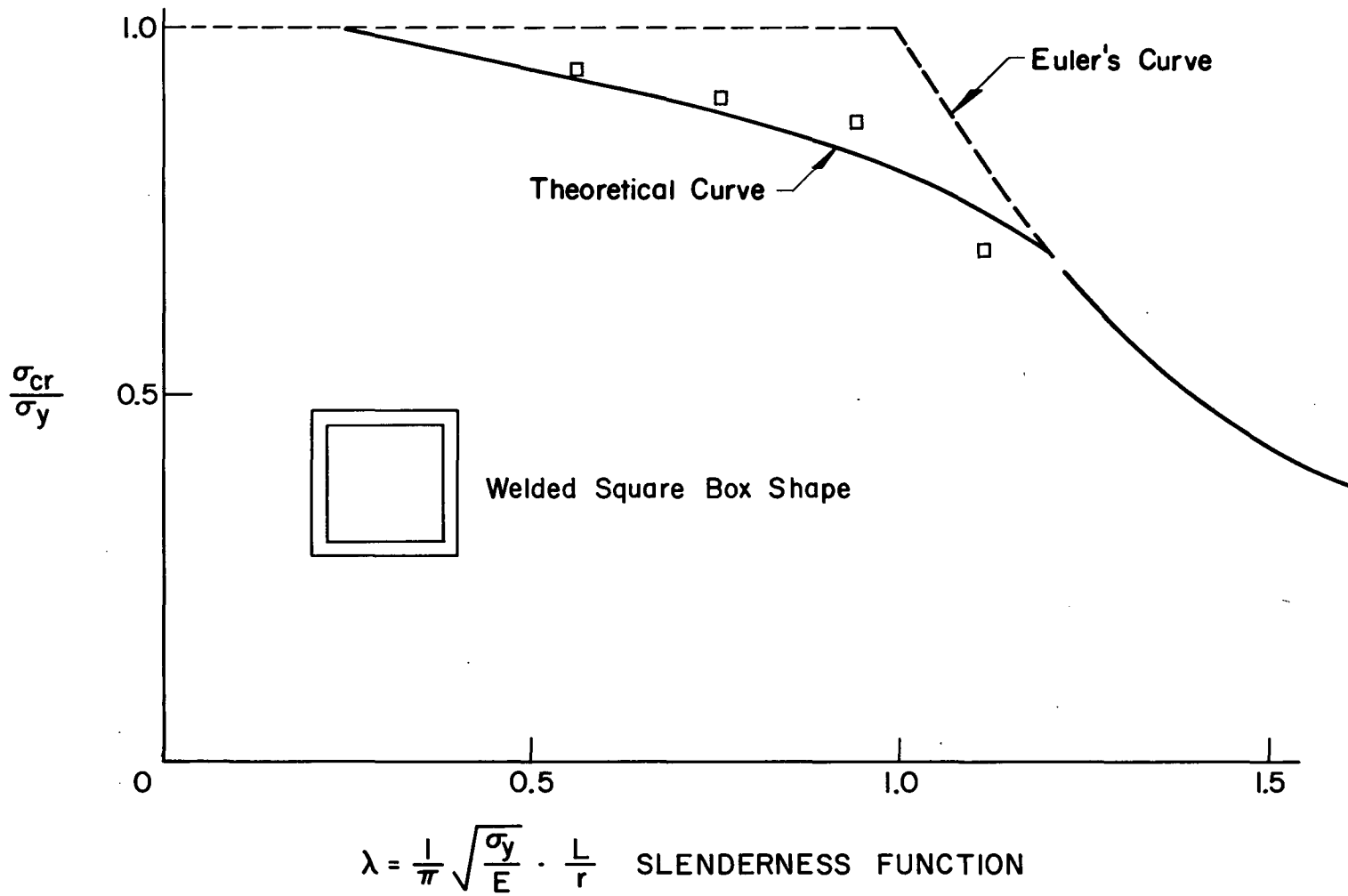


Fig. 21 COLUMN CURVES FOR WELDED SQUARE BOX SHAPES OF T-1 STEEL

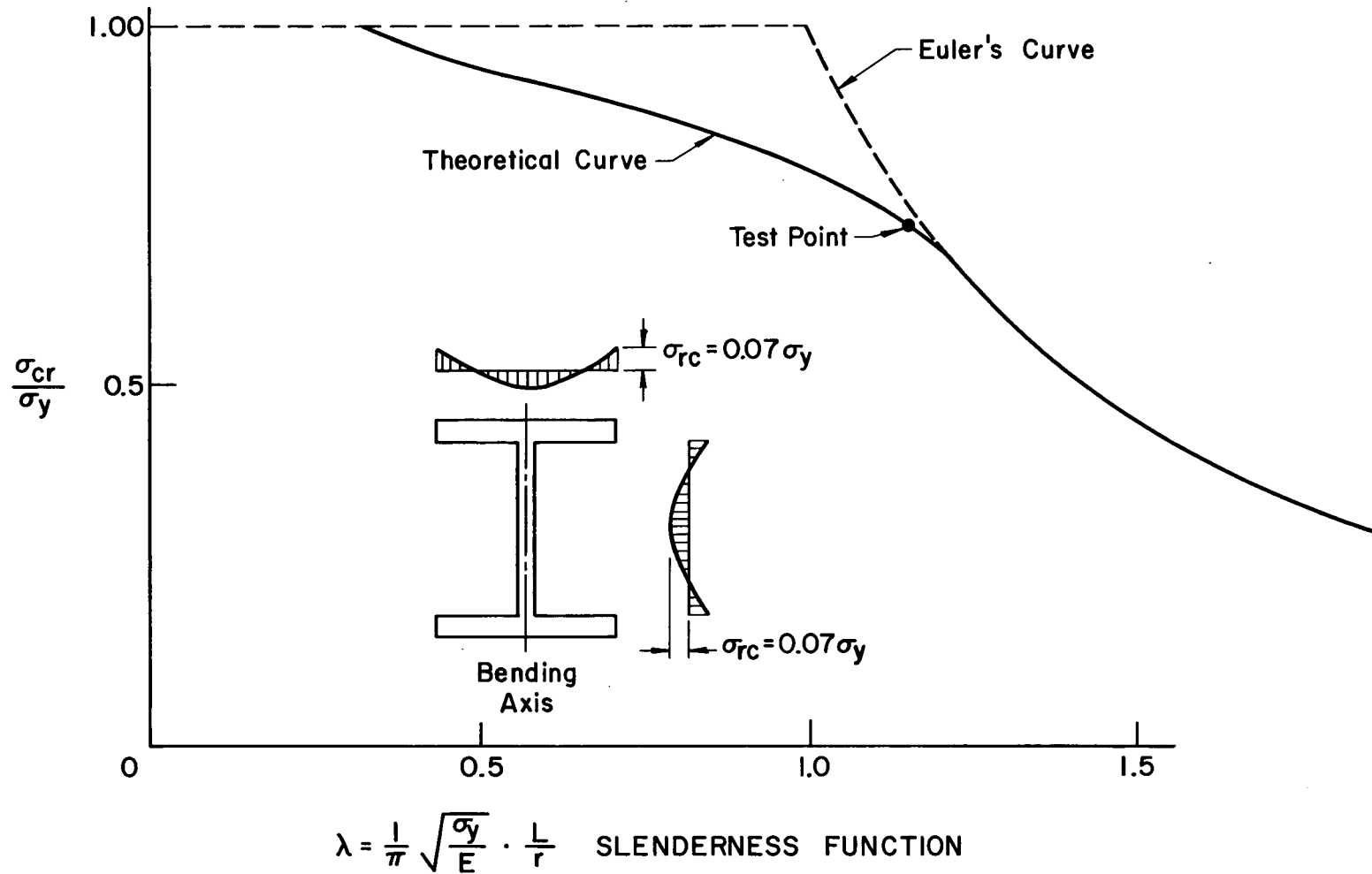


Fig. 22 COLUMN STRENGTH CURVES FOR H-SHAPES OF 5 Ni-Cr-MO-V STEEL

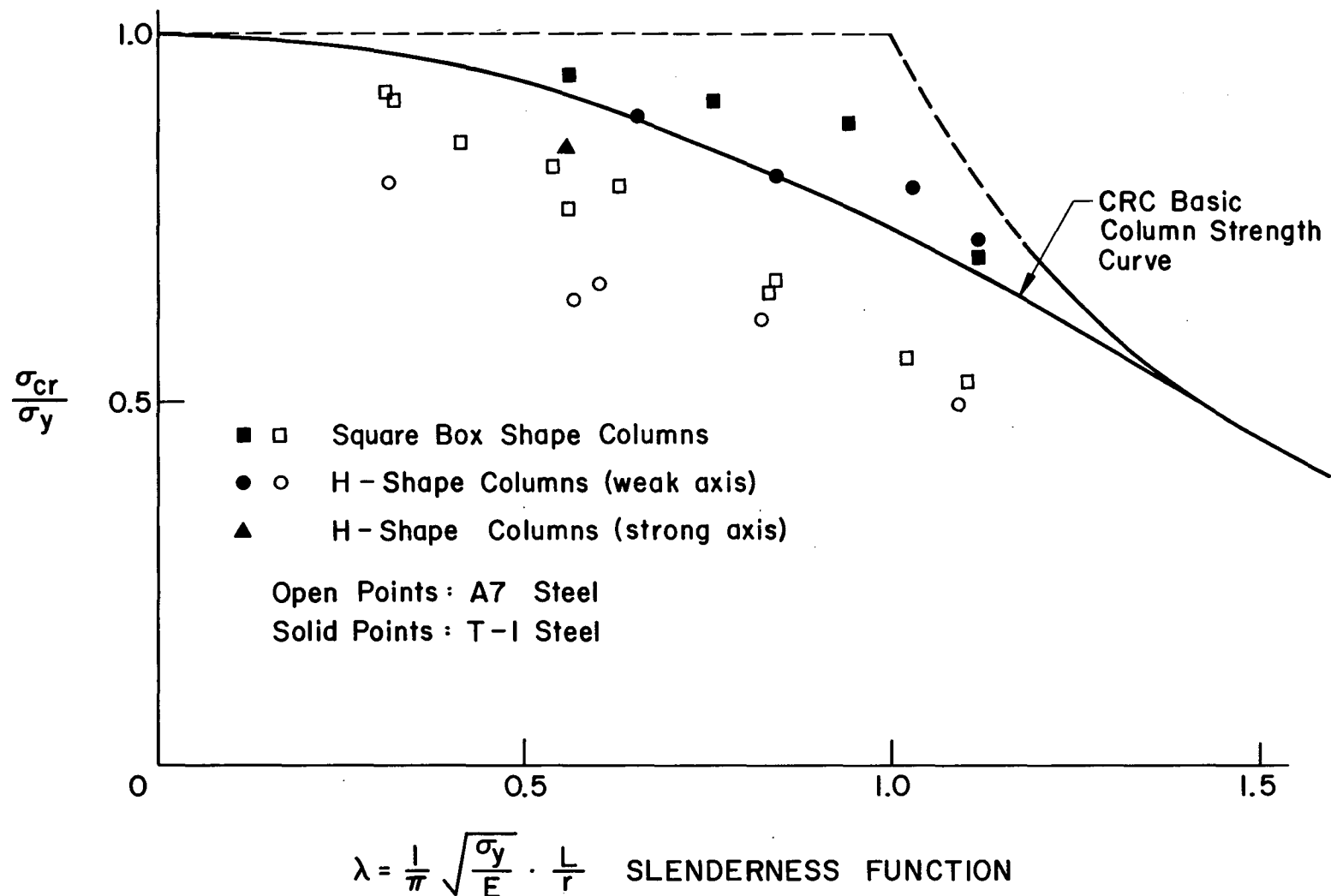


Fig. 23 WELDED COLUMN STRENGTH

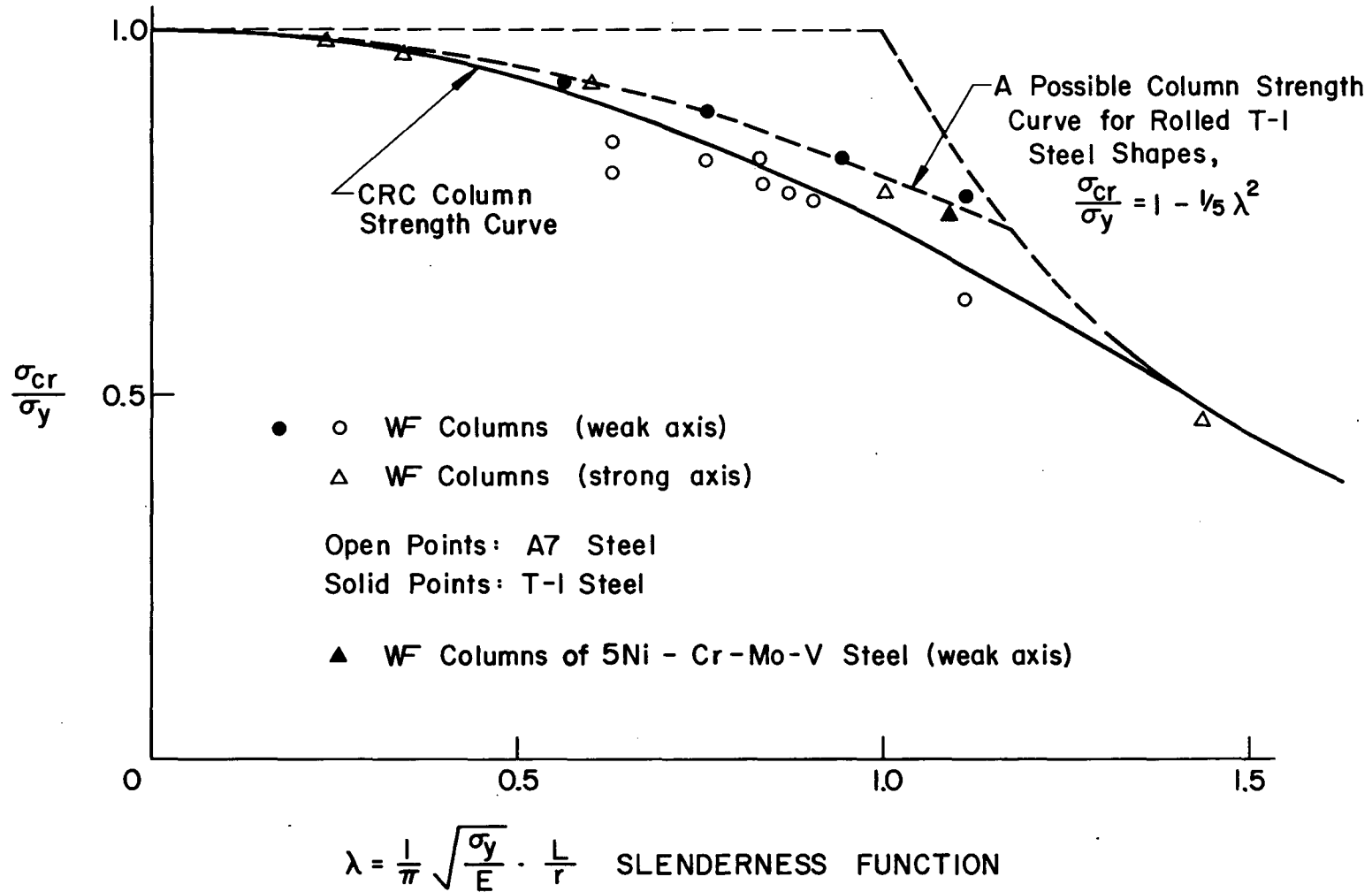
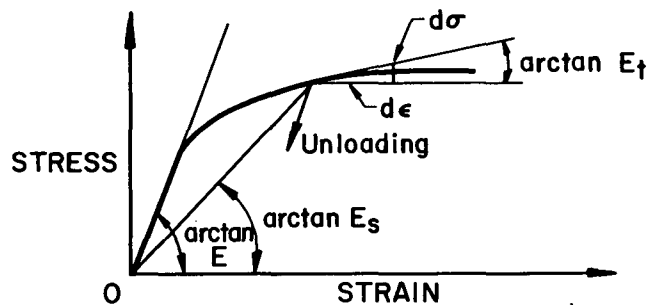
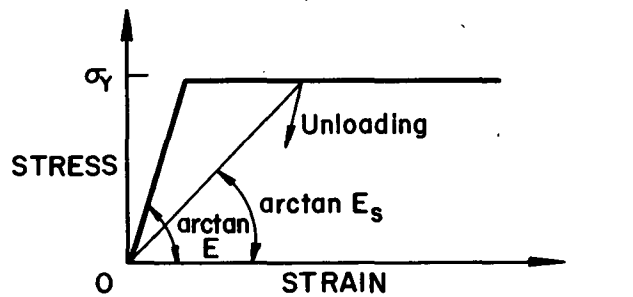


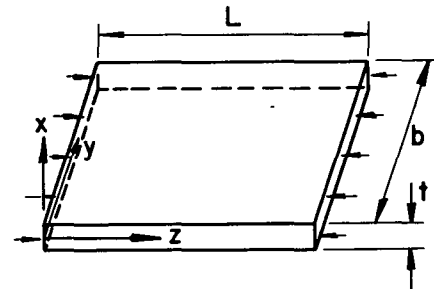
Fig. 24 ROLLED COLUMN STRENGTH



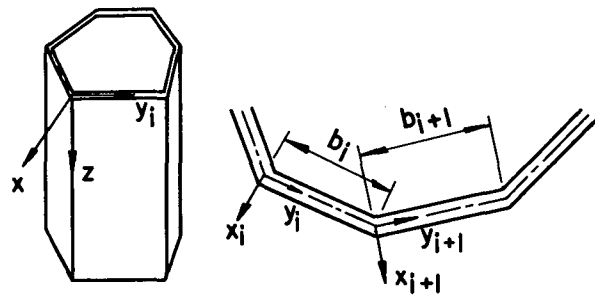
(a) General Case



(b) Idealized Relationship for Steel
(Elastic Perfectly Plastic Material)



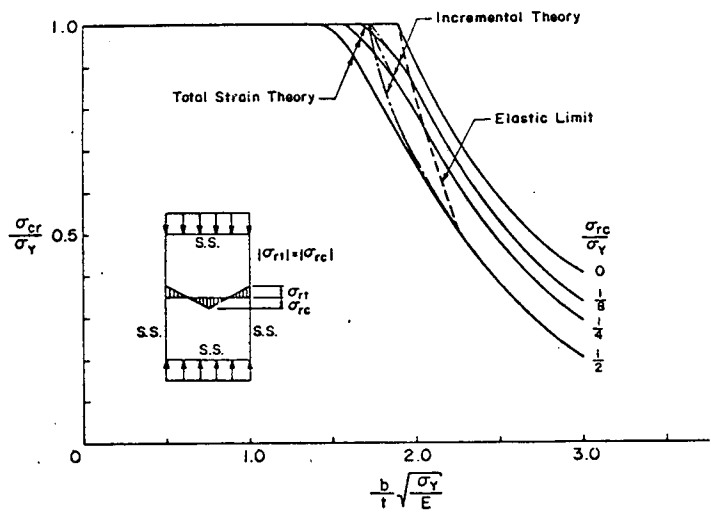
(a) Coordinate Axes for Plates



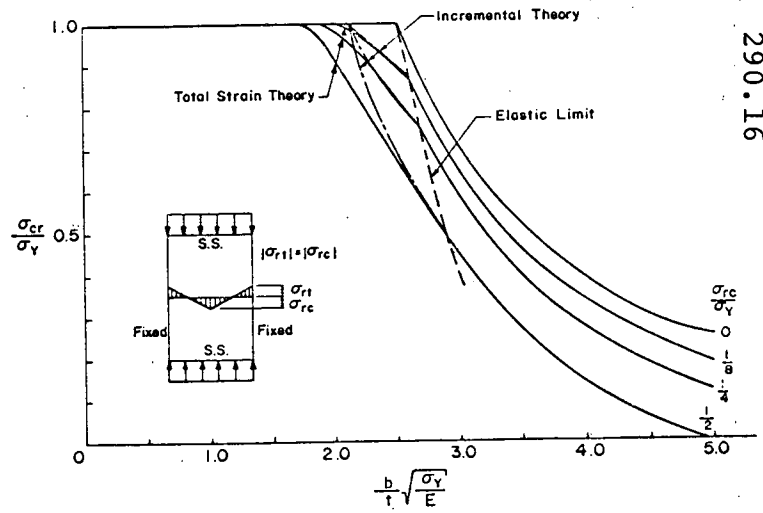
(b) Coordinate Axes for Plate Assemblies

Fig. 25 STRESS-STRAIN RELATIONSHIP

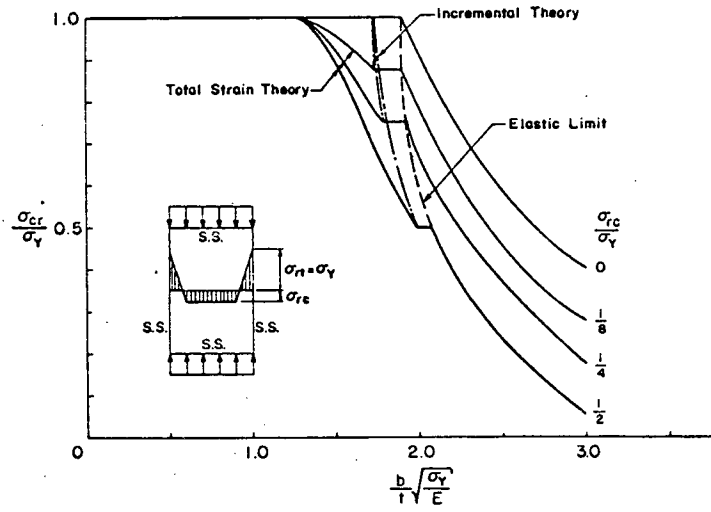
Fig. 26 COORDINATE AXES FOR
ANALYSIS OF LOCAL BUCKLING



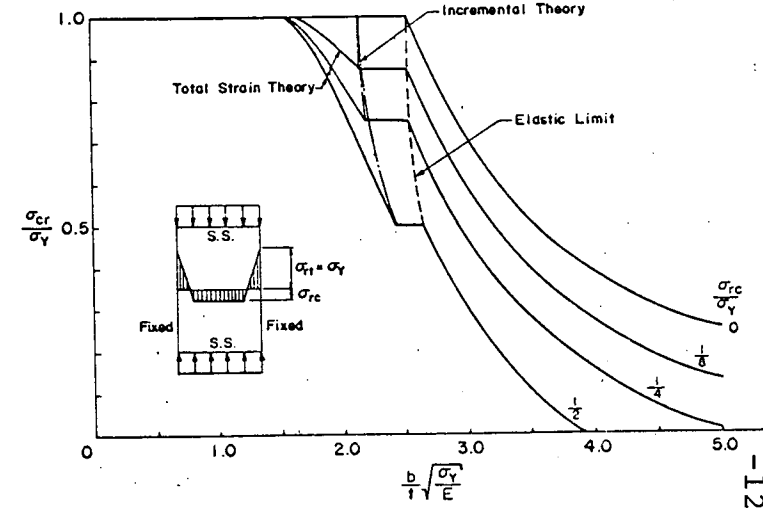
(a) With Residual Stress of Cooling Pattern



(a) With Residual Stress of Cooling Pattern



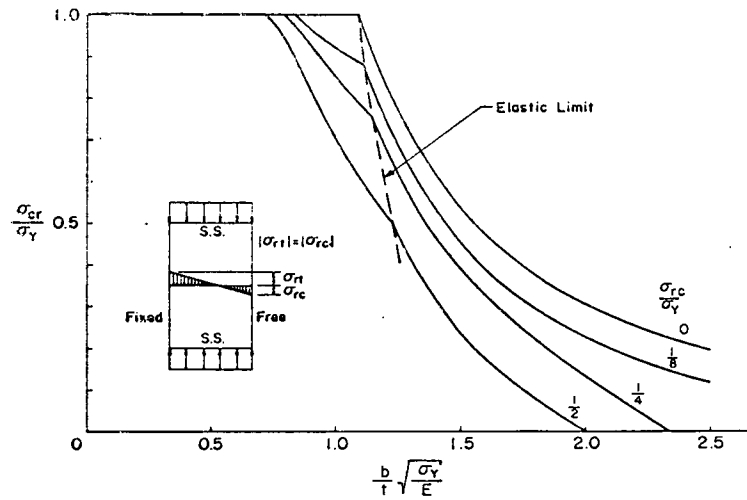
(b) With Residual Stress of Welding Pattern



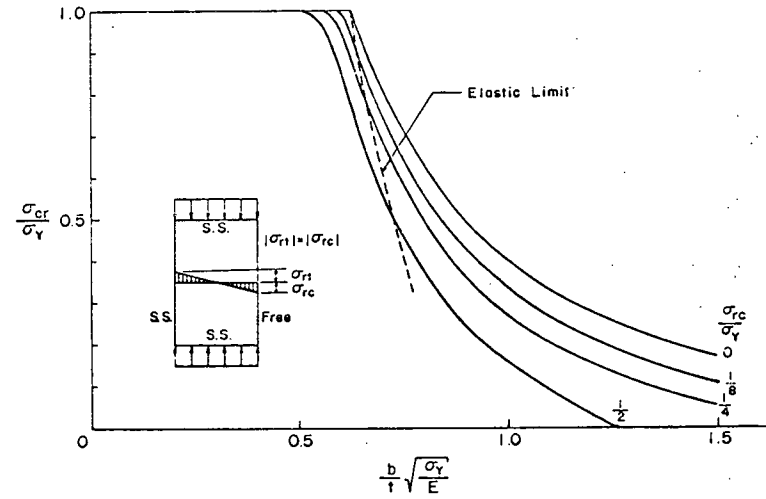
(b) With Residual Stress of Welding Pattern

FIG. 27 PLATE BUCKLING CURVE (S.S. PLATE AT UNLOADED EDGES)

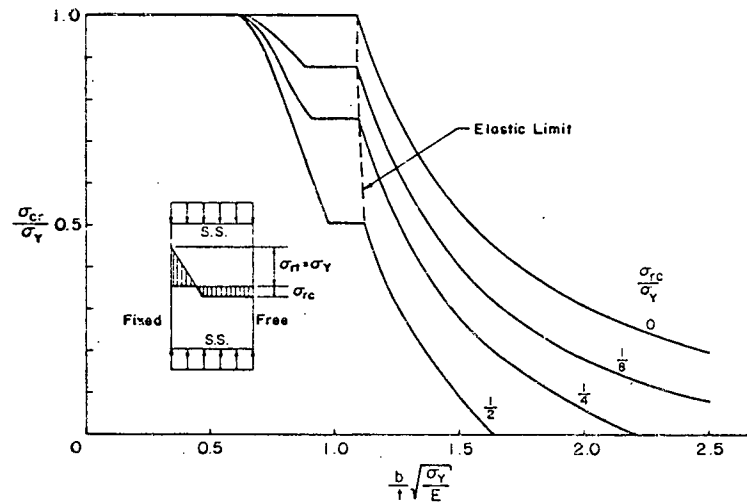
FIG. 28 PLATE BUCKLING CURVE (PLATE FIXED AT UNLOADED EDGES)



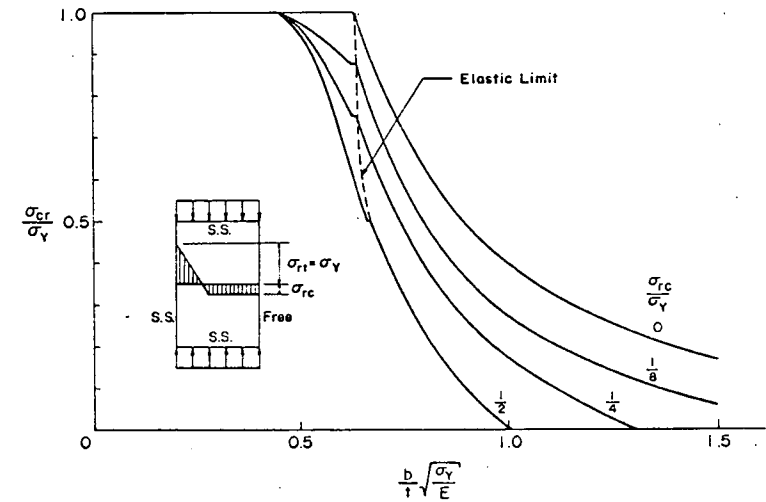
(a) With Residual Stress of Cooling Pattern



(a) With Residual Stress of Cooling Pattern



(b) With Residual Stress of Welding Pattern



(b) With Residual Stress of Welding Pattern

FIG. 29 PLATE BUCKLING CURVE (PLATE FIXED AND FREE AT UNLOADED EDGES, TOTAL STRAIN THEORY)

FIG. 30 PLATE BUCKLING CURVE (PLATE S.S. AND FREE AT UNLOADED EDGES, TOTAL STRAIN THEORY)

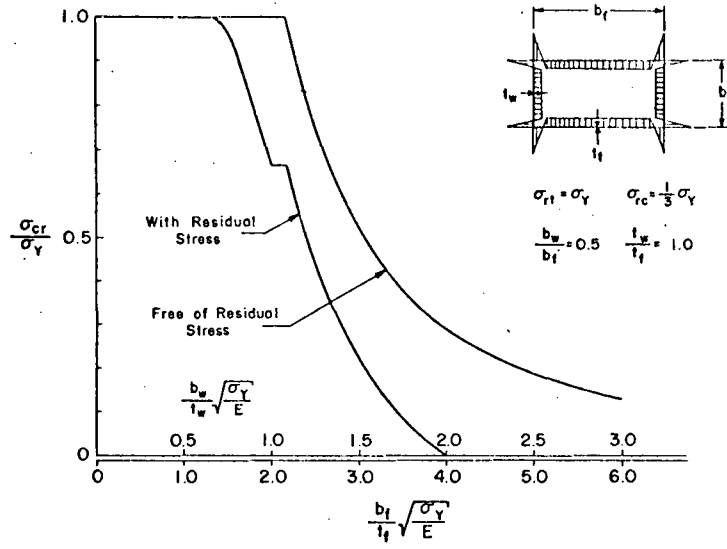
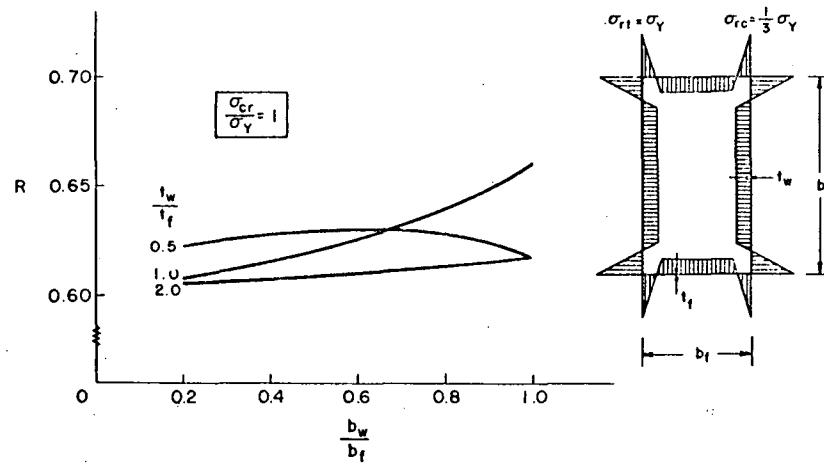
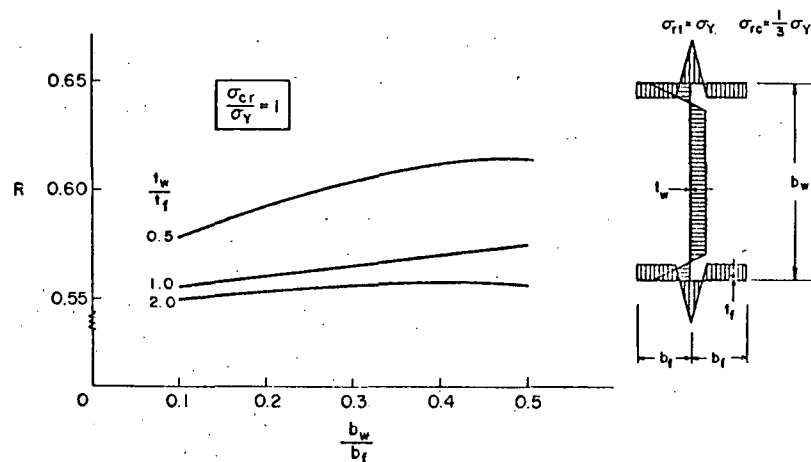


FIG. 31 LOCAL BUCKLING CURVE

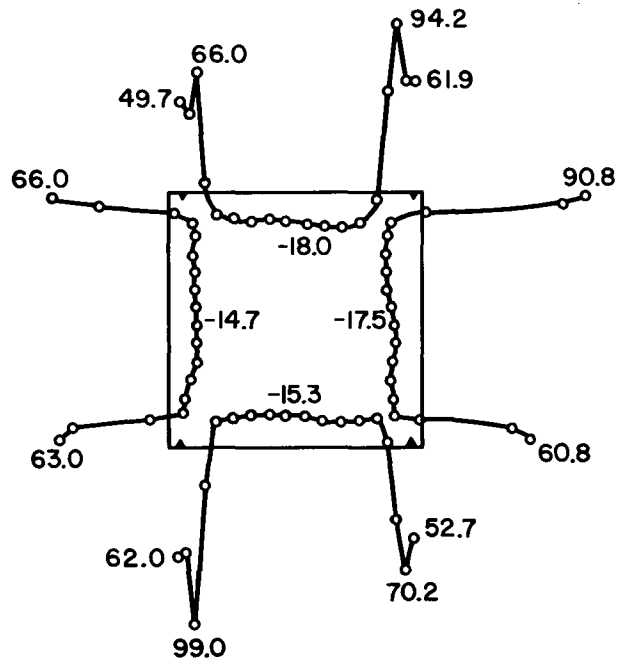


(a) Box-Column



(b) H-Column

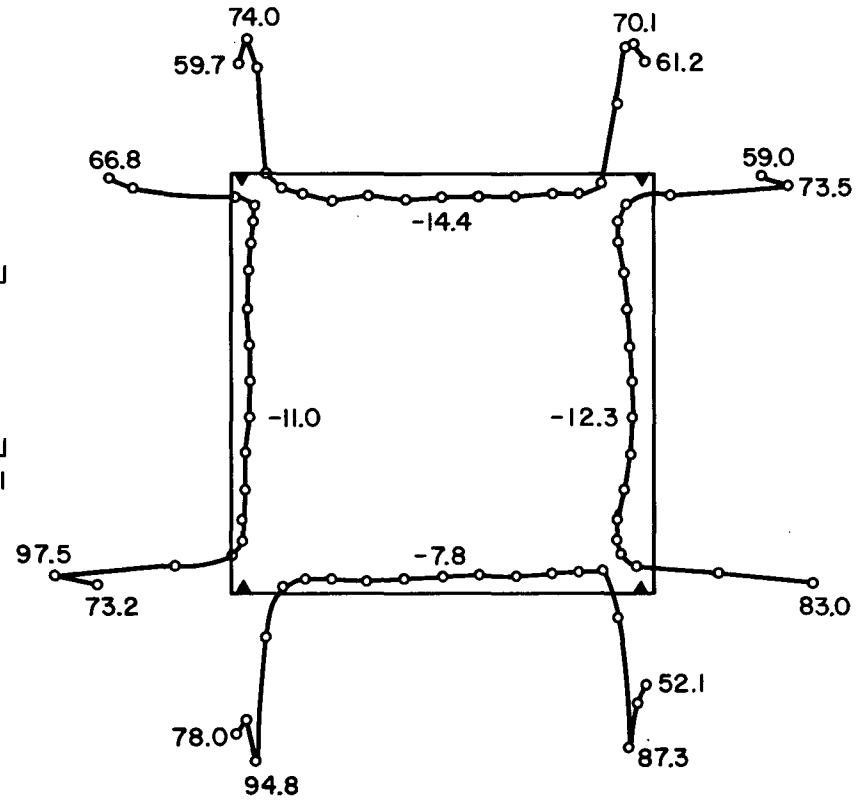
FIG. 32 REDUCTION FACTOR OF WIDTH-THICKNESS RATIO



Piece 1 (T-1A, T-1B)

2 IN.

40 KSI



Piece 2 (T-2A, T-2B)

Fig. 33 RESIDUAL STRESS DISTRIBUTIONS IN TEST SPECIMENS

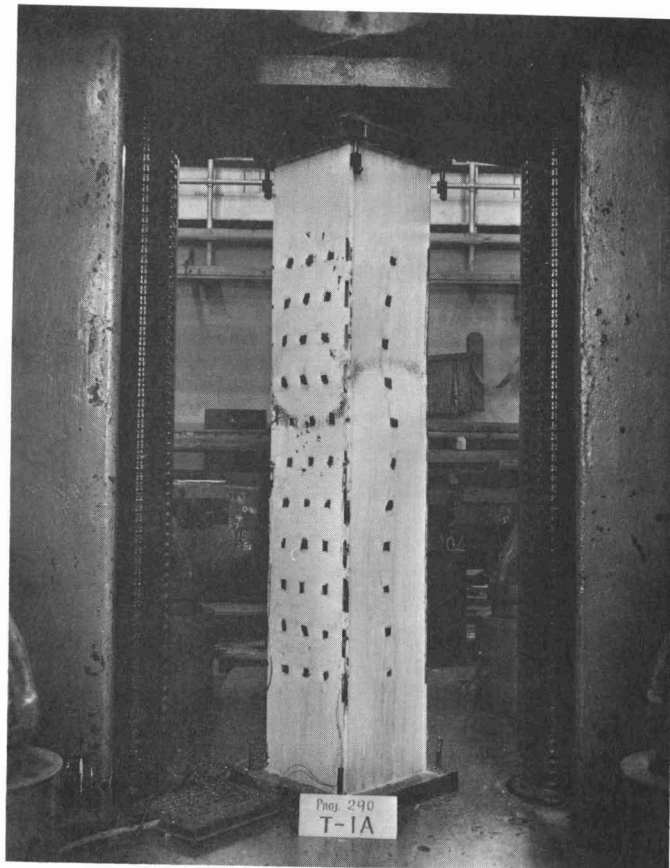


Fig. 34 Test Set-Up (Specimen at Ultimate Load)

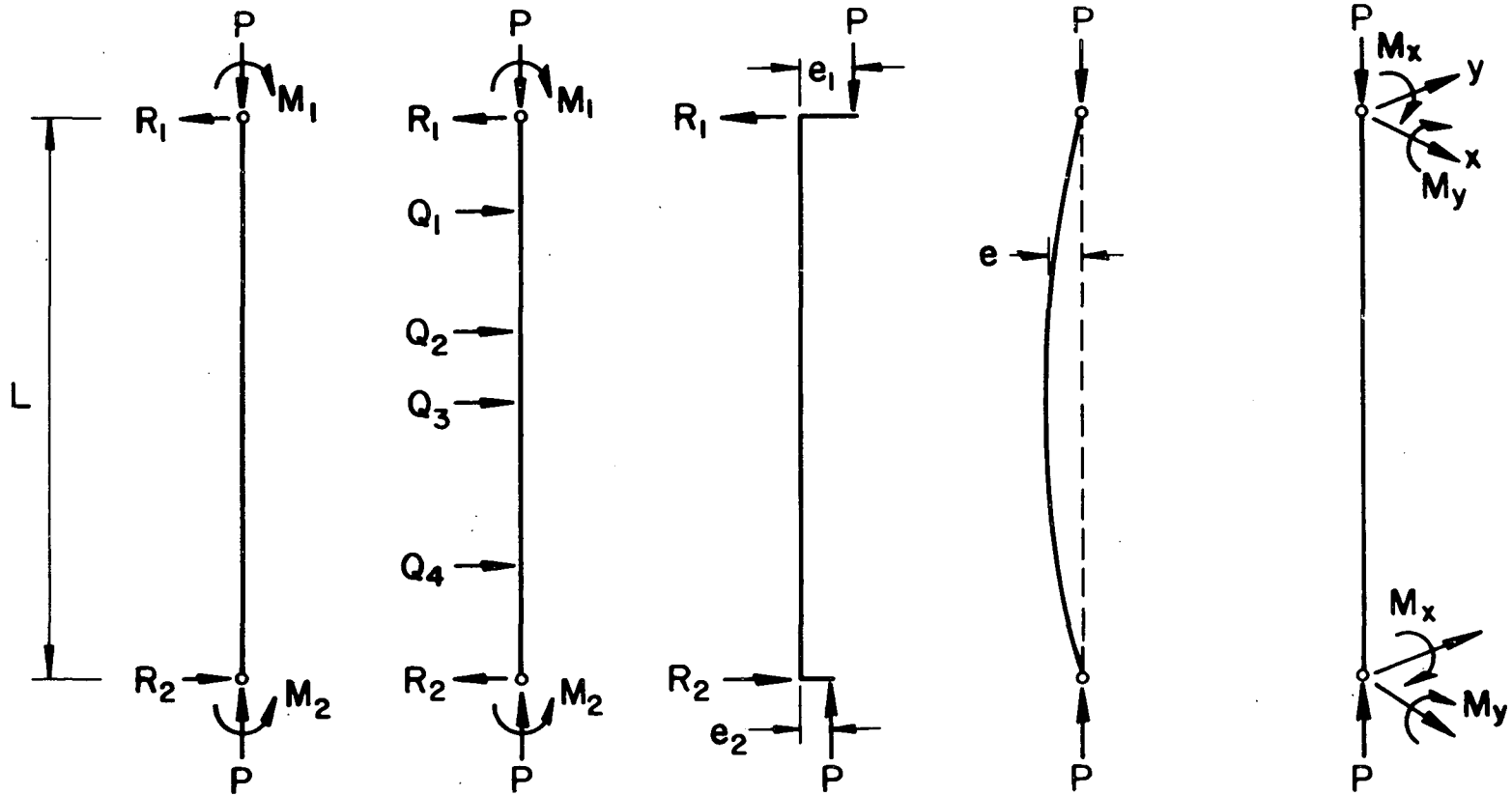


Fig. 37 Several Typical Beam-Columns

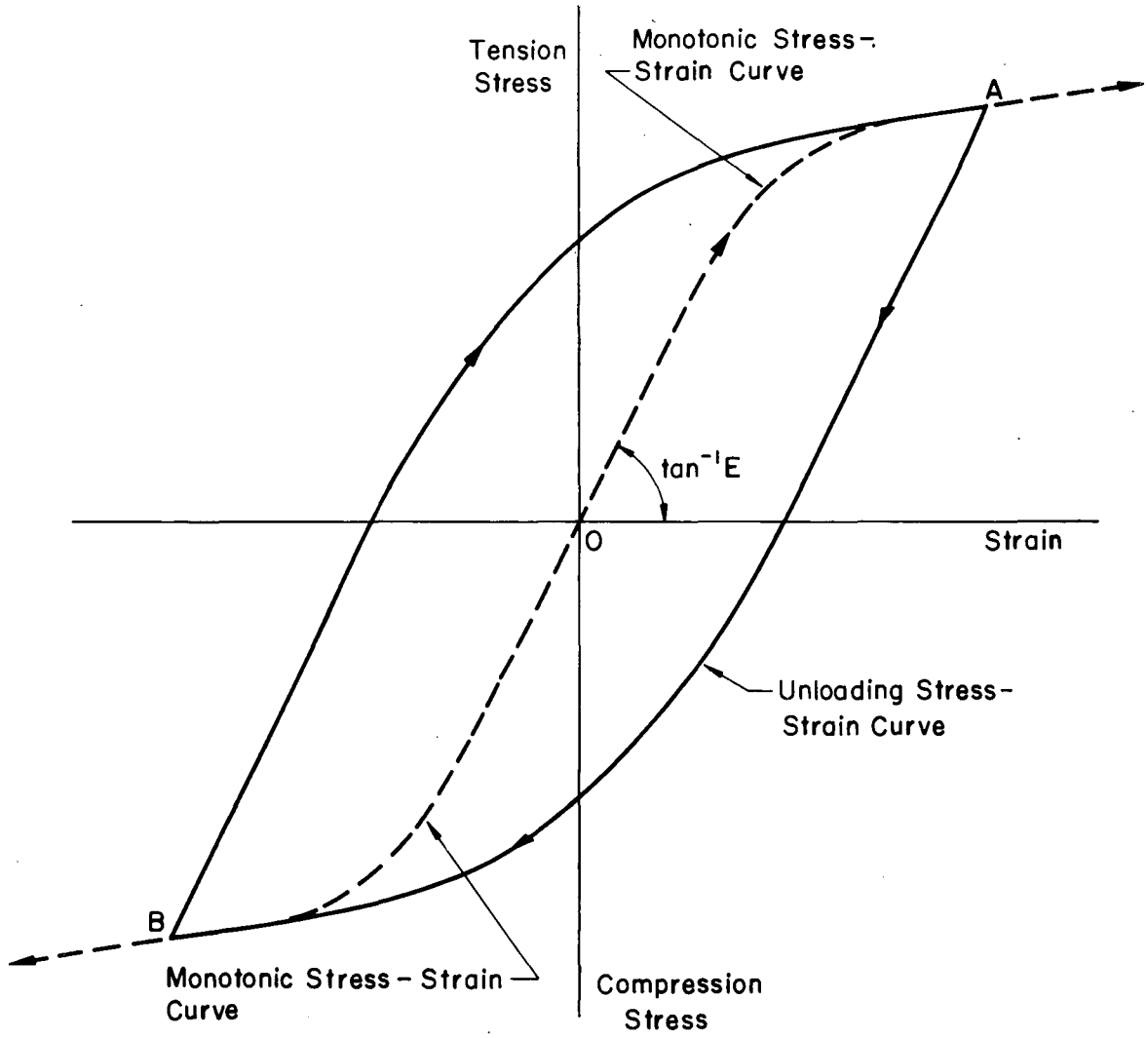


Fig. 38 Unloading Stress-Strain Curve

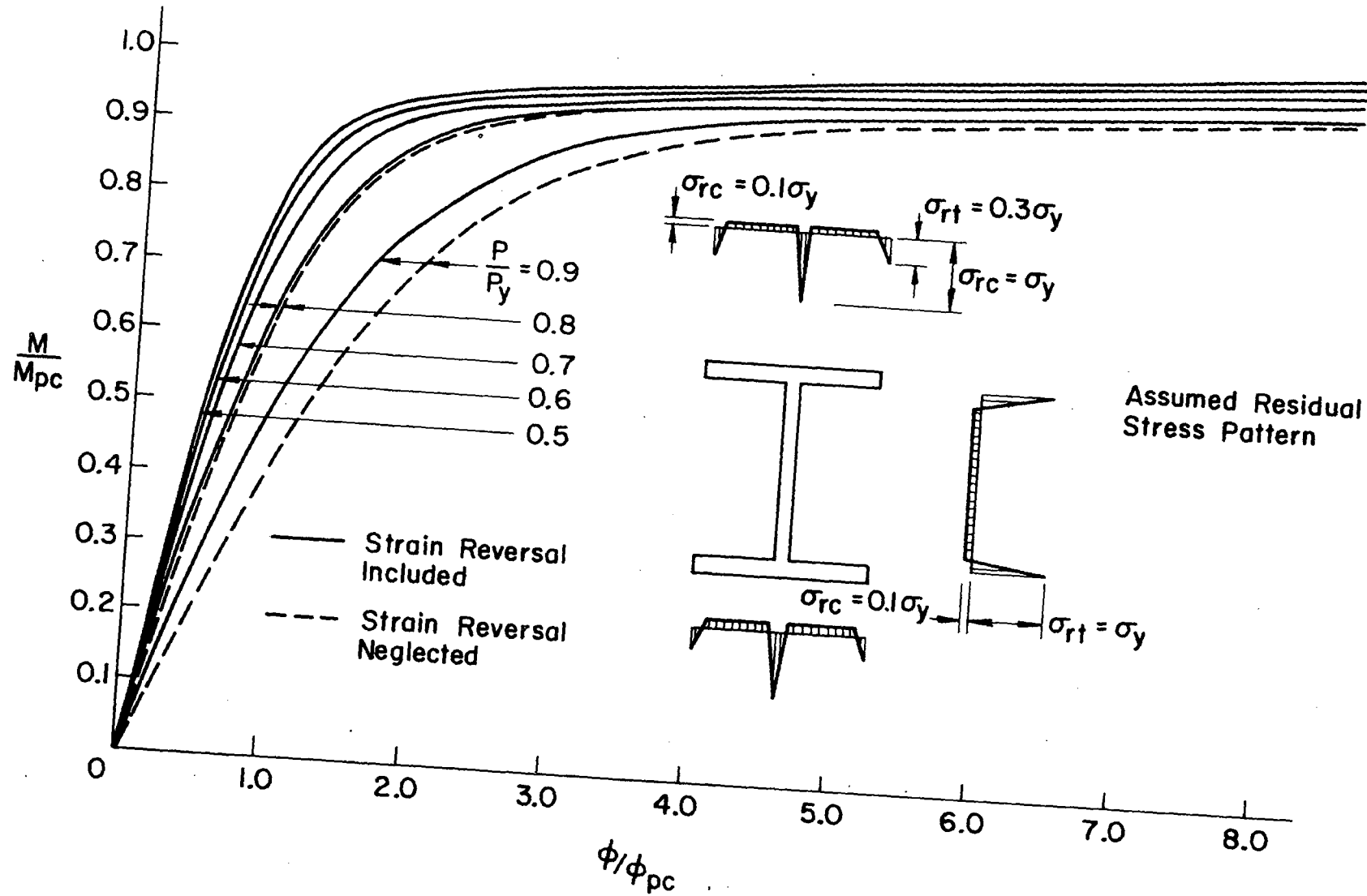


Fig. 39 Moment-Curvature-Thrust Relationship

Curve No.	1	2	3	4	5
Residual Stress	A	B	B	C	C
Stress-Strain Curve *	E	E	P	E	P

* E - Elastic Perfectly Plastic $\sigma - \epsilon$ Curve
P-T-1 Steel $\sigma - \epsilon$ Curve

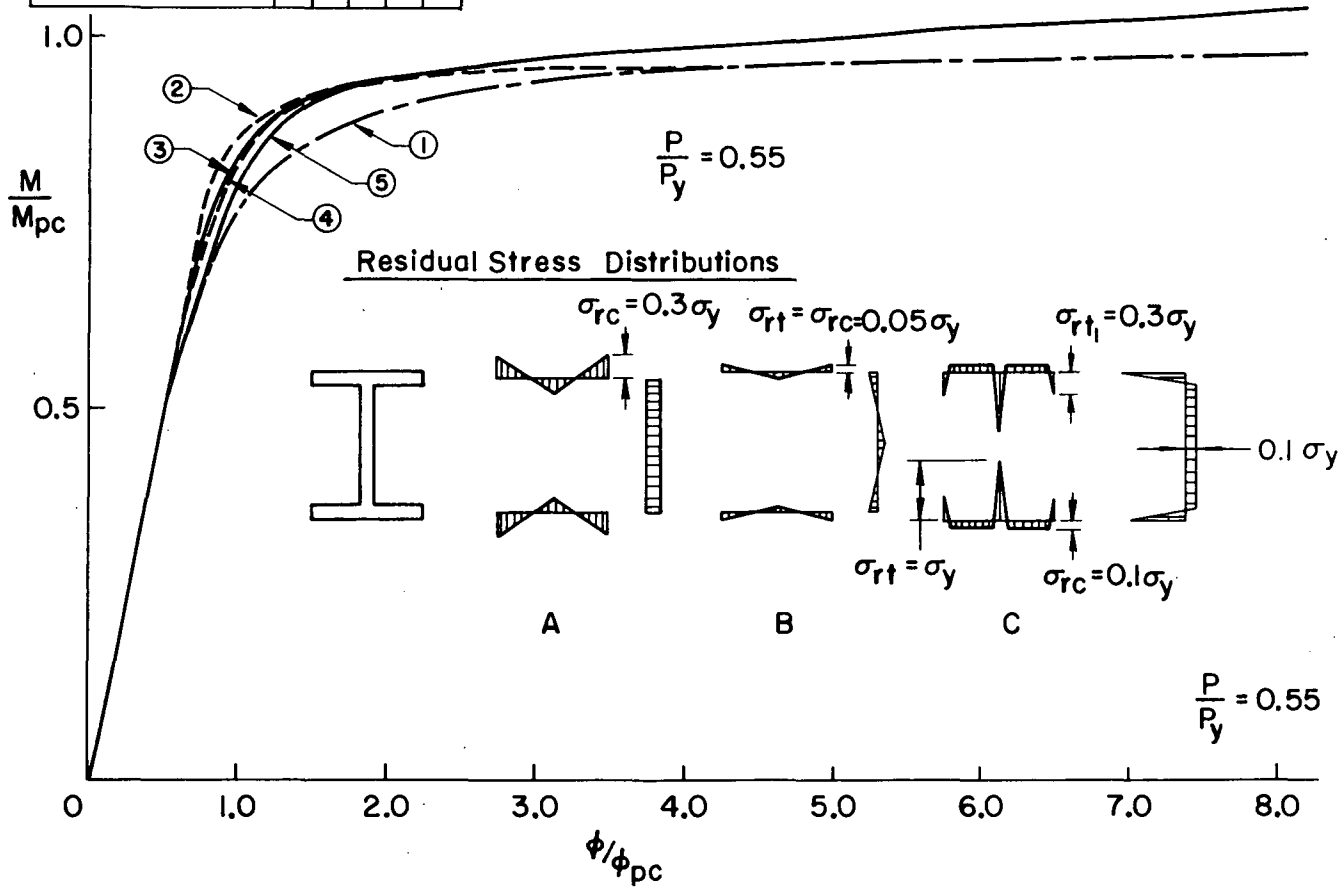
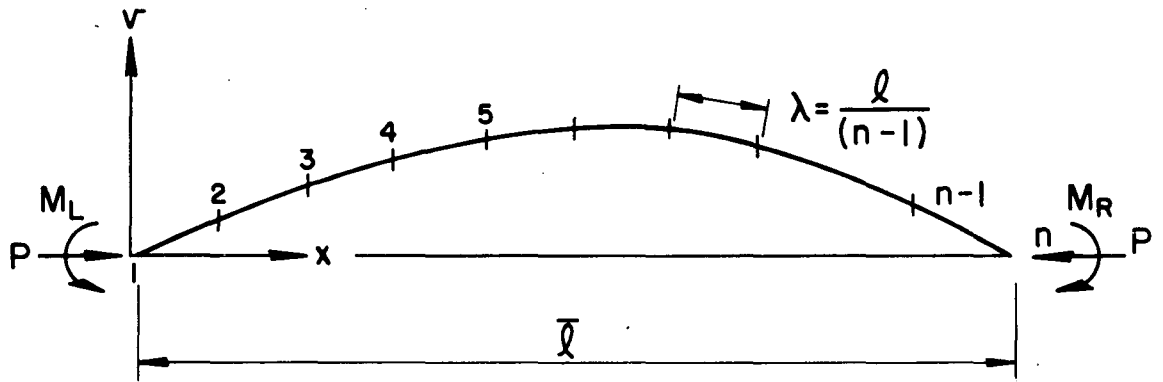
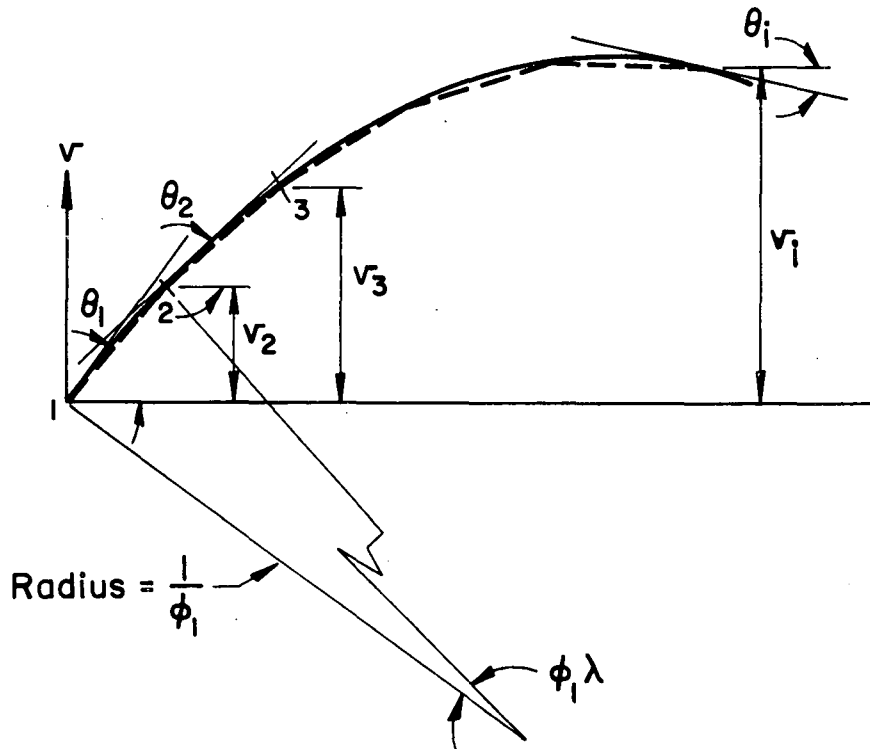


Fig. 40 Comparison of Moment-Curvature-Thrust Curves



(a)



(b)

Fig. 41 Numerical Procedure for Calculating Load-Deflection Relationship

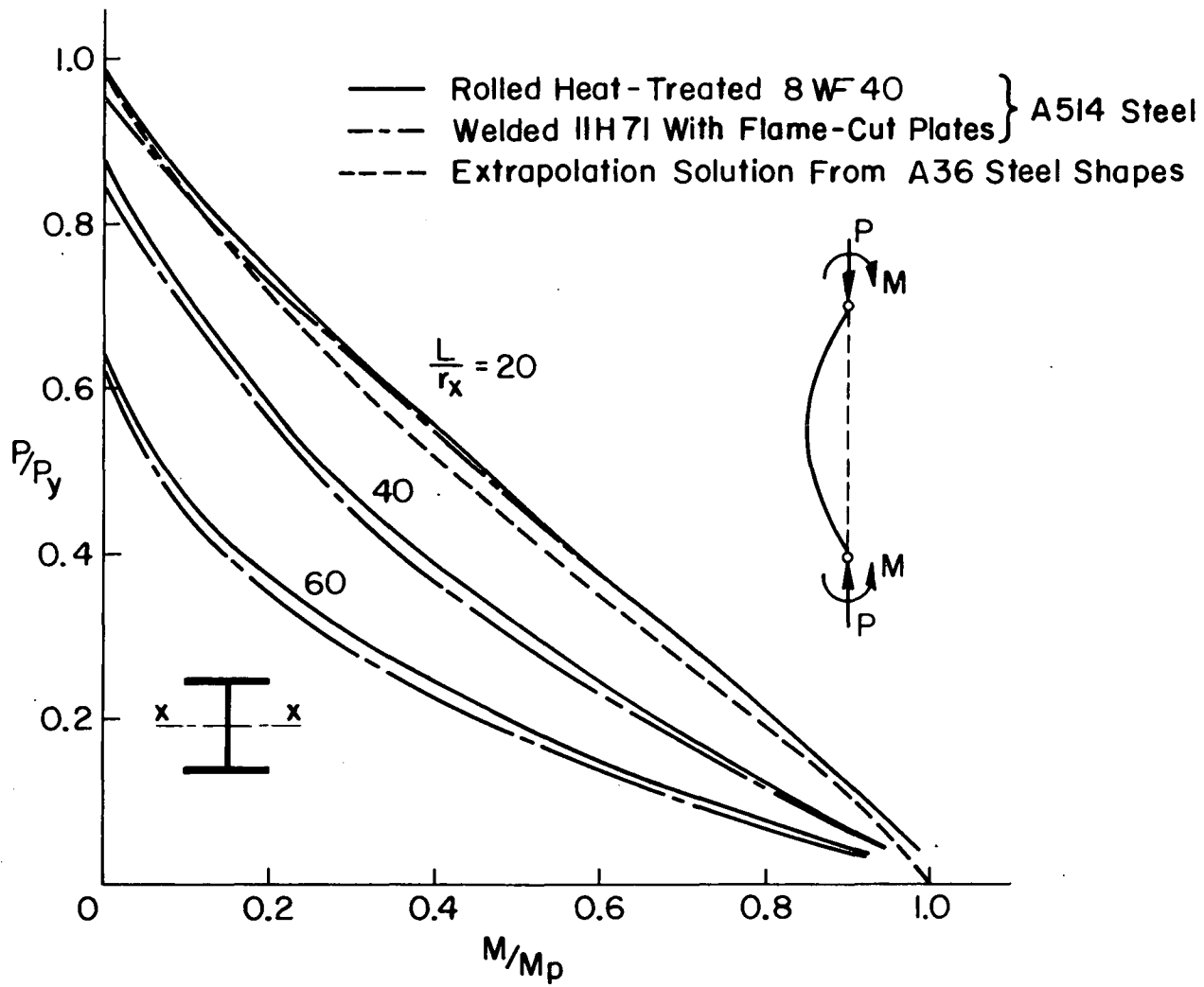
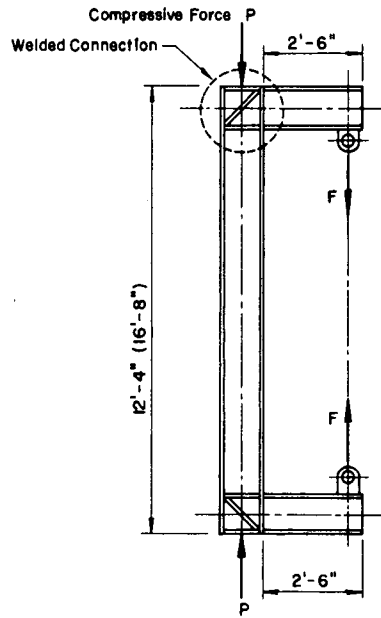
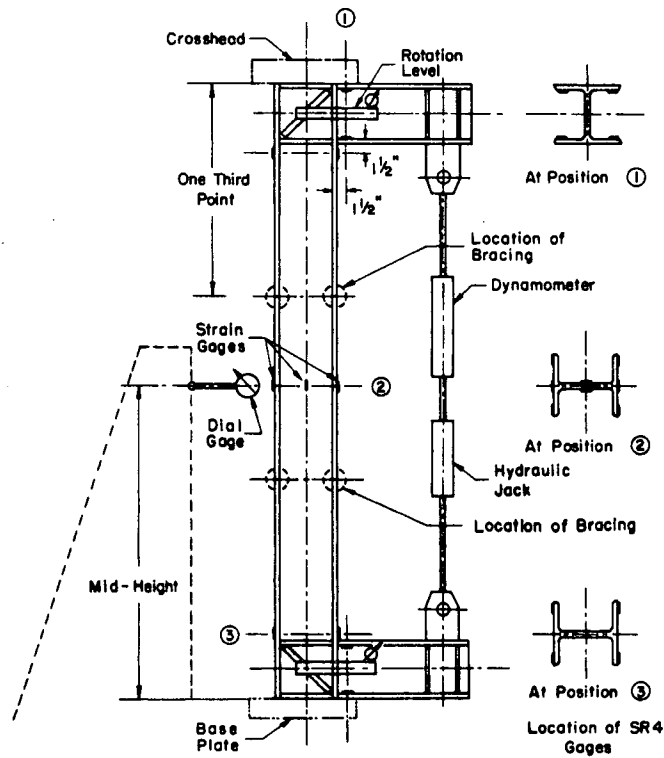


Fig. 42 Interaction Curves for A514 Steel Beam-Columns

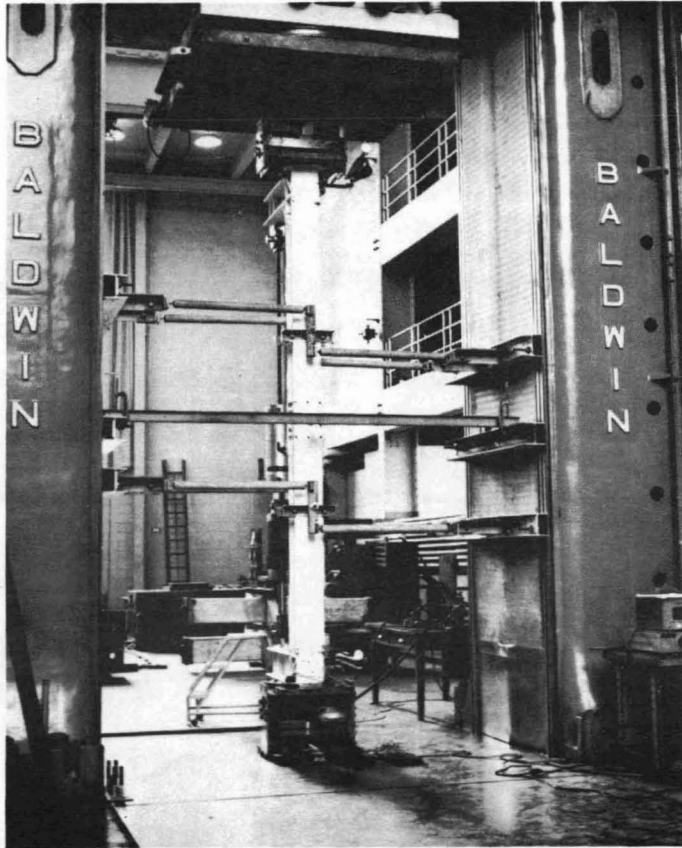


(a) GENERAL LAYOUT

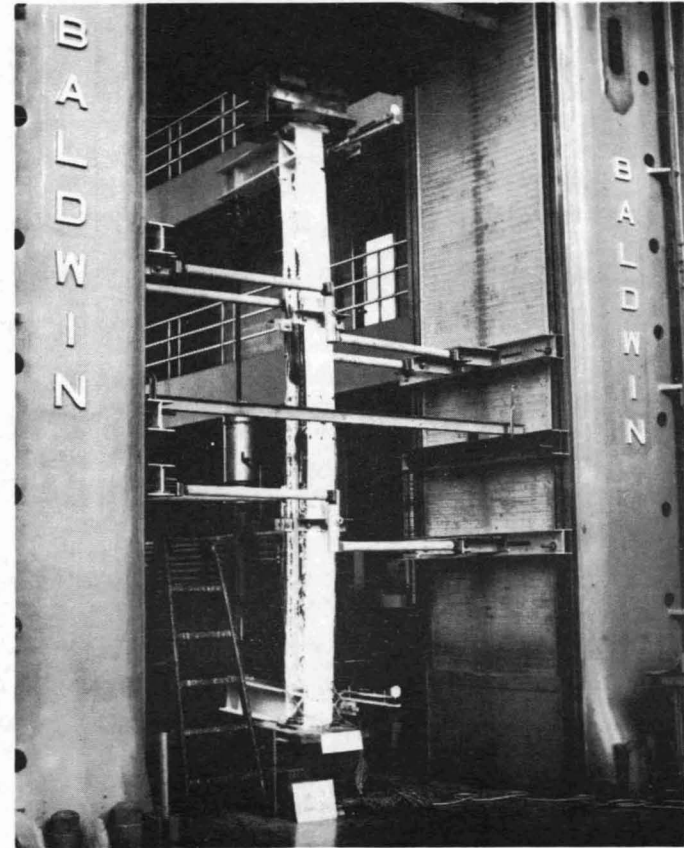


(b) INSTRUMENTATION

Fig. 43 Detail of the Beam-Column Specimen



(a) Beginning of Test



(b) End of Test

Fig. 44 Beam-Column in Testing Machine

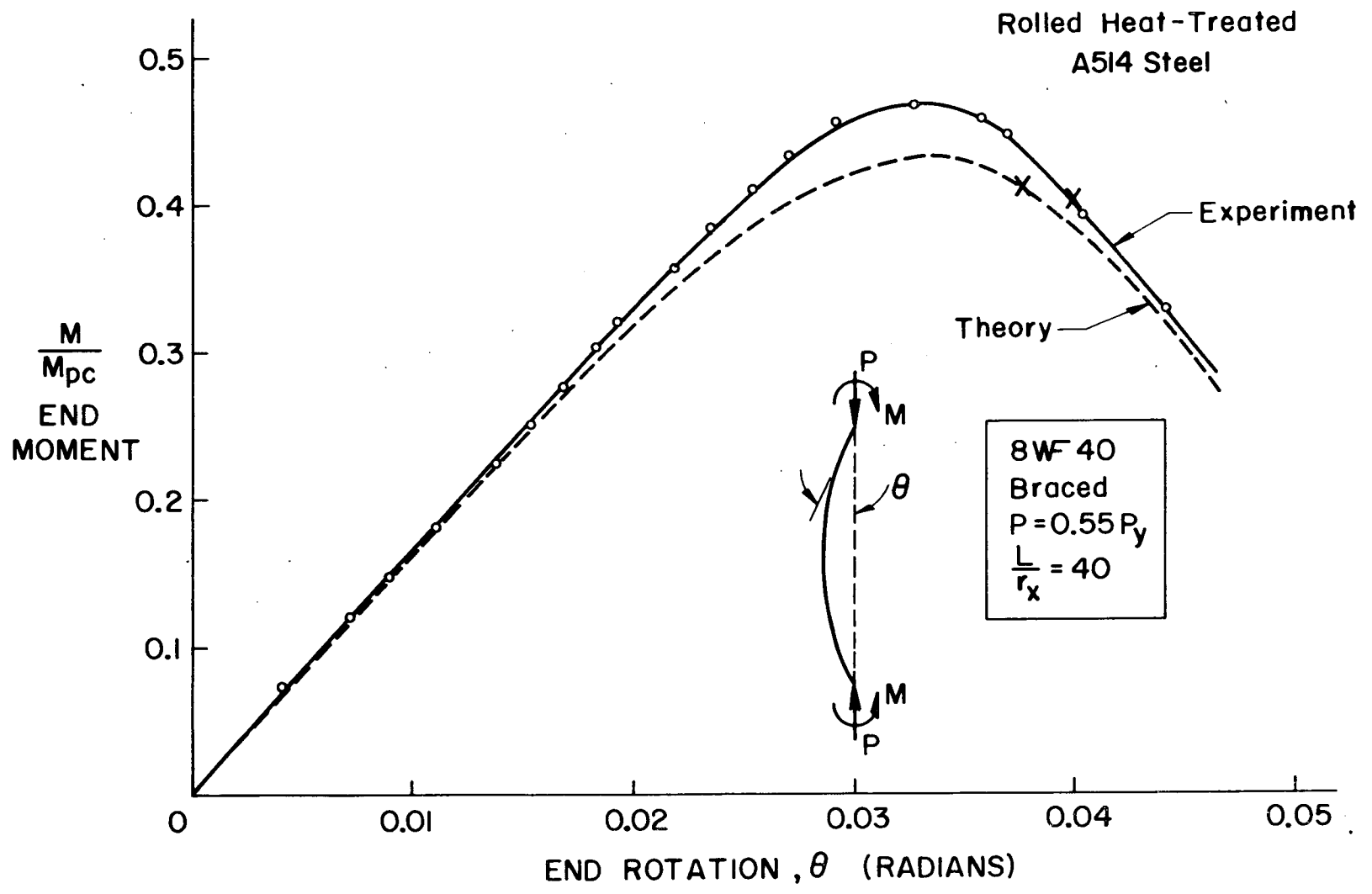


Fig. 45. Load-Deformation Relationship and Test Results

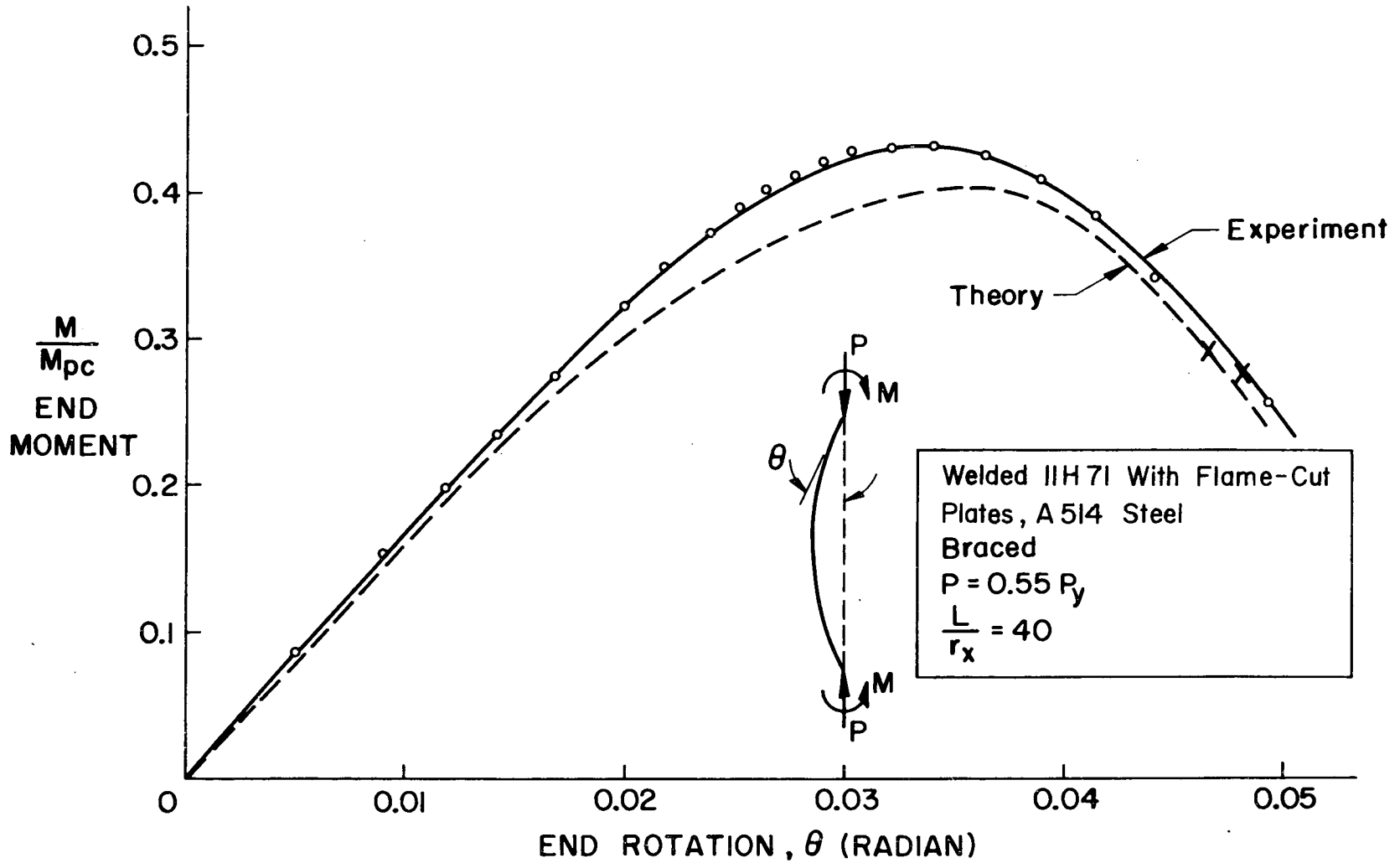
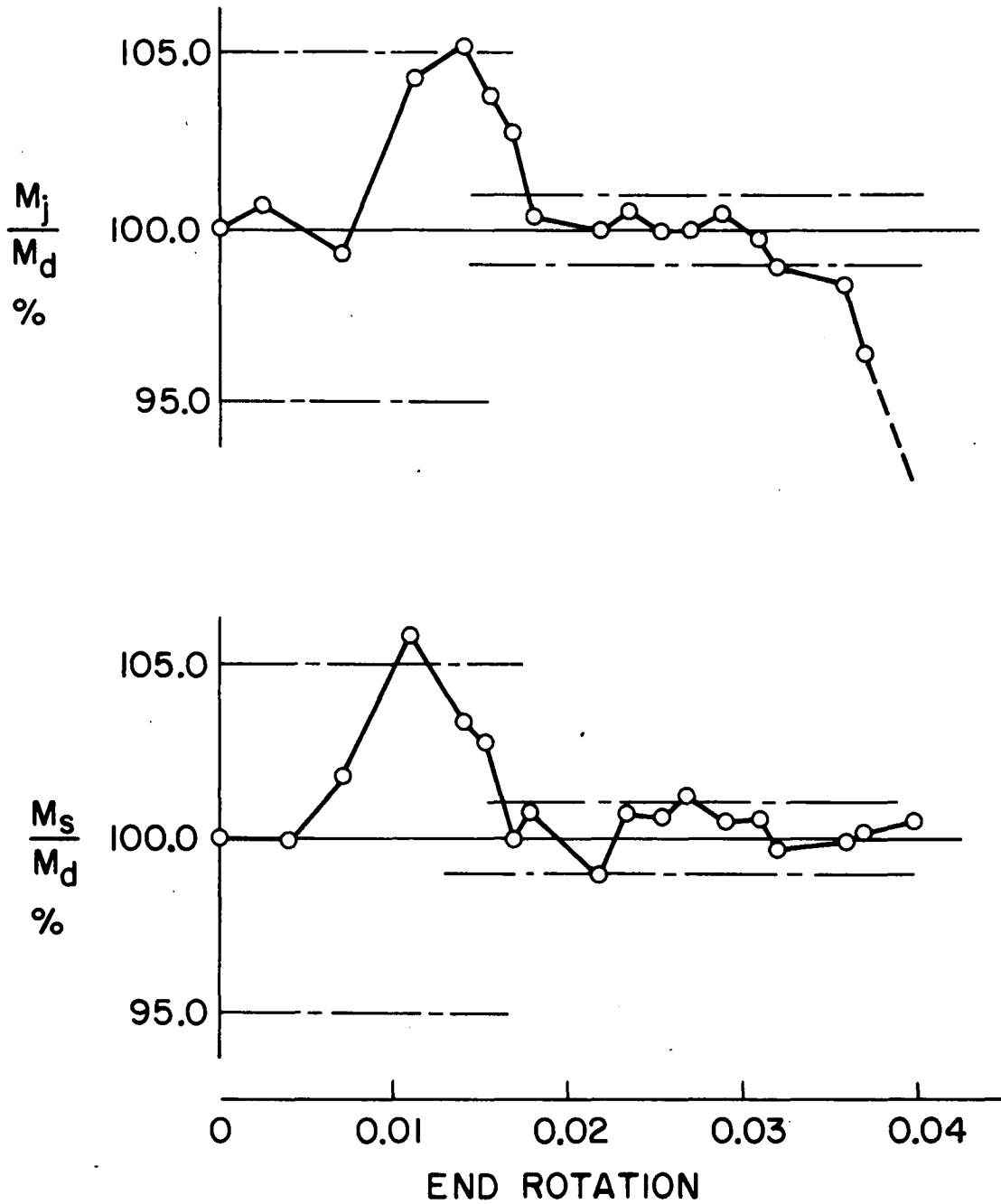


Fig. 46 Load-Deformation Relationship and Test Results



M_j Hydraulic Jack Reading
 M_d Dynamometer Reading
 M_s Strain Gage Reading

Fig. 47 Difference of the Moment Readings

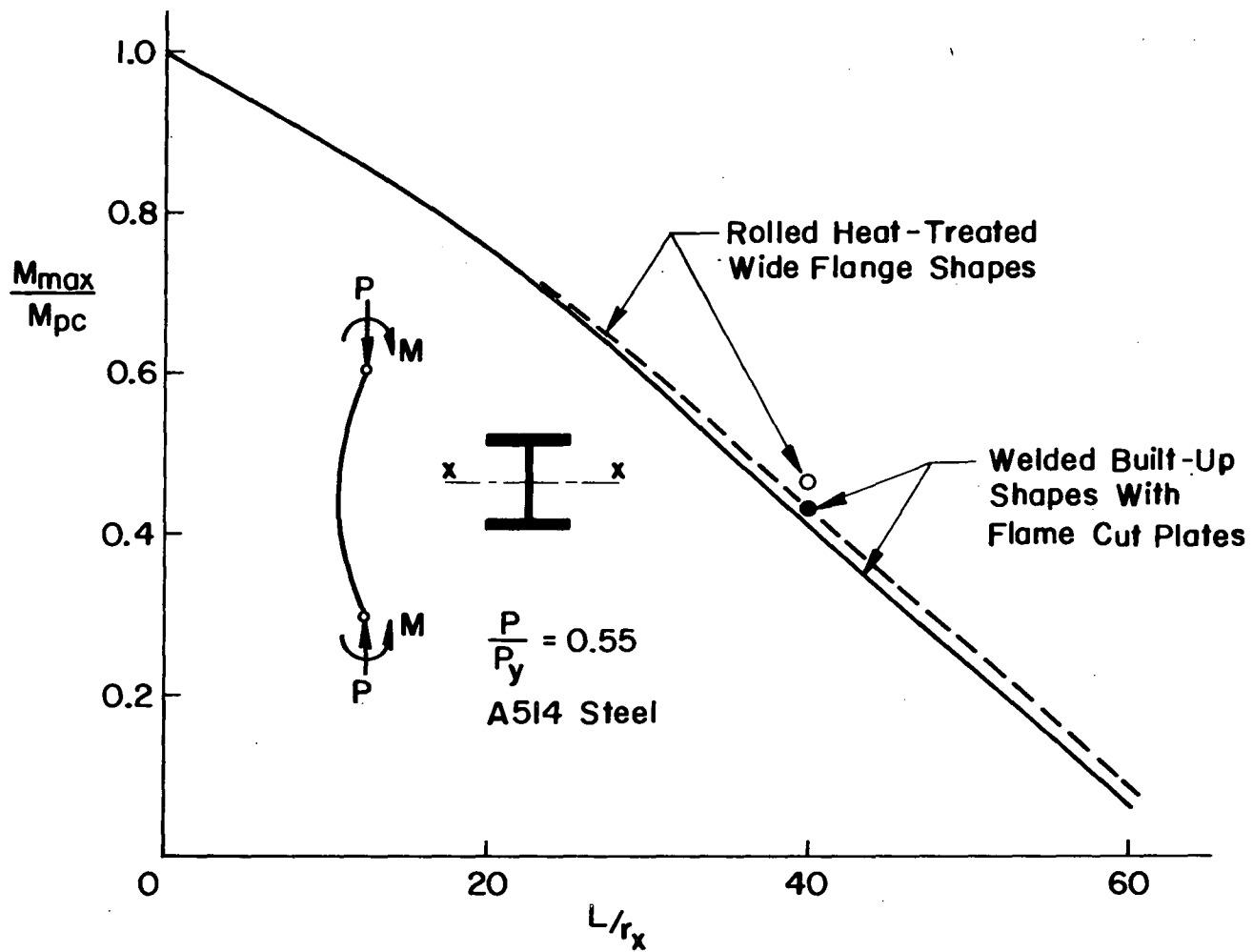


Fig. 48 Comparison Between Test Results and Theoretical Solutions

12. REFERENCES

1. Bijlaard, P. P.
THEORY OF THE PLASTIC STABILITY OF THIN PLATES,
Pub. Int. Assoc., Bridge and Structural Engr.,
Zurich, Vol. 6, 1940-1941.
2. Ilyushin, A. A.
THE ELASTO-PLASTIC STABILITY OF PLATES, NACA
TM 1188, 1949.
3. Stowell, E. Z.
A UNIFIED THEORY OF PLATE BUCKLING OF COLUMNS
AND PLATES, NACA Rep. 898, 1948.
4. Handelman, G. H. and Prager, W.
PLASTIC BUCKLING OF A RECTANGULAR PLATE
UNDER EDGE THRUST, NACA Rep. 946, 1961.
5. Ramberg, N. and Osgood, W. R.
DESCRIPTION OF STRESS-STRAIN CURVES BY THREE
PARAMETERS, NACA, N.T. No. 902, NACA, 1943.
6. American Society for Testing and Materials
ASTM STANDARDS, Part 3, A370-617, 1961.
7. Beedle, L. S. and Tall, L.
BASIC COLUMN STRENGTH, Proceedings, ASCE,
Vol. 86, No. ST7, July 1960.
8. Johnston, B.
CRC GUIDE TO DESIGN CRITERIA FOR COMPRESSION
MEMBERS, 2nd edition, 1966.
9. Cozzone, F. P. and Melcon, M. A.
NON-DIMENSIONAL BUCKLING CURVES -- THEIR
DEVELOPMENT AND APPLICATION, Journal,
Aeronaut Science, Vol. 13, No. 10, P511,
Oct. 1946.
10. Tall, L.
WELDED BUILT-UP COLUMNS, Ph.D. Dissertation
Lehigh University, May, 1961.

11. Boulton, N. S. and Lance Martin, H. E.
RESIDUAL STRESSES IN ARC-WELDED PLATES, Proc.
Inst. Mech. Engrs. Vol. 133, 1936.
12. Gruning, M.
DIE SCHRUMPFSPANNUNGEN BEIM SCHWEISSEN, Der
Stahlbau, 1934.
13. Rodgers, O. E., and Fetcher, R., Jr.
THE DETERMINATION OF INTERNAL STRESSES FROM
TEMPERATURE HISTORY OF A BUTT-WELDED PLATE,
Welding Journal, Vol. 17, November 1938.
14. Weiner, J.
AN ELASTOPLASTIC THERMAL STRESS ANALYSIS
OF A FREE PLATE, Journal App. Mech. (3)
Vol. 23, 1956.
15. Tall, L.
RESIDUAL STRESSES IN WELDED PLATES, A
THEORETICAL STUDY, Welding Journal, Vol. 43,
January 1964.
16. Estuar, F.
WELDING RESIDUAL STRESSES AND THE STRENGTH
OF HEAVY COLUMN SHAPES, Ph.D. Dissertation,
Lehigh University, 1966.
17. Alpsten, G. A.
THERMAL RESIDUAL STRESSES IN HOT-ROLLED
STEEL MEMBERS, Fritz Lab Report 337.3,
December 1968.
18. Odar, E., Nishino, F., and Tall, L.
RESIDUAL STRESSES IN "T-1" CONSTRUCTIONAL
ALLOY STEEL PLATES, Welding Research Council
Bulletin No. 121, April, 1967.
19. Odar, E., Nishino, F., and Tall, L.
RESIDUAL STRESSES IN WELDED BUILT-UP "T-1"
SHAPES, Welding Research Council Bulletin
No. 121, April 1967.
20. Odar, E., Nishino, F., and Tall, L.
RESIDUAL STRESSES IN ROLLED HEAT-TREATED
"T-1" SHAPES, Welding Research Council
Bulletin No. 121, April, 1967.

21. Shanley, F. R.
THE COLUMN PARADOX, Journal of the
Aeronautical Sciences, Vol. 13, No. 12,
December, 1946.
22. Shanley, F. R.
INELASTIC COLUMN THEORY, Journal of the
Aeronautical Sciences, Vol. 14, No. 5,
May, 1947.
23. Tall, L., Editor-in-Chief
STRUCTURAL STEEL DESIGN
Ronald Press, New York, 1964.
24. Column Research Council
THE BASIC COLUMN FORMULA, CRC Tech.
Memo. No. 1, May 1952.
25. Yu, C. K. and Tall, L.
A PILOT STUDY ON THE STRENGTH OF 5Ni-Cr-Mo-V
STEEL COLUMNS, Experimental Mechanics,
Vol. 8, No. 1, January, 1968.
26. Nishino, F. and Tall, L.
EXPERIMENTAL INVESTIGATION OF THE
STRENGTH OF "T-1" STEEL COLUMNS, Fritz
Laboratory Report No. 290.9, June 1969.
27. Estuar, F. R. and Tall, L.
TESTING OF PINNED-END STEEL COLUMNS
Special Technical Publication, No. 419,
ASTM, August 1966.
28. Bijlaard, P. P.
THEORY OF THE PLASTIC STABILITY OF THIN
PLATES, Pub. Int. Assoc., Bridge and
Structural Engrg., Zurich, Vol. 6, 1940-41.
29. Bijlaard, P. P.
SOME CONTRIBUTIONS TO THE THEORY OF
ELASTIC AND PLASTIC STABILITY, Pub. Int.
Bridge and Structural Engrg., Zurich,
Vol. 8, 1947.
30. Bijlaard, P. P.
THEORY AND TESTS ON THE PLASTIC STABILITY
OF PLATES AND SHELLS, Jour. Aero. Sci.,
Vol. 16, No. 9, September 1949.

31. Collatz, L.
EIGENWERTPROBLEME UND IHRE NUMERISCHE
BEHANDLUNG, Chelsea Publishing Co.,
New York, 1948.
32. Salvadori, M. G., and Baron, M. L.
NUMERICAL METHODS IN ENGINEERING,
Prentice-Hall, Englewood Cliffs, New
Jersey, 1952.
33. Nishino, F., and Tall, L.
RESIDUAL STRESS AND LOCAL BUCKLING
STRENGTH OF STEEL COLUMNS, F.L. Report
No. 290.11, 1967. To be published.
34. Ueda, Y.
ELASTIC, ELASTIC-PLASTIC AND PLASTIC
BUCKLING OF PLATES WITH RESIDUAL STRESSES,
Ph.D. Dissertation, Lehigh University, 1962.
35. Lundquist, E. E.
LOCAL INSTABILITY OF SYMMETRICAL
RECTANGULAR TUBES UNDER AXIAL COMPRESSION,
NACA TN 686, 1939.
36. Stowell, E. Z., and Lundquist, E. E.
LOCAL INSTABILITY OF COLUMNS WITH I-Z-
CHANNEL-AND RECTANGULAR-TUBE SECTIONS,
NACA TN 743, 1939.
37. Nishino, F., Ueda, Y. and Tall, L.
EXPERIMENTAL INVESTIGATION OF THE BUCKLING
OF PLATES WITH RESIDUAL STRESSES, ASTM
Special Technical Publication No. 419,
August 1967
38. Hu, P. C., Lundquist, E. E. and Batdorf, S. B.
EFFECT OF SMALL DEVIATIONS FROM FLATNESS
ON EFFECTIVE WIDTH AND BUCKLING OF PLATES
IN COMPRESSION, NACA TN 1124, 1946.
39. Nishino, F. and Tall, L.
RESIDUAL STRESS AND LOCAL BUCKLING STRENGTH
OF STEEL COLUMNS, Fritz Laboratory Report
No. 290.11, January, 1967.
40. Von Karman, T.
DIE KNICKFESTIGKEIT GERADER STÄBE, Physikalische
Zeitschrift, Vol. 9, p. 136, 1908.
UNTERSUCHUNGEN ÜBER KNICKFESTIGKEIT, Mitteilungen
über Forschungsarbeiten auf dem Gebiete des
Ingenieurwesens, No. 81, Berlin, 1910.

41. Westergaard, H. M. and Osgood, W. R.
STRENGTH OF STEEL COLUMNS, Trans. ASME,
Vols, 49, 50, APM-50-9, p. 65, 1928.
42. Jezek, K.
DIE TRAGFÄHIGKEIT DES EXZENTRISCH BEANSPRUCHTEN
UND DES QUERBELASTETEN DRUCKSTABES AUS EINEM
IDEAL PLASTISCHEN MATERIAL, Sitzungsberichte
der Akademie der Wissenschaften in Wien, Abt.
IIa, Vol. 143, 1934.
43. Chwalla, E.
THEORIE DES AUSSERMITTIG GEDRÜCKTEN STABES AUS
BAUSTAHL, Der Stahlbau, 7(21), p. 161-165,
October, 1934, 7(22), p. 173-176, October, 1934,
7(23), p. 180-184, November, 1934.
DER EINFLUSS DER QUERSCHNITTSFORM AUF DAS
TRAGVERMÖGEN AUSSERMITTIG GEDRUCKTER BAUSTAHLSTÄBE,
Der Stahlbau, 8(25), p. 193-197, December, 1935,
8(26), p. 204-207, December 1935.
AUSSERMITTIG GEDRÜCKTE BAUSTAHLSTÄBE MIT ELASTISCH
EINGESPANNTEN ENDEN UNTER VERSCHIEDEN GROSSEN
ANGRIFFSHEBELN, Der Stahlbau, 10(7), p. 49-53,
March 1937, 10(8), p. 57-60, April 1937.
44. Driscoll, G. C., Jr., et.al.
PLASTIC DESIGN OF MULTI-STORY FRAMES, Lehigh
University, 1965.
45. Batterman, R. H. and Johnston, B. G.
BEHAVIOR AND MAXIMUM STRENGTH OF METAL COLUMNS,
ASCE Journal, Structural Division, Vol. 93,
No. ST2, April, 1967.
46. Malvick, A. J. and Lee, L. H. N.
BUCKLING BEHAVIOR OF AN INELASTIC COLUMN, ASCE
Journal, Mechanics Division, Vol. 91, No. EM3,
Proc. Paper C372, June, 1965, pp. 113-127.
47. Birnstiel, C. and Michalos, J.
ULTIMATE LOAD OF H-COLUMNS UNDER BIAxIAL BENDING,
ASCE Journal, Structural Division, Vol. 59,
No. ST2, Proc. Paper 3503, April, 1963, pp.
161-197.
48. Ojalvo, N.
RESTRAINED COLUMNS, Proc. ASCE, 86 (EM5),
October, 1960.

49. Levi, V.
PLASTIC DESIGN OF BRACED MULTI-STORY FRAMES,
Ph.D. Dissertation, Lehigh University, 1962.
50. Galambos, T. and Lay, M.
END-MOMENT END-ROTATION CHARACTERISTICS FOR
BEAM-COLUMNS, Fritz Laboratory Report 205A.35,
May, 1962.
51. Lay, M.
THE STATIC LOAD-DEFORMATION BEHAVIOR OF PLANAR
STEEL STRUCTURES, Ph.D. Dissertation, Lehigh
University, 1964.
52. Lay, M.
THE MECHANICS OF COLUMN DEFLECTION CURVES,
Fritz Laboratory Report No. 278.12, June 1964.
53. Lu, L. W. and Kamalvand, H.
ULTIMATE STRENGTH OF LATERALLY LOADED COLUMNS,
Fritz Laboratory Report No. 273.52, November,
1966.
54. Galambos, T. V. and Prasad, T.
ULTIMATE STRENGTH TABLES FOR BEAM-COLUMNS,
Bull, No. 78, WRC, New York, 1962.
55. Levi, V. and Driscoll, G. C., Jr.
RESPONSE OF COLUMN TO IN-PLANE LOADING, Fritz
Laboratory Report No. 273.10, Lehigh University,
1963.
56. Ojalvo, M. and Fukumoto, Y.
NOMOGRAPHS FOR THE SOLUTION OF BEAM-COLUMN
PROBLEMS, Bull. No. 78, WRC, New York, 1962.
57. Yu, C. K. and Tall, L.
A514 STEEL BEAM COLUMNS, Fritz Laboratory
Report No. 290.15, October, 1968. To be
published.
58. Okuto, K.
A PILOT EXPERIMENTAL INVESTIGATION OF A514
STEEL BEAM COLUMNS, M.S. Thesis, Lehigh
University, 1967.
59. Lay, M. G., Aglietti, R. A. and Galambos, T. V.
TESTING TECHNIQUES FOR RESTRAINED BEAM-COLUMNS,
Fritz Laboratory Report No. 270.7, October, 1963.

60. Van Kuren, R. C. and Galambos, T. V.
BEAM COLUMN EXPERIMENTS, ASCE Journal
Structural Division, Vol. 90, No. ST2,
April, 1964.
61. Yarimici, E., Yura, J. A. and Lu, L. W.
TECHNIQUES FOR TESTING STRUCTURES
PERMITTED TO SWAY, Experimental Mechanics,
August, 1967.